

The ubiquitin proteasome system in Huntington's disease

A thesis presented for the degree of Doctor of Philosophy (PhD)

Rushee Singh Jolly

Department of Anatomy and Developmental Biology,
University College London

2007



UMI Number: U591759

All rights reserved

INFORMATION TO ALL USERS

The quality of this reproduction is dependent upon the quality of the copy submitted.

In the unlikely event that the author did not send a complete manuscript and there are missing pages, these will be noted. Also, if material had to be removed, a note will indicate the deletion.



UMI U591759

Published by ProQuest LLC 2013. Copyright in the Dissertation held by the Author.
Microform Edition © ProQuest LLC.

All rights reserved. This work is protected against
unauthorized copying under Title 17, United States Code.



ProQuest LLC
789 East Eisenhower Parkway
P.O. Box 1346
Ann Arbor, MI 48106-1346

For my parents

I, Rushee Singh Jolly, confirm that the work presented in this thesis is my own. Where information has been derived from other sources, I confirm that this has been indicated in the thesis.

Abstract

Huntington's disease (HD) is an autosomally dominant, progressive movement disorder, caused by an expansion in the polyglutamine tract of huntingtin protein. HD is pathologically characterised by the presence of insoluble, proteinaceous neuronal intranuclear inclusions (NIIs) and dystrophic neurite inclusions (DNIs) in affected neurons that can be immunostained for ubiquitin and other proteins involved in the ubiquitin-proteasome system (UPS). The UPS is a highly conserved mechanism for degradation of both normal and misfolded proteins in eukaryotic cells. This has led to suggestions that the UPS is inhibited in HD. This study utilises microscopy, biochemistry and fluorometric assays to examine the molecular composition of aggregates and the potential dysfunction of the UPS in the R6/2 mouse line, an established model of HD. The ultrastructure of aggregates is shown to be predominantly amorphous and granular in appearance and likely to be formed through the process of transglutamination. Immunohistochemical data shows that certain chaperones, ubiquitin-like proteins (UBLs) and proteins involved in the UPS localise to NIIs and DNIs differentially. Fluorometric assays demonstrate that the proteasome exhibits a differential profile in R6/2 mice where both chymotrypsin-like and PGPH-like activities are markedly increased whilst trypsin-like activity is decreased relative to litter-mate control mice. Furthermore, these activity changes may be explained by alterations in proteasome regulation, levels and maturation. These results suggest that, in the R6/2 line, the proteasome is not inhibited by the presence of mutant huntingtin, rather that there are alterations of the catalytic activities of the proteasome. It appears that NII's act not only as focal points of proteolysis, but also of proteasome biogenesis. This is consistent with, and extends, the concept of clastosomes.

Acknowledgements

There are many people to whom I am extremely grateful for their help, expertise and encouragement throughout my PhD and I shall attempt to mention them here.

Firstly, I would like to express my gratitude and respect to my supervisor, Prof. Stephen W. Davies. Throughout the course of my doctoral studies, Steve has always been supportive, patient and open to my ideas. His scientific knowledge is formidable and his enthusiasm, infectious. I feel truly privileged to have learnt from him.

I would like to thank Mark Turmaine and Dr. Elizabeth Slavic-Smith for teaching me electron microscopy. Mark's knowledge, skills and practicality have proved invaluable to me; he is a tremendous asset to the department. Additionally, Elizabeth taught me confocal microscopy and (bravely!) proofread large chunks of my work. I am extremely grateful to Dr. Christian Specht who taught me the basics of Western blotting and immunoprecipitation techniques. During his time at UCL, Christian often went out of his way to help me and was both an inspiration and friend. I also must thank Dr. Louise Donnelly and Samir Nuseibeh, both of Imperial College London, for their help and use of equipment in the fluorometric experiments, which form the crux of this work. I still cannot believe that the UCL Anatomy department does not have a working fluorimeter!

I would also like to thank all the members of the Davies lab, past and present, for creating such a friendly and sociable work atmosphere; Lee-Jay Bannister, Barbara Cozens, Aysha Raza, Elizabeth Slavic-Smith and Mark Turmaine. And what a stroke of luck to have had a supervisor as hooked on music and food as me!

Lastly, but certainly not least, my deepest thanks go to my family. My mother, father and sisters, Schon and Nish, provided the impetus for me to finish my thesis. Words cannot express how much their love, understanding and support mean to me and I shall forever be grateful.

Contents

	Page number
Abstract	3
Acknowledgments	4
Contents	5
Figures	9
Abbreviations	11

Chapter 1: Introduction

1.1 Introduction to Huntington's disease

1.1.1 Neuropathology in Huntington's disease	13
1.1.2 Genetics of Huntington's disease	16
1.1.3 Huntingtin	18
1.1.4 Polyglutamine expansion diseases	20
1.1.5 Protein aggregation in HD and other polyglutamine expansion diseases	22
1.1.6 Mechanisms of protein aggregation in polyglutamine disorders	24
1.1.7 The R6/2 model of HD	27

1.2 The Ubiquitin-Proteasome System

1.2.1 An overview of the ubiquitin proteasome pathway	32
1.2.2 Structure of the proteasome	33
1.2.3 Proteasome assembly	38
1.2.4 Regulation of proteasome activity	39
1.2.5 The proteasome in HD and other polyglutamine disorders	41
1.2.6 Ubiquitin-like proteins	44

1.2.7 Ubiquitin-like proteins in polyglutamine expansions diseases	46
1.3 The chaperone family of proteins	48
1.3.1 Chaperones in polyglutamine expansion diseases	49
1.4.1 Aims of the project	50

Chapter 2 : Materials and Methods

2.1 Materials	52
2.1.1 Standard solutions	52
2.1.2 Transgenic mice	52
2.2 Microscopy methods	53
2.2.1 Preparation of tissue for immunohistochemistry or immunofluorescence	53
2.2.2 Preparation of tissue for electron microscopy	53
2.2.3 Immunohistochemistry	54
2.2.4 Antibodies for immunohistochemistry	55
2.2.5 Double-labelled immunofluorescence	56
2.2.6 Antibodies for immunofluorescence	57
2.2.7 Electron microscopy	58
2.3 Protein biochemistry	59
2.3.1 Preparation of tissue for electrophoresis	59
2.3.2 SDS-PAGE	59
2.3.3 Western blotting	60
2.3.4 Antibodies for Western blotting	61

2.3.5 Coomassie blue staining	62
2.3.6 Preparation of tissue for immunoprecipitation	62
2.3.7 Immunoprecipitation of ubiquitinated proteins	62
2.4 Proteolysis activity assays	63
2.4.1 Preparation of tissue for proteolysis assays	63
2.4.2 Proteolytic activity assay	64
2.4.3 Proteasomal and protease activity assay	64
2.4.4 Statistics	65

Chapter 3 : Results

3.1 Overview	66
3.2 Molecular composition of aggregates in R6/2 transgenic mice	68
3.2.1 Aggregates are amorphous structures containing Nε(γglutamyl)lysine bonds	68
3.2.2 Expanded polyglutamine proteins are ubiquitinated in R6/2 mice	74
3.2.3 20s, 19s and 11s proteasomal subunits relocate to aggregates in R6/2 brains	76
3.2.4 Chaperones relocate to aggregates in R6/2 brains	80
3.3 Proteolytic activity in brains of R6/2 mice	83
3.3.1 Altered total proteolysis in R6/2 mice	84
3.3.2 Altered proteasomal and non-proteasomal proteolysis in R6/2 mice	86
3.3.3 Alterations in proteasomal subunits in R6/2 mice	88
3.4 Proteasomal regulation in R6/2 transgenic mice	91
3.4.1 Levels of 11s and 19s proteasomal regulatory proteins in R6/2 mice	92
3.4.2 No change in immunoproteasome subunits	94
3.4.3 Levels and localisation of PA200 and PI31k	94

3.5 Additional components of the UPS in the R6/2 transgenic model	98
3.5.1 Additional components of the UPS machinery associate with NIIs	98
3.5.2 Ubiquitin-like proteins redistribute to neuronal intranuclear inclusions	100
 Chapter 4 : Discussion	
4.1 Molecular composition of polyglutamine containing aggregates	105
4.1.1 Clues about the ultrastructure of protein aggregates in R6/2 mice	106
4.1.2 Protein recruitment to nuclear and neurite aggregates	111
4.2 Proteolysis in the R6/2 model	122
4.2.1 Altered Proteolysis in the R6/2 model	122
4.2.2 Regulation of the proteasome in the R6/2 model	130
4.3 Future studies	138
 Conclusions	140
Appendix	141
References	143

Figures

	Page number
Fig. 1 Brain sizes between HD and control	14
Fig. 2 Currently identified polyglutamine expansion diseases	21
Fig. 3 Construct of the transgene in the R6/2 line	28
Fig. 4 An overview of the phenotype and neuropathology of the R6/2 mouse	29
Fig. 5 An overview of the ubiquitin-proteasome system (UPS)	34
Fig. 6 An overview of proteasome structures and variations	35
Fig. 7 Inclusions in the R6/2 mouse model	72/3
Fig. 8 Huntingtin is ubiquitinated in the R6/2 model	75
Fig. 9 Components of the UPS localise to aggregates	78
Fig. 10 Table showing which proteasome subunits localise to aggregates	79
Fig. 11 Chaperones aggregate in NIIs in R6/2 mice	81
Fig. 12 Table showing which chaperones localise to aggregates in R6/2 mice	82
Fig. 13 Rate of trypsin, chymotrypsin and PGPH peptidase activities in R6/2 mice	85
Fig. 14 Rate of trypsin, chymotrypsin and PGPH proteasomal and protease activities in R6/2 mice	87
Fig. 15 Relative contributions of the proteasome and non-proteasomal proteases to total proteolysis in R6/2 mice and litter mate controls	89
Fig. 16 Altered expression / localisation of proteasome subunits in R6/2 mice	90
Fig. 17 Levels of 11s and 19s regulatory subunits in R6/2 mice	93
Fig. 18 Levels of immunoproteasome subunits in R6/2 mice	95
Fig. 19 Altered expression / localisation of proteasome regulatory components PA200 and PI31k in R6/2 mice	97

Fig. 20	Altered expression / localisation of proteasome maturation protein (POMP) and E2 ubiquitinating enzyme in R6/2 mice	99
Fig. 21	Altered expression / localisation of ubiquitin-like proteins (UBLs) in R6/2 mice	102
Fig. 22	Redistribution of UBLs in R6/2 mice	103
Appendix 1	Table showing the yeast and mammalian nomenclature for the 20s, 19s and 11s proteasomal subunits	141
Appendix 2	Representative images demonstrating the “*” scoring scale used for strength of immunohistochemical staining	142

Abbreviations

ALS	Amyotrophic lateral sclerosis
CNS	Central nervous system
DNI	Dystrophic neurite inclusion
DRPLA	Dentatorubral-Pallidoluysian atrophy
HD	Huntington's disease
IFN- γ	Interferon- γ
LMC	Litter-mate control
MJD	Machado-Joseph disease
NII	Neuronal intranuclear inclusion
PBS	Phosphate buffered saline
POMP	Proteasome maturation protein
SBMA	Spinal bulbar muscular atrophy
SCA	Spinocerebellar ataxia
SUMO	Small ubiquitin-like modifier protein
UBL	Ubiquitin-like protein
UPS	Ubiquitin-proteasome system
WHS	Wolf-Hirschhorn syndrome
WT	Wild-type

CHAPTER 1

Introduction

1.1 Introduction to Huntington's disease

Huntington's disease (HD) is a progressive, autosomally dominant neurodegenerative disease that was named after the Long Island physician, George Huntington, who provided the first accurate description of this illness. In his seminal paper "*On Chorea*", published in 1872 in the Philadelphia based journal *The Medical & Surgical Reporter*, Huntington made key observations regarding the age of onset, psychiatric disturbances and hereditary nature of this disease, which are still considered to be definitive features of the disease.

HD is clinically characterised by psychiatric abnormalities, hyperkinesia, and cognitive decline. The psychiatric abnormalities can include hypersexuality, suicidal tendencies, depression or anti-social behaviour. These behavioural changes appear before the involuntary writhing, chorea-form movements, which are characteristic of the disease. HD patients can, but do not always, experience cognitive decline to varying degrees (Nance, 1998). The juvenile variant of HD, which accounts for approximately 1-7% of HD cases presents differently with symptoms that are more parkinsonian in nature (such as bradykinesia, rigidity and tremor) and with slightly less cognitive impairment than the adult onset variant

(Gomez-Tortosa et al., 1998; Rasmussen et al., 2000; Nance and Myers, 2001; Seneca et al., 2004).

Typically, HD will present in the fourth or fifth decade, although there are several known modulators of the age of onset (see 1.1.2). The typical time course from disease onset to death is 15-25 years. Juvenile HD, defined as presenting before 20 years of age, can occur as early as 2 years of age and typically results in a shorter disease time course (Foroud et al., 1999).

1.1.1 Neuropathology in Huntington's disease

The neuropathological changes in HD are quite striking. HD brains weigh ~30% less than age-matched control (de la Monte et al., 1988), with reduction in the size of most regions of the brain. There is thinning of the cerebral cortex and severe atrophy of areas of the striatum (particularly the caudate nucleus and putamen), which is accompanied by a consequent enlargement of the lateral ventricle. All of these features are visible macroscopically (de la Monte et al., 1988; Rosas et al., 2003) (Figure 1).

There are numerous quantitative studies detailing the extent of neuronal loss from the striatum and cortex, some of which also indicate marked astrocytosis and microglial activation (Hedreen et al., 1991; Myers et al., 1991; Hedreen and Folstein, 1995; Pavese et al., 2006). Although there is severe degeneration in the

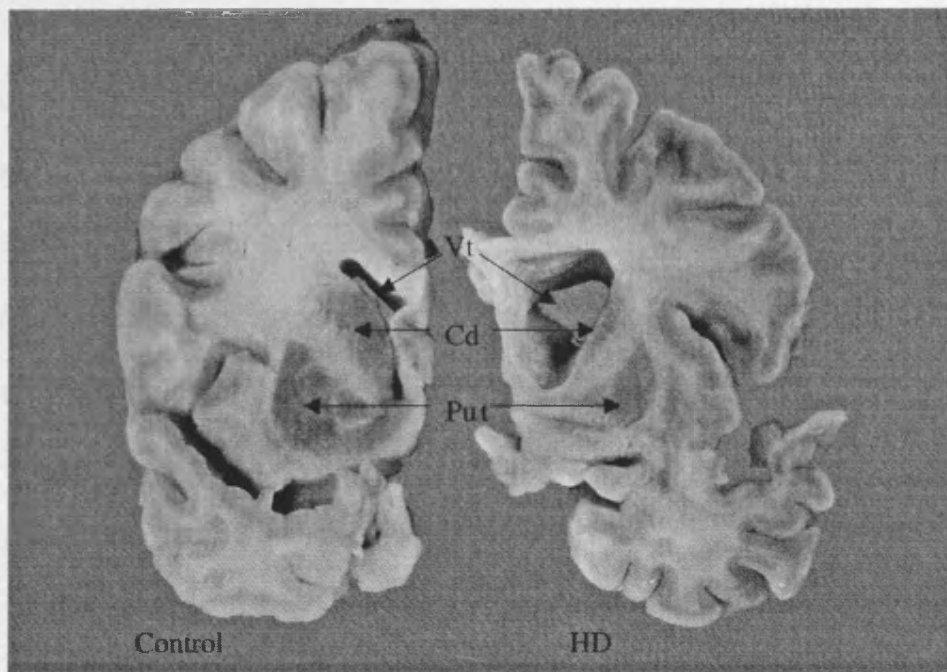


Figure 1: Neuropathology in Huntington's disease brains. Gross neuronal atrophy is macroscopically visible in coronally sectioned cerebral hemispheres in an HD brain (right) when compared to an age-matched control (left). Particularly evident is the enlarged ventricle (Vt), thinned caudate nucleus (Cd) and atrophied putamen (Put). *Photograph taken from (Gutekunst et al., 2002)*

HD striatum, the pattern of neuronal loss is far from uniform. In early stage HD, there appears to be a preferential loss of three types of strial projection neurons (those that project to the globus pallidus external segment, substantia nigra pars reticulata and substantia nigra pars compacta) which is accompanied by a much more gradual loss of globus pallidus internal segment-projecting neurons. However, in late stage HD, all four populations are reduced (Deng et al., 2004). In addition, virtually all striatal chemospecific interneurons (those that contain calretinin, NADPH, parvalbumin, calbindin or ChAT) are spared in HD, thus leading to their increased density throughout the course of the disease (Cicchetti et al., 2000).

Using Golgi impregnations to visualise the dendritic morphology of spiny striatal neurons, both proliferative and degenerative changes have been described. In moderate grades of HD, the proliferative changes dominate (dendritic curving, branching and increased spine numbers), whereas in severe grades of HD, the degenerative changes predominate, such as truncated dendritic arbors, dendritic swellings and significant loss of spines (Graveland et al., 1985; Ferrante et al., 1991).

A grading system exists to classify the severity of the neuropathology in HD, ranging from 0-4, with 4 being classed as the most severe grade. This scale was devised using both macroscopic and microscopic criteria from post-mortem tissue of 163 clinically diagnosed HD cases and correlates well with the clinical manifestations of the disease. Grade 0 cases, although clinically diagnosable with HD, do not show any gross or microscopic pathology, demonstrating that detectable anatomical changes follow

behavioural disorders. Grade 1 cases show moderate astrocytosis and up to 50% neuronal loss in the caudate nucleus. Grades 2-4 show increasing astrocytosis, enlargement of the lateral ventricle and severe neuronal loss in the caudate nucleus (as much as 95%) and putamen (Vonsattel et al., 1985).

HD is characterised by the presence of insoluble protein aggregates in both the nucleus and neurites of affected neurons. These have become one of the defining pathological features of HD and are described later in detail (see 1.1.5).

1.1.2 Genetics of Huntington's disease

The prevalence of HD worldwide varies considerably with area - some areas have high occurrences (Venezuela) and in some areas HD is almost none existent (eg. Finland, Japan). Epidemiological studies show variance in the prevalence of HD in European populations, but most figures seem to fall within the region of 4-8 per 100,000 (Harper, 1992).

In 1993, the Huntington's Disease Collaborative Research Group mapped the gene responsible for HD to a region on chromosome 4 (4p16.3), named IT15 ("interesting transcript 15"). This gene, spanning 67 exons, encoded a large protein of unknown function, which was subsequently named huntingtin. In HD, there is an expansion of the trinucleotide CAG repeat sequence (which codes for glutamine) found in exon 1 of

IT15 (Huntington's Disease Collaborative Research Group, 1993). Polyglutamine tract lengths in huntingtin protein are polymorphic and in normal populations are typically between 14-26 glutamines; tracts between 27-35 repeats are not associated with HD (but may expand in paternal / maternal transmission); individuals with tracts between 36-39 repeats display reduced penetrance – ie. a proportion of individuals develop HD. However, 40 polyglutamine repeats appears to be the threshold for disease – any higher numbers of CAG repeats, and HD will present (Myers, 2004).

There is an inverse correlation between the length of the polyglutamine tract and the age of onset; large repeats of 60 or more typically result in juvenile onset HD (Gusella and MacDonald, 2000; Wexler et al., 2004). Juvenile HD cases with polyglutamine repeat lengths as high as 214 have been reported (Seneca et al., 2004). But, whilst there exists a significant correlation between polyglutamine tract length and age of onset of disease, the repeat length only accounts for 65-71% of the variance in the age of onset (Rosenblatt et al., 2001; Wexler et al., 2004). Epidemiological studies have shown that the variation in age of onset that is not attributable to repeat size, is due to genetic modifiers in 40-56% of cases and environmental causes in 44-60% of cases (Djousse et al., 2003; Wexler et al., 2004). It has been shown that approximately 1% of the variance in age of onset is due to the repeat length in the normal allele; suprisingly, the longer the repeat length in the normal allele, the later the age of onset (Djousse et al., 2003).

Patients that are homozygous for the HD gene do not differ clinically from heterozygous patients, in terms of severity or course of the disease, demonstrating that HD is a completely phenotypically dominant disorder (Wexler et al., 1987).

1.1.3 Huntingtin

Huntingtin is a large 348 kDa protein consisting of 3,144 amino acids (Huntington's Disease Collaborative Research Group, 1993) and shares little sequence homology with other known proteins. However, huntingtin does contain three prominent motifs: a polyglutamine tract after the first 18 amino acids, which is immediately followed by a polyproline tract and 10 HEAT (htt, elongation factor 3, the regulatory A subunit of protein phosphatase 2A and TOR1) repeats, which are clustered into three domains in the N-terminal region of the protein. Polyglutamine / polyproline tracts are thought to be involved in transcription and HEAT repeats have been suggested to play a role in transport, microtubule dynamics and chromosome separation (Harjes and Wanker, 2003).

Although expressed ubiquitously in humans and rodents, huntingtin is particularly highly expressed in the brain and testes, with no obvious pattern of expression that mirrors the pathology seen in HD. Subcellularly, Huntingtin is found with the cytoskeleton, in the cytoplasm associated with a variety of organelles, such as the golgi

complex, vesicle membranes, and has even been shown to localise to the nucleus (Li et al., 1993; DiFiglia et al., 1995; Sharp et al., 1995; Jeong et al., 2006).

The details of huntingtin's cellular functions have remained elusive. In spite of this, several proteins have been found that associate with huntingtin (mainly through the N-terminal portion) and they can largely be grouped into proteins that are either involved in transcription (eg. TBP), trafficking and endocytosis (eg. HAP1), signalling (eg. Grb2) or metabolism (eg. HIP2) (Li and Li, 2004). To date, roles in various cellular functions have been suggested, such as modulation of dendritic morphology, transcriptional regulation, cellular transport and survival (Harjes and Wanker, 2003; Cattaneo et al., 2005). Several groups have shown that homozygous disruption of the mouse huntingtin gene results in embryonic lethality, thus highlighting the importance of huntingtin in development (Duyao et al., 1995; Zeitlin et al., 1995). The fact that mice expressing huntingtin with expanded (Mangiarini et al., 1996) or deleted polyglutamine stretches (Clabough and Zeitlin, 2006) are viable, demonstrate that this portion of the protein is not essential for development.

Interestingly, a condition called Wolf-Hirschhorn Syndrome (WHS), which is caused by a hemizygous deletion of the distal short arm of chromosome 4, has a disease phenotype (facial dysmorphism and mental / growth retardation) completely distinct from that of HD, which demonstrates that HD is not caused simply by a loss of huntingtin activity (Gandelman et al., 1992). A recent study found that one of the functions of huntingtin was to regulate body weight, with overexpression causing

weight gain (Van Raamsdonk et al., 2006). As one of the features of HD is an increasing loss of body weight, often despite a high calorific intake, it is possible that some of the features of HD could be as a result of loss of normal huntingtin function.

1.1.4 Polyglutamine expansion diseases

HD is one of a family of polyglutamine expansion diseases, which includes dentatorubropallidoluysian atrophy (DRPLA), spinal and bulbar muscular atrophy (SBMA) and various spinocerebellar ataxias (SCA's). To date, nine polyglutamine expansion diseases have been identified (Figure 2). Importantly, in all of these diseases the expanded polyglutamine stretch is present in seemingly unrelated proteins, yet they exhibit striking similarities – an autosomal dominant pattern of inheritance (except SBMA, which is X-linked), the presence of neuronal intranuclear inclusions (see chapter 1.1.5), the relationship of repeat length to age of onset / severity of disease and a progressive nature to neurological dysfunction (Ordway et al., 1997). Another feature of HD and indeed all polyglutamine expansion diseases, is that they exhibit a feature called anticipation. Anticipation is defined as the tendency for inherited disorders to present at an earlier age in successive generations, often with increasing severity. In the case of polyglutamine disorders, this is usually brought about by a continued expansion of the polyglutamine tract in successive generations, although much less common and smaller polyglutamine contractions have also been reported (La Spada et al., 1994).

Disease Name(s)	Protein containing polyQ expansion	Function of normal protein	Primary sites of neuropathology	Normal polyQ lengths	Reported disease allele lengths
HD (Huntington's disease)	Huntingtin	Unknown	CN, PU, GPe	6-35	36-121
DRPLA (Dentatorubro-pallidoluysian atrophy) or Haw river syndrome	Atrophin-1	Transcriptional co-repressor	CE (DN), RN, GPe, STN	3-35	49-88
SBMA (Spinal & bulbar muscular atrophy) or Kennedy's disease	Androgen receptor	Steroid receptor	AHC	11-38	38-62
SCA-1 (Spinocerebellar ataxia-1)	Ataxin 1	Regulatory factor in gene expression?	CE (PC & DN), RN, IO, pons, AHC, pyramidal tracts	6-44	40-81
SCA-2	Ataxin 2	Unknown	CE (PC), IO, pons, SNpc, AHC	15-29	35-59
SCA-3 or Machado-Joseph Disease (MJD)	Ataxin 3	Involved in de-ubiquitination??	CE (monolayer cells), pons, SNpc, SNpr, AHC	12-41	55-84
SCA-6	Isoform of α_{1A} Ca ²⁺ channel subunit	Calcium channel subunit	CE (PC, MG)	4-17	20-30
SCA-7	Ataxin 7	Histone acetylation??	CE (PC, MG), pons, IO, AHC, retina	4-35	37-220
SCA-17	TATA-binding protein	Transcription factor	CE (PC), CA, PU, thalamus	29-42	47-55

Figure 2: Currently identified polyglutamine expansion diseases. Table demonstrating that polyglutamine expansion diseases occur in proteins with seemingly unrelated function. The threshold of polyglutamine tract length resulting in disease is fairly similar between diseases and has been reported to be as high as 220 repeats in SCA-7. The regions of neuropathology (atrophy, cell death etc) in these diseases also greatly varies, highlighting the role that the disease protein plays in the selective vulnerability of neurons. AHC=Anterior horn cells; CA=Caudate; CE=Cerebellum; CN=Caudate nucleus; DN=Dentate nucleus; GPe=Globus pallidus, external segment; IO=Inferior olive; MG=Molecular & granular layers; PC=Purkinjee cells; PU=Putamen; RN=Red nucleus; SNpc=Substantia nigra pars compacta; SNpr= Substantia nigra pars reticulata; STN=Sub-thalamic nucleus. *Adapted and compiled from several sources (Gusella and MacDonald, 2000; Nakamura et al., 2001; Zhang et al., 2002; Rudnicki and Margolis, 2003; Scheel et al., 2003; Tarlac and Storey, 2003; van Roon-Mom et al., 2005).*

The common features in these disorders imply that a polyglutamine expansion above a certain threshold confers a gain of function on a protein, regardless of its normal cellular function. It has been shown that insertion of a 146 CAG repeat stretch into exon 3 of murine hypoxanthine phosphoribosyltransferase (HPRT), a protein unrelated to identified repeat expansion diseases, results in a delayed onset, progressive neurological phenotype, accompanied by neuronal intranuclear inclusions (Ordway et al., 1997). This rather eloquently demonstrates that polyglutamine expansion causes neurological dysfunction regardless of the context of the protein which it lies in. Certainly, the context of the protein may have an effect on the nuances between these diseases – region of affected neurons (Figure 2), disruption of normal function of protein etc. For example, in SBMA, the polyglutamine expansion lies within the androgen receptor (AR) and accompanying motor dysfunction are a range of testosterone-related dysfunctions – muscle wasting, gynecomastia and testicular atrophy.

1.1.5 Protein aggregation in HD and other polyglutamine expansion diseases

One of the pathological hallmarks of HD is the presence of insoluble, proteinaceous aggregates present in both the nucleus and neurites of affected neurons in the cortex and striatum, termed neuronal intranuclear inclusions (NIIs) and dystrophic neurite inclusions (DNIs), respectively (Davies et al., 1997; DiFiglia et al., 1997). NIIs and DNIs can be visualised at the electron microscopic level – in fact nuclear inclusions

were first noted in studies on HD tissue as early as 1979 (Roizin et al., 1979). Typically, NIIs are non membrane-bound circular structures that have a pale, granular appearance at the ultrastructural level, are on average $1.65 (\pm 0.05) \mu\text{m}$ in diameter and occupy approximately 10-20% of the nuclear area (Davies et al., 1997). DNIs are also non membrane-bound structures that tend to be slightly ovoid in shape with a length of between $3.5\text{-}12\mu\text{m}$. In adult-onset HD, DNIs are much more frequent than NII's, and in juvenile-onset HD, this trend is reversed (DiFiglia et al., 1997). These inclusions can be visualised by immunohistochemical staining using antibodies raised against either huntingtin or ubiquitin (see 1.2.1). However, analysis of both HD brains and a transgenic mouse model of HD (see 1.1.7) has shown that DNIs and NIIs can only be detected with antibodies raised against the N-terminal portion (and not C-terminal) of huntingtin, suggesting that inclusions are made up of N-terminal fragments (DiFiglia et al., 1997; Sieradzan et al., 1999). Further evidence comes from the work of Lunkes *et al.*, who used a panel of antibodies against huntingtin to ascertain what length of huntingtin fragments were present in inclusions in HD brains. They showed that NIIs are primarily made up of N-terminal fragments of huntingtin and that whilst the DNIs are also made up of N-terminal fragments, some were slightly larger than those found in NIIs (Lunkes et al., 2002). In spite of this, C-terminal huntingtin antibodies still have not been shown to label inclusions in HD (Stephen Davies, UCL, UK, personal communication).

It has been suggested that some of the cellular dysfunction in HD results from proteins which are sequestered into aggregates, therefore unable to perform their normal

cellular functions. A wide variety of proteins have been shown to be recruited to polyglutamine inclusions including chaperones (see 1.3), proteasome components (see 1.2) and transcription factors, such as TBP (van Roon-Mom et al., 2002) and CBP (McCampbell et al., 2000).

1.1.6 Mechanisms of protein aggregation in polyglutamine disorders

There are two main mechanisms which have been suggested to explain how expanded polyglutamine-containing proteins aggregate – hydrogen bonding by polar zipper formation and covalent cross-linking by transglutamination.

In 1993, Howard Green postulated that transglutaminase, an enzyme expressed in brain and other tissues, catalyses the formation of specific isopeptide bonds (ϵ -(γ -glutamyl) lysine crosslinks) between glutamine and lysine residue in side chains of adjacent proteins (Green, 1993). Huntingtin has been shown to be a substrate of transglutaminase *in vitro* and additionally, that longer polyglutamine stretches produce polymers at a higher rate (Kahlem et al., 1998). One study showed that transglutaminase selectively co-immunoprecipitates and localises with truncated, but not full length huntingtin, and that it modifies proteins associated with huntingtin, but not huntingtin itself. The authors suggest that after proteolytic processing of huntingtin, transglutaminase may be involved in aggregation (Chun et al., 2001). The link between short huntingtin fragments and increased *in vitro* aggregation caused by

transglutaminase (when compared to larger fragments) has also been demonstrated (Karpuj et al., 1999). Whilst there is limited evidence to suggest that aggregates in HD brains are caused by transglutamination, studies have shown that there is an increase in transglutaminase in HD brains (Karpuj et al., 1999; Lesort et al., 1999) and that HD cerebrospinal fluid has a 3-fold increase in ϵ -(γ -glutamyl) lysine (Jeitner et al., 2001).

In 1994, based on the properties of a synthesized polyglutamine containing peptide, Max Perutz suggested that glutamine repeats could function as “polar zippers”, by hydrogen bonding main chain and side chain amides to form tightly linked β -sheets (Perutz et al., 1994). However, support for this method of aggregation is far from conclusive and often conflicting. In one study, purified GST-fused huntingtin proteins containing a variety of disease-length polyglutamine tracts (51, 83 and 122 glutamines), but not proteins containing shorter polyglutamine tracts (20 and 30 glutamines), were found to aggregate *in vitro*, but only after proteolytic cleavage of the GST domain. As purified proteins were used in these preparations and electron microscopic analysis showed the presence of fibrils, the authors concluded that huntingtin aggregates are likely to form amyloid-like structures *in vivo* (Scherzinger et al., 1997). A problem with this theory is that small 10 glutamine tract proteins have also been shown to oligomerize *in vitro* (Stott et al., 1995), yet polymerized huntingtin aggregates are not detected in the normal population (ie. huntingtin with tracts of 35 glutamines or less). In HD post-mortem tissue, Congo red (an amyloidophilic stain) stained green birefringent inclusions have been detected, although in smaller numbers than ubiquitin-positive inclusions (Huang et al., 1998; McGowan et al., 2000),

showing that this may occur in polyglutamine diseases, but may not be the main mechanism for aggregation. However, another study failed to Congo red stain any inclusions in HD post-mortem tissue (Karpuj et al., 1999). A relatively recent paper described several species of mutant huntingtin-GST structures (including spherical, annular, amorphous and fibrillar) with both spherical and annular structure formation attenuated by Hsp70 and Hsp40; the authors concluded proposed two models of fibril formation. In one, pathways that encourage spherical, annular and amorphous structures essentially competed with pathways that promoted fibril formation. In the other, spherical oligomers were prerequisites to fibril formation and annular and amorphous were metastable by-products that compete with pathways promoting fibril formation (Wacker et al., 2004). However, these experiments were performed *in vitro* and it remains to be seen whether these structures form *in vivo*.

It remains to be seen whether either of these hypotheses regarding polyglutamine aggregation turn out to be correct. What is clear, however, is that proteins with expanded polyglutamine stretches adopt novel conformations which result in protein aggregation. Typically, the fate of misfolded proteins in a cell may go down two possible routes: either corrective folding, for example through the actions of chaperones (see 1.3), or degradation, the main mechanism of which being the ubiquitin-proteasome system (see 1.2).

1.1.7 The R6/2 model of HD

The identification of the relevant genes in HD and other polyglutamine disorders prompted the generation of several murine models, which serve to act as powerful tools for investigating the neurobiology of these diseases. Although several murine models of HD exist, including various knock-in, YAC or BAC approaches, without doubt, the most established and well characterised murine model remains the R6/2 model. This transgenic model was created by inserting a 2kb fragment encoding exon 1 of human huntingtin protein, containing approximately ~145 polyglutamine repeats, and the human huntingtin promotor (Figure 3). This model exhibits a progressive neurological phenotype that recapitulates many of the features of HD, including resting tremor, movements akin to chorea and stereotypic involuntary movements. The onset of these motor disturbances is usually around 8-9 weeks of age, and death usually occurs from 13 weeks old onwards (Mangiarini et al., 1996). Depending on the tasks assessed, cognitive decline can be detected in the R6/2 mice as early as 3.5 weeks postnatally (Lione et al., 1999). Furthermore, R6/2 mice exhibit decreased body weight, with decreases of 30-40% when compared to litter-mate controls, and on a gross neuropathological level, R6/2 brains weigh 20% less (see Figure 4). Detailed neuropathological studies have been carried out on R6/2 brains with Nissl staining revealing no abnormal brain architecture, and GFAP (glial fibrillary acidic protein) and F4/80 immunohistochemistry revealing no reactive astrocytosis (Mangiarini et al., 1996). Immunohistochemical analysis, using antibodies raised against either ubiquitin

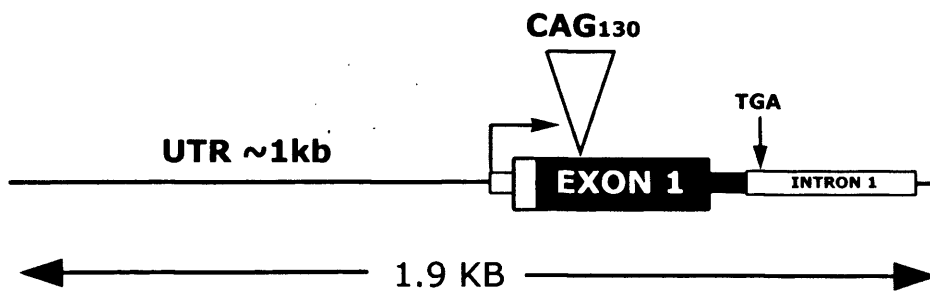


Figure 3: Construct of the transgene in the R6/2 line. R6/2 mice express exon 1 of human Huntingtin protein (under the control of the human Huntingtin promoter) with a polymorphic polyglutamine stretch of ~ 130-150 repeats. (*Picture by L. J. Bannister, UCL; adapted from Mangiarini et al., 1996*)

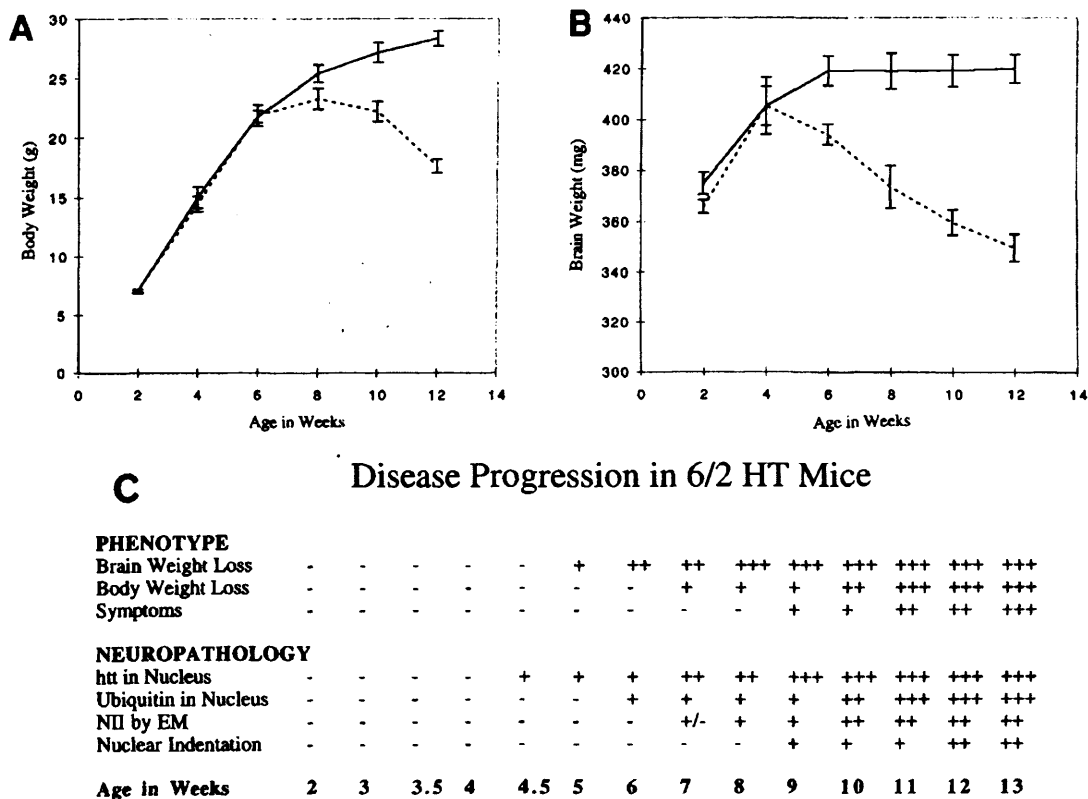


Figure 4: An overview of the phenotype and neuropathology in the R6/2 mouse. The progressive decreases in (A) body and (B) brain weight correlates with (C) neuropathological changes in R6/2 mice. Initially huntingtin is present in the nucleus at ~4.5 weeks and is then ubiquitinated at 6 weeks. This immunohistochemical detection of NIIs precedes their detection by ultrastructural analysis. Dotted and continuous lines in (A) and (B) represent R6/2 and LMC mice, respectively. Taken from Davies et al. (1997).

or the N-terminus of Huntingtin, detected the presence of NIIs (Davies et al., 1997) and DNIs (DiFiglia et al., 1997) in R6/2 brains as early as 4 weeks of age, which precedes the motor symptoms. It is worth mentioning that although retrospective literature searches reveal that NIIs were noted in ultrastructural studies in HD brains as early as 1979 (Roizin et al., 1979), it was their identification in R6/2 brains that led to their subsequent detection and status as a pathological hallmark of HD in human tissue (DiFiglia et al., 1997). This emphasises the relevance of this model in producing findings that relate to polyglutamine disease in humans. Additionally, in a recent publication studying the chronology of behavioural and neuropathological changes in R6/2 mice (Figure 4), the authors concluded that this model very closely resembles many key aspects of human HD (Stack et al., 2005).

1.2 The Ubiquitin-Proteasome System (UPS)

The levels of proteins in a cell are dictated by the rates of protein synthesis and degradation. The main methods of protein degradation in a cell are either lysosomal degradation, macroautophagy or via the ubiquitin-proteasome system. Whilst there is evidence to suggest that both lysosomal degradation and macroautophagy have roles in the clearance of misfolded proteins in neurodegenerative disease (Qin et al., 2003; Ravikumar et al., 2005), this thesis is concerned with the role of the UPS in HD.

The UPS is a highly conserved mechanism of degradation of both normal and misfolded proteins in eukaryotic cells. The proteasome complex is thought to constitute as much as 1% of eukaryotic cellular protein (Hershko and Ciechanover, 1998). It has been suggested that 80-90% of cellular protein degradation is attributable to the proteasome, with the lysosome responsible for the remainder (Rock et al., 1994). Components of the ubiquitin-proteasome system have been implicated in cellular functions as diverse as regulation of translation, activation of transcription factors (eg. NF- κ B) and kinases, cell-cycle control, DNA repair, endosomal transport and labelling of membrane proteins for degradation in lysosomes (Weissman, 2001; Klimaschewski, 2003). With such a variety of important cellular functions it is, perhaps, not surprising that this system has been implicated in human disorders from cancer to neurodegenerative disease.

In eukaryotic cells, proteasomes are found distributed in both the nucleus and cytoplasm, although the levels in either compartment vary with cell type. In the cytoplasm, proteasomes are typically concentrated on the surface of the endoplasmic reticulum and cytoskeletal networks and in the nucleus proteasomes are found distributed throughout the nucleoplasm (excluding the nucleolus), occasionally forming multiple focal points once again, depending on cell type. Generally, in CNS neurons, immunostaining with antibodies against proteasome subunits seems to label nuclei much more intensely than the cytoplasm (Wojcik and DeMartino, 2003). However, certain proteasome subunits are expressed at very low levels in the brain, such as immunoproteasome subunits and 11s β (see 1.2.2)(Rechsteiner et al., 2000),

which effectively can alter the “type”, and therefore proteolytic profile (see 1.2.4), of proteasomes present in differing tissues (Noda et al., 2000).

1.2.1 An overview of the ubiquitin proteasome pathway

Unlike proteases compartmentalized in lysosomes, the proteasome is widespread throughout the cell and, as such, requires a highly specific and regulated mechanism of selecting proteins for degradation. This is achieved by “tagging” target proteins with polyubiquitin chains which are subsequently recognised by the proteasome and then degraded. Ubiquitin is a small 8.6 kDa protein that covalently binds to lysine residues on target proteins via an enzymatic cascade. Initially, a ubiquitin-activating enzyme (E1) binds ubiquitin in an ATP-dependent manner. The ubiquitin molecule is then transferred to a ubiquitin conjugating enzyme (E2) which subsequently catalyses its transfer to the ubiquitin-ligating enzyme (E3)-bound target protein. Based upon the presence of certain motifs, E3 enzymes can be classed as HECT (Homologous to the E6-AP Carboxyl Terminus) or RING finger ligases. RING finger ligases catalyse the transfer of ubiquitin directly from the E2 enzyme to the substrate, whilst HECT E3 ligases bind ubiquitin from E2 enzymes and then transfer it to the substrate. Through sequential addition of further ubiquitin molecules a polyubiquitin chain is generated. Lys-48 polyubiquitinated proteins (see below) are then targeted and recognised by the proteasome and degraded into smaller peptides. Additionally, deubiquitinating enzymes coordinate with this process to remove ubiquitin molecules for recycling

(Figure 5) (Weissman, 2001; Ciechanover and Brundin, 2003). It should be mentioned at this point that there are several types of polyubiquitin chain; there are several lysine residues in the ubiquitin protein (Lys-6, Lys-11, Lys-27, Lys-29, Lys-33, Lys-48, or Lys-63) and the function of polyubiquitin chains are different depending on which ubiquitin lysine residue the Gly-76 of subsequent ubiquitins in the chain binds to (Voges *et al.*, 1999). For example, whilst Lys-48 polyubiquitinated chains are known to signal proteasomal degradation, Lys-11 polyubiquitin residues have also been shown to signal proteasomal degradation but only *in vitro* and Lys-63 chains can signal several pathways, including protein trafficking and autophagy (Pickart & Fushman, 2004; Tan *et al.*, 2007).

1.2.2 Structure of the Proteasome

The central component of the UPS is a multisubunit proteolytic complex referred to as the 20S core particle. The 20S complex is made up of four stacked heptameric rings which form a cylindrical shape with a central “pore” channel. The identical two outer rings are each composed of seven α -subunits (α_{1-7}), whilst the identical inner two rings are each made up of seven β -subunits (β_{1-7}) (Figure 6)(Bochtler *et al.*, 1999). There are three main proteolytic activities of the mammalian 20S core particle: chymotrypsin-like, trypsin-like and peptidylglutamyl peptide hydrolysing (PGPH or caspase-like)

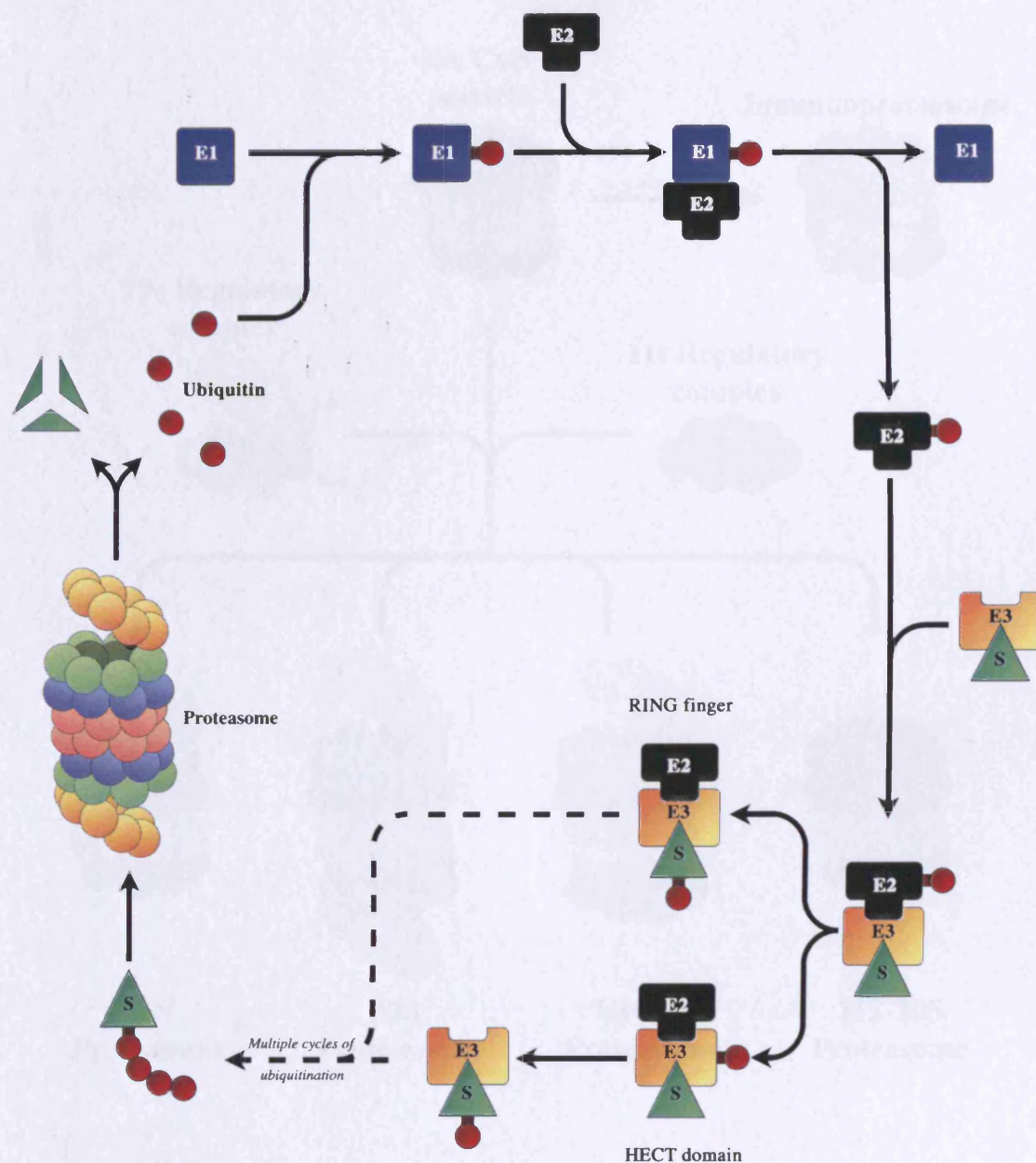


Figure 5: An overview of the Ubiquitin-Proteasome System. Schematic illustrating the process of ubiquitination and subsequent degradation of proteins. Ubiquitin is first activated by E1 enzymes and then transferred to E2 enzymes. E3 enzymes then catalyse the transfer of ubiquitin either directly (in the case of RING finger E3s) or indirectly (in the case of HECT domain E3s) to the bound substrate (S). After multiple cycles of ubiquitination, a polyubiquitin chain is generated signalling the degradation of the substrate by the proteasome into small peptides and the recycling of ubiquitin molecules via deubiquitination. *Adapted from Weissman (2001) and Ciechanover & Brundin (2003).*

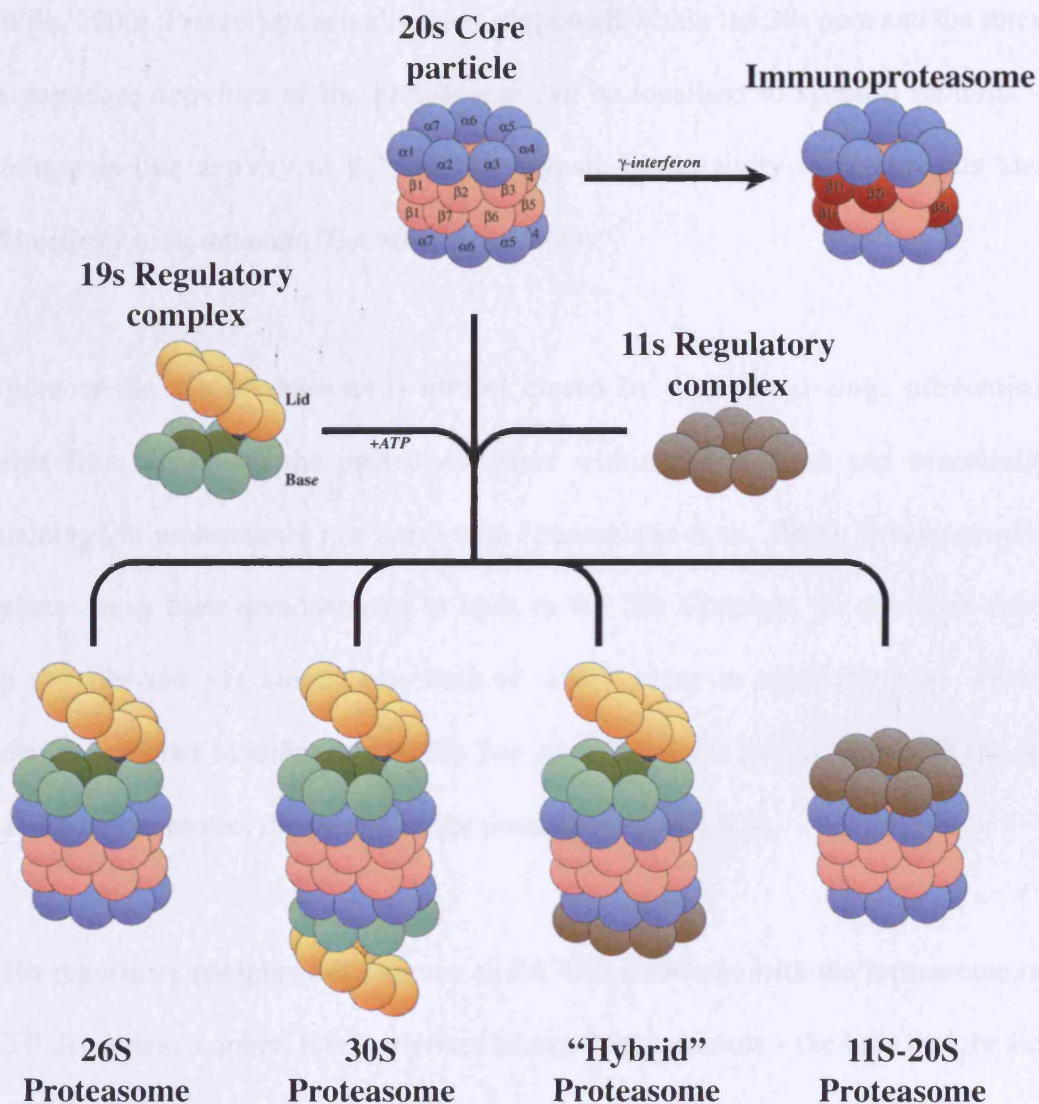


Figure 6: An overview of proteasome structures and variations. 20s core particles are composed of 2 outer heptameric α -rings and 2 inner heptameric β -rings. Upon γ -interferon stimulation, immunoproteasomes are formed, where the catalytic subunits $\beta 1$, $\beta 2$ and $\beta 5$ are replaced by $\beta 1i$, $\beta 2i$ and $\beta 5i$. Both 19s and 11s regulatory complexes can bind (alone or in combination) to the α -ring of the 20s core particle to activate and alter the proteolytic profile of the proteasome. Adapted from Ferrell et al. (2000) and Cascio et al. (2002).

which cleave after hydrophobic, basic and acidic amino acids, respectively (Orlowski and Wilk, 2000). Proteolysis actually takes place well within the 20s pore and the three main peptidase activities of the proteasome can be localised to specific subunits – chymotrypsin-like activity to β_1 -subunits, trypsin-like activity to β_2 -subunits and PGPH activity to β_5 -subunits (Bochtler et al., 1999).

The pore of the 20s proteasome is almost closed by the tight α -ring, preventing proteins from accessing the proteolytic sites within the channel and essentially maintaining 20s proteasomes in a latent state (Baumeister et al., 1998). Several protein complexes have been demonstrated to bind to the 20s complex, the principal ones being the 19s and 11s complexes, both of which serve to open the pore. These complexes can bind to either end of the 20s proteasome via interactions with the α -ring and alter the proteolytic profile of the proteasome (see 1.2.4).

The 19s regulatory complex (also known as PA700) associates with the proteasome in an ATP-dependent manner. It is comprised of two subcomplexes – the base and the lid (Glickman et al., 1998). The base is composed of 6 ATPase (Rpt1-6)* and 3 non-ATPase (Rpn1, 2 & 10) subunits and opens the proteasomal pore when it binds to the 20s α -ring (Ferrell et al., 2000)(Figure 6). Additionally, the base subcomplex has been shown to have chaperone-like activity *in vitro* and may serve to unfold the targeted protein and translocate it into the pore (Braun et al., 1999). The lid is comprised of 8 non-ATPase subunits (Rpn 3, 5, 6, 7, 8, 9, 11 & 12) and is necessary for deubiquitination (Ferrell et al., 2000). Specific functions have been mapped to

individual subunits within the proteasome. For example, Rpn10 contains polyubiquitin binding sites and is thought to target polubiquitinated substrates to the proteasome (Young et al., 1998) as does Rpt5 (Lam et al., 2002). Additionally, the lid subunit, Rpn11, is thought to be responsible for deubiquitination of polyubiquitinated substrates (Verma et al., 2002).

** - The proteasome subunits are here referred to by their well-known yeast nomenclature to avoid confusion. However, the mammalian nomenclature can be found in the appendix.*

The 11s regulatory complex (also known as PA28 or 11sREG) is a heptameric ring that binds to the 20s α -subunits in a similar manner to the 19s complex. The 11s complex is heteromeric, comprised of two distinct subunits (sharing ~50% homology) termed 11s α and 11s β (Ahn et al., 1995). Another protein sharing significant sequence homology with 11s α/β , has also been shown to activate the proteasome and was subsequently named 11sy. 11sy is thought to form homomeric rings (Realini et al., 1997; Tanahashi et al., 1997). 11s α and β , and to a lesser extent 11sy, have been shown to be induced by interferon- γ (IFN- γ) (Rechsteiner et al., 2000).

Various types of proteasomes can be visualised by incubation of proteasome complexes and subsequent visualisation by negative staining electron microscopy. This *in vitro* method reveals the possible existence of several different species of proteasome – 20s proteasome, singly-capped (19s-20s) and doubly-capped (19s-20s-

19s) proteasomes with 19S complexes, singly-capped (11s-20s) and doubly-capped (11s-20s-PA28) proteasomes with 11s complexes as well as a hybrid proteasome with a 11s and 19s complex bound to either end (19s-20s-11s)(Figure 6) (Cascio et al., 2002).

Additional variations of proteasomes can be achieved as three different 20s subunits have been shown to be induced by IFN- γ . In this situation, the three catalytically active subunits (β 1, β 2 & β 3) are substituted by three “immuno” subunits - β 1i (also known as LMP2), β 2i (also known as MECL-1) and β 5i (also known as LMP7) – which serves to alter the proteolytic profile of the proteasome, by forming *de novo* “immunoproteasomes” (1.2.4; Figure 6).

1.2.3 Proteasome assembly

Much of the work on early stage proteasome assembly comes from archaebacterium and considerably less data comes from mammalian cells. Many of the β -subunits (β 1, β 2, β 5, β 6 & β 7) exist as precursors that undergo limited proteolysis of the propeptide to reveal their active sites during biogenesis. It is thought that the formation of the α -ring is one of the earliest events in 20s proteasome biogenesis. α -rings have been shown to self-assemble using recombinant α -7 to “seed” ring formation (Gerards et al., 1998). Based on studies immunoprecipitating early intermediate stage mouse proteasomes, the α -ring is then bound to β 2, β 3 and β 4 subunits (Nandi et al., 1997).

Subsequent addition of the remaining β -subunits and the binding of proteasome maturation protein (POMP) is required before half-proteasomes dimerize to form a short-lived, inactive but complete “preholoproteasome”. This is thought to interact with the chaperone Hsc70 and concomitantly, propeptide sequences are autolytically cleaved. POMP is then degraded by the newly formed proteasome (Heinemeyer et al., 2004). Two other proteins have been described to play a role in proteasome formation, PAC1 and PAC2 (proteasome assembling chaperone), and are thought to form heterodimers that associate with proteasome precursors and are degraded after 20s formation (Hirano et al., 2005).

1.2.4 Regulation of Proteasome activity

As 20s proteasomes are thought to exist in a latent state (due to channel closure and therefore inability of proteins to access the proteolytic sites within the pore) and are implicated in numerous cellular functions, it is essential that there are a variety of mechanisms in place to regulate its activity. A number of proteins and complexes have been identified (such as 19s, 11s, PA200 and PI31K) which can bind to the 20s proteasome and alter its proteolytic profile (Rechsteiner and Hill, 2005).

19s complexes bind to the 20s α -ring and are thought to open the 20s channel. Studies have shown that the 19s regulatory complex, and subsequent 26s formation, enhances the catalytic activity of the proteasome by approximately 2-3 fold (Hoffman and Rechsteiner, 1994).

Both 11 α / β complexes and 11 γ rings can also bind to the 20s α -ring and alter the proteolytic activity of the 20s core particle. Whilst it has been shown that 11 α / β complexes markedly stimulate all three catalytic activities to a greater extent than 19s regulatory complexes (by as much as 60x depending on the substrate used) (Dubiel et al., 1992; Ma et al., 1992), 11 γ exhibits a different pattern of activation with stimulation of trypsin-like activities and relative inhibition of chymotrypsin-like and PGPH activities (Li et al., 2001; Li and Rechsteiner, 2001).

PA200 is a 200 kDa protein (which also has 160 and 60 kDa variants) that was originally identified from its association with proteasomes in rabbit reticulocyte lysates (Hoffman et al., 1992; Ustrell et al., 2002). PA200 has been shown to stimulate all three catalytic activities of the proteasome, particularly chymotrypsin-like activity (Ustrell et al., 2002), and has been shown to bind to 20s α -subunits and subsequently open the 20s channel (Ortega et al., 2005).

A relatively small 31 kDa protein, PI31K, purified from bovine red blood cells (Chu-Ping et al., 1992) has been shown to inhibit both chymotrypsin-like and PGPH activity, but leave trypsin-like activity relatively unaffected. Further *in vitro* investigations have revealed that PI31K can bind to 20s core particles and compete with both 11s (Zaiss et al., 1999) and 19s regulatory complexes (McCutchen-Maloney et al., 2000), implying that PI31K also binds via the 20s α -subunits.

It has also been shown that under certain conditions, such as stimulation with interferon- γ , β_1 , β_2 and β_5 subunits can be replaced by “immunoproteasome” subunits (LMP2, MECL-1 and LMP7, respectively), which display different proteolytic activities. Immunoproteasomes typically display enhanced trypsin-like and decreased PGPH and chymotrypsin-like activities (Dahlmann et al., 2000).

Other proteins, such as valosin-containing protein (VCP or p97), could indirectly affect the rate of proteasomal breakdown in a cell. VCP is an abundant 97 kDa protein that binds to both polyubiquitin chains and components of the 26s proteasome. It is thought to act as a shuttling factor and has been demonstrated to be involved in the targeting of polyubiquitinated substrates to the proteasome (Dai et al., 1998). Loss of VCP function has been shown to result in a build up of ubiquitinated proteins (Dai and Li, 2001). Interestingly, VCP has been shown to be present, with Dorfin (an E3 ligase with which it interacts), in ubiquitinated aggregates from post mortem Parkinson’s disease and amyotrophic lateral sclerosis (ALS) tissue and has been suggested to play a role in their formation (Ishigaki et al., 2004).

1.2.5 The proteasome in HD and other polyglutamine disorders

The accumulation of insoluble, ubiquitinated, mutant protein-containing aggregates in polyglutamine diseases strongly favours the implication that the cell is unable to fully degrade these novel proteins. As NIIs are immunopositive for antibodies against

ubiquitin, it seems unlikely that there is a perturbation of the enzymatic mechanisms involving ubiquitination. It has been postulated that proteins with expanded polyglutamine tracts may undergo impaired cleavage, accumulate within the central proteolytic chamber of the proteasome and inactivate it (Goellner and Rechsteiner, 2003).

As NIIs and DNIs in HD have been shown to contain both huntingtin protein and ubiquitin, it has been assumed that it is the huntingtin protein within inclusions that is ubiquitinated. As a number of proteins are present in aggregates, it is possible that proteins other than mutant huntingtin are ubiquitinated. However, an *in vitro* study has shown that expression of a truncated huntingtin protein (1-540 amino acids of huntingtin including 44 glutamines) interacts with a ubiquitin-conjugating enzyme, hE2-25K, in the yeast two-hybrid system. Furthermore, huntingtin is a target for ubiquitination in transformed lymphoblasts derived from a patient heterozygous for HD (Kalchman et al., 1996).

Studies on transfected cells have yielded conflicting reports as to whether polyglutamine containing proteins can (Michalik and Van Broeckhoven, 2004) or cannot (Holmberg et al., 2004; Venkatraman et al., 2004) be degraded by the proteasome. In a conditional mouse model of HD, reduced numbers of inclusions were detected (in a proteasome-dependent manner) when expression of the transgene was suppressed, indicating that *in vivo*, polyglutamine containing aggregates can be

degraded after formation and that this occurs via the proteasome (Martin-Aparicio et al., 2001).

Equally unclear is whether expanded polyglutamine stretches actually inhibit the proteasome or not. Studies from transfected cells expressing truncated N-terminal huntingtin (Jana et al., 2001; Waelter et al., 2001; Rangone et al., 2005) and aggregates of polyglutamine containing proteins (Bence et al., 2001) have resulted in varying degrees of proteasomal impairment. However, *in vivo* studies have produced inconsistent results. One study measuring chymotrypsin and PGPH proteolysis in HD patient brains and fibroblasts, found that both activities were decreased (Seo et al., 2004). However, this study measured total proteolysis (both proteasomal and non-proteasomal protease) and did not measure trypsin peptidase activity. A recent paper has underlined the importance of all the three main proteolytic activities of the proteasome being assayed to ascertain a thorough view of proteasome function (Kisselev and Goldberg, 2005). In another study, where all three peptidase activities were assayed in the HD94 conditional mouse model of HD, selective increases were demonstrated in trypsin and chymotrypsin like activity. This was attributed to increased expression of immunoproteasome subunits LMP2 and LMP7, which were shown to be present in very few aggregates in the HD94 cortex (Diaz-Hernandez et al., 2003).

1.2.6 Ubiquitin-like proteins

Subsequent to the discovery of ubiquitin, a family of small ubiquitin-related proteins have been identified called ubiquitin-like proteins (UBLs). These proteins are categorised as UBLs based upon their tertiary structure – the presence of a ubiquitin superfold or β -grasp fold – and not upon their primary structure, although some UBLs do share significant sequence homology with one another (Mayer et al., 1998; Hochstrasser, 2000). UBLs bind to substrate proteins through a series of E1, E2 and E3 enzymes in a similar manner to the prototype UBL, ubiquitin, although only a few E3 enzymes have been identified for non-ubiquitin UBLs. Additionally, as lysine side chains represent common binding targets for many UBLs, their binding can often be viewed as competitive. Attachment of various UBLs have been shown to affect functions as diverse as degradation, transcription, DNA repair, signal transduction, autophagy and cell-cycle control (Kerscher et al., 2006). Indeed, the number of UBLs, enzymes involved and the various functions implicated would mean that this mechanism rivals other post-translational modifications such as phosphorylation in terms of significance to the cell. Whilst many UBLs have been discovered (a trend which looks likely to continue), there are certain UBLs, such as SUMO, NEDD8 and ubiquilin (contains a UBL sequence within the larger protein sequence) that either have relatively well characterised or are pertinent to this study and therefore only these shall be discussed here.

There are 4 identified members of the SUMO (Small ubiquitin-like modifier; also known as sentrin) family: SUMO1, SUMO2, SUMO3 and relatively recently, SUMO4 (Muller et al., 2001; Guo et al., 2004). In humans, mSUMO1, a 101 amino acid protein shares ~50% sequence homology with the closely related SUMO2/3 (Muller et al., 2001) and ~18% with ubiquitin itself (Bayer et al., 1998). Unlike ubiquitin, SUMO1 is unable to form polypeptide chains, whereas SUMO2/3 can readily form polySUMO chains, implying distinct functionality (Tatham et al., 2001). SUMOylation has been implicated in functions such as nuclear transport, signal transduction and cell-cycle control (Muller et al., 2001). Additionally, SUMO has also been shown to competitively bind to lysine residues on NF κ B α with ubiquitin, demonstrating that SUMOylation regulates the degradation of proteasomal targets (Desterro et al., 1998). As well as the previous example, SUMO has been shown to regulate the ubiquitination and therefore stability of other proteins (Buschmann et al., 2000). Furthermore, it has been demonstrated that there are increases in levels of SUMO2/3 conjugates in response to cellular stressors, such as oxidation and heat (Saitoh and Hinchey, 2000).

Out of all the UBLs identified, NEDD8 (also known as RUB1) is the protein that has the most similar primary sequence to ubiquitin. Whilst not acting as a direct signal for proteasomal degradation, NEDD8's identified functions centre on it's ability to regulate ubiquitin ligating enzymes (E3). Binding of NEDD8 to sites on target E3s prevents binding of E3 inhibitors (Welchman et al., 2005). This can serve to regulate downstream ubiquitination, and therefore degradation.

Ubiquilin is a UBL that has been shown to interact with a variety of seemingly unrelated proteins and is of particular interest here because of two key facets. Firstly, ubiquilin proteins contain domains that allow them to bind to both polyubiquitin chains and key subunits of the 19S proteasome regulatory complex. These binding attributes imply that ubiquilin may act as shuttling protein to mediate the delivery of polyubiquitinated proteins to the proteasome (Ko et al., 2004). Secondly, and somewhat perversely, ubiquilin has been shown to decrease the degradation of certain proteins and also their ubiquitination. This is thought to be through competitive binding which would essentially block ubiquitin chain elongation (Massey et al., 2004). Like SUMO proteins, ubiquilin can compete with ubiquitin for binding and therefore can alter the degradation of proteins.

1.2.7 Ubiquitin-like proteins in polyglutamine expansions diseases

Out of all of the UBLs, perhaps the most ones most implicated in neurodegeneration are the SUMO family. SUMO1 immunoreactive NIIs have been described in DRPLA patients and cellular models (Terashima et al., 2002). Furthermore, increased levels of high molecular weight SUMO1-conjugates have been described in transgenic mice expressing mutant ataxin-1 with an expanded polyglutamine tract as well as increased SUMO-1 immunoreactivity in brains of HD, DRPLA, SCA1 and MJD patients (Ueda et al., 2002). Indeed, the polyglutamine containing protein, ataxin-1, has been shown to be a target of SUMOylation, although increasing the polyglutamine tract length has

been shown to decrease SUMO-1 binding (Riley et al., 2005). Overexpression of a mutant form of SUMO-1 activating enzyme in a *Drosophila* model of SBMA enhances polyglutamine induced degeneration (Chan et al., 2002). Additionally, and perhaps more pertinent to this study, SUMOylation of mutant huntingtin exon 1 fragments in *Drosophila* model of HD exacerbated neurodegeneration, which the authors suggested was not simply due to competitive binding with ubiquitin for lysine residues (Steffan et al., 2004). This, taken together with a study that showed that SUMO-1 deletion or overexpression ameliorates or enhances NII frequency and cell death implies that SUMO-1 may act to accelerate polyglutamine pathology (Terashima et al., 2002). Interestingly, in PC12 cells, inhibition of the proteasome resulted in the appearance of SUMO-1 immunopositive nuclear inclusions (Pountney et al., 2003).

There is little data concerning NEDD8 in the pathology of polyglutamine disorders. However, in one study examining SBMA, HeLa cells transfected with polyglutamine expanded androgen receptor produced aggregates than were immunopositive for antibodies raised against NEDD8 (Stenoien et al., 1999).

To date, there are few studies examining the UBL ubiquitin in polyglutamine expansion diseases. In one, N-terminal Huntingtin with 150 glutamine repeats was expressed in Neuro2A cells and the subsequent nuclear aggregates produced were isolated and shown to contain ubiquitin. This was also confirmed in double-labelled immunofluorescence studies in R6/2 mice, although it was unclear whether DNIs also stained immunopositive (Doi et al., 2004). Another recent study showed that

overexpression of ubiquilin in HeLa cells and primary neurons reduced aggregation and cell death induced by overexpression of GFP-tagged Huntingtin (with 74 glutamine repeats) (Wang et al., 2006).

1.3 The chaperone family of proteins

The molecular chaperone (heat shock) family of proteins are a group of proteins that were originally identified based on their appearance during cellular stress and the subsequent discovery of their role in preventing protein aggregation and misfolding by promoting their correct conformation. Chaperones are an abundant and highly conserved family of cellular proteins and are widespread throughout the eukaryotic cell (Hartl, 1996). They can broadly be classified into four subfamilies: the Hsp70 family, the Hsp90 family, the small heat shock proteins and the chaperonins.

The Hsp70 proteins include the constitutive Hsc70 and inducible Hsp70 homologues as well as the Hsp40 family of co-chaperones (which serve to regulate Hsp70 function). The action of Hsp70 proteins is ATP-dependent, and can be regulated by the Hsp40 proteins (and other proteins, such as BAG-1). Hsp70 proteins have been shown to be involved in refolding after translation and during cellular stress (Hartl, 1996). Interestingly, two proteins, CHIP (C-terminal of Hsp-70 interacting protein) and BAG-1 (Bcl-2 associated gene product 1) have been shown to act as a link between the chaperone system and the UPS.

The cytoplasmic Hsp90 family of proteins, also ATP-dependent, are generally thought to be involved in the regulation of signal transduction networks (Pratt, 1997). Hsp90 proteins are interesting here because they have been shown to be involved in the regulation (suppression) of chymotrypsin-like and PGPH activities of the proteasome (Lu et al., 2001).

The role of the ATP-independent small heat shock proteins (sHsp's), which include Hsp27 and α B-crystallin, is not well understood, although they have an established role in preventing aggregation formation under cell stress. Typically, they exist as an active dimer and have been known to function alongside other chaperones (eg. Hsp70).

The chaperonin family (eg. Hsp60) seems to function slightly differently from the other chaperones in that they form a barrel-like structure as a prerequisite to activity. Chaperonins are, for example, involved in the folding of the cytoskeletal protein actin (Martin and Hartl, 1997).

1.3.1 Chaperones in other polyglutamine expansion diseases

There is a breadth of data to suggest that chaperones are involved in the pathology of polyglutamine diseases. Several studies have detailed the co-localisation of chaperones



(particularly Hsp70 and Hsp40) with aggregates in models of polyglutamine diseases (Cummings et al., 1998; Stenoien et al., 1999; Warrick et al., 1999; Jana et al., 2000).

Furthermore, decreases of Hsp70 and Hsp27 have been described in transformed lymphoblastoid cells from SCA-7 patients (Tsai et al., 2005). It is possible that either sequestration in aggregates or a reduction in chaperone levels could contribute to the formation of aggregates and toxicity of expanded polyglutamine containing proteins.

There is evidence to support this in an *in vitro* model expressing exon 1 of Huntingtin (with 150 glutamines), where reduced numbers of aggregates and decreased toxicity are exhibited when cells are co-transfected with the brain-enriched chaperone, MRJ (Chuang et al., 2002). Other studies have also demonstrated a cell-protective effect of chaperones on polyglutamine-induced pathology including a reduction in aggregation (Warrick et al., 1999; Cummings et al., 2001; Novoselova et al., 2005).

1.4 Aims of the project

This study aims to examine the role of the UPS in the R6/2 mouse line (Mangiarini et al., 1996), an established model of HD and attempts to shed light into several key questions regarding the neuropathology in this model: What is the ultrastructure of the aggregates in this model? Is it the huntingtin protein that is ubiquitinated in these mice? What proteasome components / chaperones are recruited to the aggregates and do the NII and dNI differ with respect to what they recruit? And importantly, if

proteasomes are sequestered into aggregates, does this result in loss of function of the proteasome? Do polyubiquitinated aggregates sequester other UPS-associated proteins? Assessing the localisation, function, activity and regulation of the UPS in this model could provide useful insights into the fundamental mechanisms of neuropathology in HD.

CHAPTER 2

Materials and Methods

2.1 Materials

2.1.1 Standard solutions

Primary antibody buffer: 0.002% (w/v) sodium azide, 0.3% (v/v) Triton-X 100, 0.1 M

Tris pH7.4

Phosphate buffer pH7.4: 77 mM Na₂HPO₄, 23 mM NaH₂PO₄, pH7.4

2.1.2 Transgenic mice

All mouse husbandry and experimental procedures were carried out in accordance with UK Home Office regulations and the Animals (Scientific Procedures) Act, 1986. The mice used in this study were either 13 week-old transgenic R6/2 (described previously) or age-matched litter-mate controls (referred to as wild-type or WT herein). R6/2 mice were donated by Professor Gillian Bates (King's College, London) and maintained by backcrossing R6/2 males with (C57BL/6 x CBA) F1 females (Harlan Olac, Bicester, UK). Only female mice were used in this study.

Mice were anaesthetised with an overdose of sodium pentobarbitone (Sagatal, 100 mg/kg, intraperitoneally) and perfused through the left cardiac ventricle with the appropriate fixative / solution.

2.2 Microscopy methods

2.2.1 Preparation of tissue for immunohistochemistry or immunofluorescence

Animals were perfused with 35-50 ml of PLP (2% (w/v) paraformaldehyde / lysine / periodate fixative in phosphate buffer pH7.4). The brains were carefully removed, submersed in PLP for 4-6 hours and transferred to cryoprotectant solution (30% (w/v) sucrose in 0.1 M Tris pH7.4) for 48 hrs at 4 °C. Brains were mounted on a SM2000R sledge microtome (Leica) with Tissue-Tek Oct compound (Miles Laboratories) and frozen with powdered solid CO₂. Sections were cut in the coronal plane (40 µm) and transferred to a dimple tray with 0.1 M Tris pH7.4.

2.2.2 Preparation of tissue for electron microscopy

Animals were perfused with 35-50 ml of EM fixative (4% (w/v) paraformaldehyde, 0.1% (v/v) glutaraldehyde in phosphate buffer pH7.4). The brains were carefully

removed and placed in fresh EM fixative overnight (4 °C). Brains were mounted onto a Series 1000 Vibratome (Agar Scientific) with cyanoacrylate (Superglue) and immersed in 0.1 M phosphate buffer pH7.4. Sections were cut in the coronal plane (200 µm) and transferred to a dimple tray with 0.1 M phosphate buffer pH7.4.

2.2.3 Immunohistochemistry

Sections were incubated, free-floating, in primary antibody diluted in primary antibody buffer (1:200; see below for antibodies used) for 72 hours at 4 °C, washed* and transferred to biotinylated secondary antibody (1:200, diluted in 0.1 M Tris pH7.4; all from Vector) for 90 minutes. Sections were removed, washed* and incubated with ABC complex (Vectastain) in 0.1 M Tris pH7.4 for 90 minutes. Sections were washed* and incubated with DAB developer solution (diaminobenzidine (25 mg / 100 ml), 0.003% (v/v) H₂O₂, 0.1 M Tris pH7.4) until dark brown areas of DAB reaction product were clearly visible. Reactions were stopped by transferring sections to 0.1 M Tris pH7.4. Sections were mounted onto gelatinized glass slides, air-dried overnight and dehydrated in a series of ethanol concentrations (5 minutes each; 70%, 80%, 90%, 95%, 100% (v/v) x 2). Slides were cleared in Histoclear (2 x 10 minutes; National Diagnostics), coverslipped with DPX solution and air-dried (24-48 hours). Slides were viewed on a DMR light microscope (Leica) and images captured using a Canon EOS D30 digital camera.

** - All washes (3 x 10 minutes) were performed in 0.1M Tris pH 7.4*

2.2.4 Antibodies for immunohistochemistry

The following proteasome antibodies, used for immunohistochemistry, were all obtained from BIOMOL, UK:

Protein (Yeast nomenclature)	Protein (Mammalian nomenclature)	Antibody Code #	Species raised in
20s α 1,2,3,5,6 & 7	iota, C3, C9, zeta, C2 & C8	PW 8195	M
20s "core"	20s "core"	PW8155	R
20s β 1	Y	PW8140	M
20s β 1i	LMP2	PW8345	R
20s β 1i	LMP2	PW8840	M
20s β 2	Z	PW8145	M
20s β 2i	MECL-1	PW8350	R
20s β 3	C10	PW8130	M
20s β 4	C7	PW8890	R
20s β 5	X	PW8895	R
20s β 5i	LMP7	PW8845	M
20s β 5i	LMP7	PW8355	R
20s β 6	C5	PW9000	R
20s β 7	N3	PW8135	M
19s Rpt1	S7	PW8165	R
19s Rpt1	S7	PW8825	M
19s Rpt2	S4	PW8305	R
19s Rpt3	S6b	PW8175	R
19s Rpt3	S6b	PW8310	R
19s Rpt3	S6b	PW8765	M
19s Rpt4	S10b	PW8220	R
19s Rpt4	S10b	PW8830	M
19s Rpt5	S6a	PW8770	M
19s Rpt6	S8	PW8320	R
19s Rpn2	S1	PW9270	M
19s Rpn6	S9	PW8370	R
19s Rpn7	S10a	PW8225	R
19s Rpn8	S12	PW8180	S
19s Rpn10	S5a	PW9250	M
19s Rpn12	S14	PW8815	R
19s Rpn12	S14	PW8835	M
11s α	PA28 α	PW8185	R
11s β	PA28 β	PW8240	R
11s γ	PA28 γ	PW8190	R

NB: 20s “core” antibody recognises $\alpha 5/\text{zeta}$, $\alpha 7/\text{C8}$, $\beta 1/\text{Y}$, $\beta 5/\text{X}$, $\beta 5\text{i}/\text{LMP7}$ and $\beta 7/\text{N3}$ subunits.

The following antibodies were also used for immunohistochemistry:

BAG (Santa Cruz Biotech., SC-939), CHIP (Abcam, AB2917), E2-25k (BIOMOL, UG9520), Hsp27 (Santa Cruz Biotech., SC-1049), Hsp40 (Santa Cruz Biotech., SC-1801), HDJ-2 / DNAJ (Neomarkers, MS-225-P1ABX), Hsp70 (Santa Cruz Biotech., SC-1060), Hsp70 (Stressgen Biotech., SPA-810), Hsc70 (Santa Cruz Biotech., SC-1059), Hsc70 (Stressgen Biotech., SPA-815), Hsp105 (Santa Cruz Biotech., SC-1804), Huntingtin (EM48) (Chemicon, MAB5374), Huntingtin N-18 (Santa Cruz Biotech., SC-8767), Glutamyl lysine isopeptide bonds (Abcam, AB422), NEDD8 (Santa Cruz Biotech., SC-5480), PI31 (Abcam, AB3893), Polyglutamine (1C2) (Chemicon, MAB1574), POMP (BIOMOL, PW9715), PA200 (Abcam, AB5620), SUMO 1 (Abcam, AB11672), SUMO 2/3 (Abcam, AB3742), Ubiquilin (Abcam, AB3341), Ubiquitin (Dako, Z0458), VCP (Santa Cruz Biotech., SC-20799).

2.2.5 Double-labelled immunofluorescence

Sections were incubated, free-floating, in primary antibodies diluted in primary antibody buffer (see below for concentrations used) for 72 hours at 4 °C, washed* and then transferred to fluorophore-tagged secondary antibodies (1:100 in 0.1 M phosphate buffer pH7.4) for 2 hours away from light. Sections were removed, washed* and mounted onto gelatinized slides, coated with Vectashield mounting medium,

coverslipped and sealed with nail varnish (all in the dark). Slides were stored at 4 °C in the dark until they were viewed on an upright confocal microscope (Leica).

** - All washes (3 x 10 minutes) were performed in 0.1 M phosphate buffer pH7.4*

2.2.6 Antibodies for immunofluorescence

The following primary antibodies were used for double-labelled immunofluorescence:

Target protein	Dilution	Species raised in	Product Number	Manufacturer
Huntingtin (EM48)	1:500	mouse	MAB5374	Chemicon
SUMO 1	1:200	rabbit	AB11672	Abcam
SUMO 2/3	1:200	rabbit	AB3742	Abcam
Ubiquitin	1:1000	rabbit	Z0458	Dako
Ubiquitin (FK2)*	1:1000	mouse	SC-939	BIOMOL

As all combinations of primary antibodies for double-labelled immunofluorescence used one primary antibody raised in rabbit and one in mouse, both anti-rabbit conjugated to FITC and anti-mouse conjugated to TRITC (both raised in donkey; Jackson Immunochemicals) were used as secondary antibodies.

** - FK2 recognises both mono and polyubiquitinated proteins, but not free ubiquitin.*

2.2.7 Electron Microscopy

Sections were osmicated in 1% (v/v) osmium tetroxide (diluted in 0.1 M phosphate buffer, pH7.4) at 4 °C for 1 hour, washed (2 x 10 mins in 0.1 M sodium acetate) and then *en-bloc* stained in 2% (v/v) uranyl acetate (diluted in 0.1M sodium acetate) at 4 °C for 1 hour. Sections were washed in 0.1 M sodium acetate (10 mins) and then in distilled water (5 mins) before dehydration through a graded ethanol series (25%, 50%, 70%, 90%, 100% (v/v) x 4 ; 5-10 mins each). Sections were cleared of alcohol through washes in propylene oxide (4 x 10 mins) and placed into a 1:1 mixture of propylene oxide and araldite resin (10 g DDSA(dodecenyl succinic anhydite), 10 g araldite and 0.8 g plasticizer (dibutyl pathalate)) for 45 minutes. Sections were transferred to fresh araldite resin on a rotator for 24 hours. Sections were then blocked-out by placing between two sheets of Melinex (ICI), weighted down and left overnight at 60 °C. Sections in polymerised resin were superglued onto resin blocks and ultrathin (~70-90 nm) sections were cut using glass knives on a Ultracut microtome (Reichert) and collected on copper-mesh grids. Sections were counter-stained in lead citrate, dried and viewed under a JEOL 1010 transmission electron microscope.

2.3 Protein biochemistry

2.3.1 Preparation of tissue for electrophoresis

Animals were briefly perfused with cold 0.1% (w/v) NaCl with Complete protease inhibitor cocktail tablets (PIC) (Roche Diagnostics GmbH, 1 tablet / 25 ml). The brains were quickly removed and homogenised in 3 ml boiling lysis buffer (1% (w/v) SDS, 1 mM Na_3VO_4 , 10 mM Tris pH7.4 with PIC, 1 tablet / 25 ml)) using a dounce homogeniser. Homogenates were microwaved for 15 seconds and centrifuged (10,000 x g, 15 °C) for 3 minutes to pellet large insoluble material. Supernatants were collected, aliquoted and stored at -80 °C. Total protein concentrations were measured using a modified Lowry assay (DC protein assay, Biorad). Aliquots of two R6/2 and two LMC samples were used for all western blot experiments and equal loading of samples was confirmed through initial western blots using antibodies against γ -tubulin.

2.3.2 SDS-PAGE

Samples were denatured at 95 °C for 3 mins) in 3 x sample buffer (125 mM Tris pH6.8, 15% (v/v) glycerol, 10% (v/v) β -mercaptoethanol, 4% (w/v) SDS, 0.05% (w/v) bromophenol blue). Precast polyacrylamide gels (either 4-15% or 4-20% (Biorad) were loaded into Mini Protean II systems (Biorad) containing cold running buffer (25 mM Tris, 192 mM glycine, 0.1% (w/v) SDS, pH8.8). Samples of total protein (10 or

20 µg) were loaded per lane. Biotinylated protein ladder (0.5 or 1 µl, Cell Signalling Technology, Inc.) was used to act as molecular weight markers. Samples were electrophoresed at 45 mA, 200 V until the tracking dye reached the end of the gel.

2.3.3 Western blotting

Gels were equilibrated in transfer buffer (50 mM Tris, 40 mM glycine, 20% (v/v) methanol) for 1 hour. Proteins were blotted overnight (30 v, 90 mA) onto nitrocellulose membranes (Amersham Pharmacia Biotech.) in ice-cold transfer buffer using a Mini Transblot (Biorad). Membranes were washed (10 mins) in wash buffer (50 mM Tris pH 7.4, 80 mM NaCl, 40 mM glycine, 2 mM CaCl₂, 0.2% (v/v) Igepal CA-630) and then incubated in blocking buffer (5% (w/v) non-fat dried skimmed milk power (eg. Marvel) in wash buffer) for 2 hours. After blocking, membranes were incubated for 1 hour with primary antibodies diluted in blocking buffer. Membranes were washed in wash buffer (3 x 10 minutes) and incubated with HRP-conjugated secondary antibodies (Calbiochem) and HRP-conjugated anti-biotin antibody (1:20,000) diluted in blocking buffer for one hour. Secondary antibodies were used at the following concentrations: anti-mouse (raised in goat), 1:20,000; anti-rabbit (raised in goat), 1:10,000; anti-goat (raised in rabbit), 1:5,000. Membranes were washed in wash buffer (3 x 10 mins), developed using ECL Plus kits (Amersham Pharmacia Biotech) according to manufacturers instructions and exposed onto Hyperfilm ECL (Amersham Pharmacia Biotech.).

2.3.4 Antibodies for western blotting

Target protein	Dilution	Species raised in	Product Number	Manufacturer
20s $\alpha_{1,2,3,5,6,7}$	1:2500	mouse	PW8140	BIOMOL
20s β_1	1:2500	mouse	PW8145	BIOMOL
20s β_2	1:2500	mouse	PW8895	BIOMOL
20s β_5	1:2500	rabbit	PW8195	BIOMOL
BAG	1:250	rabbit	SC-939	Santa Cruz Biotechnology
CHIP	1:750	rabbit	AB2917	Abcam
E2-25k	1:4000	rabbit	UG9520	BIOMOL
Hdj-2	1:250	mouse	MS-225P0	Neomarkers
Hsc-70	1:250	goat	SC-1059	Santa Cruz Biotechnology
Hsp-40	1:250	goat	SC-1801	Santa Cruz Biotechnology
Hsp-70	1:250	goat	SC-1060	Santa Cruz Biotechnology
Huntingtin (EM48)	1:1250	mouse	MAB5374	Chemicon
Huntingtin N-18	1:200	goat	SC-8767	Santa Cruz Biotechnology
Isopeptidase	1:250	mouse	AB422	Abcam
LMP2	1:2000	rabbit	PW8205	BIOMOL
LMP7	1:2000	rabbit	PW8200	BIOMOL
MECL-1	1:2000	rabbit	PW8150	BIOMOL
NEDD8	1:250	goat	SC-5480	Santa Cruz Biotechnology
PA28 α	1:4000	rabbit	PW8185	BIOMOL
PA28 β	1:4000	rabbit	PW8240	BIOMOL
PA28 γ	1:4000	rabbit	PW8190	BIOMOL
PI31	1:500	goat	AB3893	Abcam
Polyglutamine (1C2)	1:4000	mouse	MAB1574	Chemicon
POMP	1:1000	rabbit	PW9715	BIOMOL
PA200	1:2000	rabbit	AB5620	Abcam
SUMO 1	1:2000	rabbit	AB11672	Abcam
SUMO 2/3	1:2000	rabbit	AB3742	Abcam
Ubiquilin	1:750	rabbit	AB3341	Abcam
Ubiquitin	1:5000	rabbit	Z0458	Dako
VCP	1:500	rabbit	SC-20799	Santa Cruz Biotechnology

2.3.5 Coomassie blue staining

To confirm equal lane loading, total protein was Coomassie stained on post-transfer gels. Gels were incubated with staining solution (35% (v/v) methanol, 15% (v/v) glacial acetic acid, 0.1% (w/v) Coomassie brilliant blue R-250 (Biorad)) until bands were visible, then rinsed (changed every 30 minutes) in destaining solution (35% (v/v) methanol, 15% (v/v) Glacial acetic acid) until background was clear. Gels were placed in drying frame (BioDesign Inc.) and air-dried.

2.3.6 Preparation of tissue for immunoprecipitation

Animals were briefly perfused with cold 0.1% (w/v) NaCl with protease inhibitor cocktail tablets (PIC) (1 tablet / 25 ml). The brains were quickly removed and homogenised in 3 ml SIP buffer (0.1 M phosphate buffer, pH7.4, PIC 1 tablet / 25 ml) using a Dounce homogeniser. Lysate protein concentrations were determined using a modified Lowry assay (DC protein assay, Biorad) and samples were diluted with SIP buffer to a concentration of 500 µg / ml.

2.3.7 Immunoprecipitation of ubiquitinated proteins

50 µl of magnetic Dynabeads coupled to protein G (DynaL Biotech) were washed twice in 0.5 ml IP buffer (0.1 M phosphate buffer, pH7.4, 0.01% (v/v) Tween-20) and

resuspended in 50 µl IP buffer. Beads were incubated with FK2 antibody (BIOMOL) for 2 hours at room temperature with gentle mixing on a rotorwheel, washed and resuspended in 50 µl IP buffer. 1 ml of sample homogenate was added to beads and incubated overnight at 4 °C with rotation. Beads were washed 3 times in 1 ml phosphate buffer (pH7.4), resuspended in 20 µl sample buffer, electrophoresed and blotted with 1C2 antibody.

All mixes were performed on a slow rotorwheel. All separation of Dynabeads from solution was performed using a magnet (Dyna Magnetic Particle Concentrator, Dynal Biotech.).

2.4 Proteolysis activity assays

2.4.1 Preparation of tissue for proteolysis assays

This proteolytic activity assay was based upon the methods of Keller *et al.*. Animals were perfused with ice-cold 0.1% (w/v) NaCl. Brains were quickly removed and homogenised in proteolysis assay buffer (5 mM MgCl₂, 5 mM ATP, 0.5 mM DTT, 10 mM Tris pH7.4) using a Dounce homogeniser. Lysate protein concentrations were determined using a modified Lowry assay (DC protein assay, Biorad) and samples were diluted with proteolysis assay buffer to a concentration of 1 µg / µl.

2.4.2 Proteolytic activity assay

SDS is a known activator of the 20s proteasome (Shibatani and Ward, 1995). For proteolysis activity assays in the presence of SDS, detergent was added to give a final concentration of 0.03% (w/v). 250 µl of sample and 2.5 µl of fluorogenic substrate (5 mM in DMSO) were incubated in 96-well plates for 30 minutes at 37°C. Proteolytic activity, as determined by the cleavage of fluorogenic substrate, and subsequent fluorescence generated was measured and recorded (every 30 mins for 4 hours, 37 °C) using a Fluostar Optima fluorimeter connected to a PC running the Optima analysis package (BMG Labtech Ltd.). Parameters (eg. gain of fluorescence, excitation / emission filters) were optimised for samples prior to experiment. All experiments were repeated in triplicate and averaged.

The following fluorogenic substrates were used: Succinyl-Leu-Leu-Val-Tyr-AMC (BIOMOL) was used to measure chymotrypsin-like proteolysis; Boc-Leu-Arg-Arg-AMC (BIOMOL) was used to measure trypsin-like proteolysis; Z-Leu-Leu-Glu-AMC (BIOMOL) was used to measure PGPH-like proteolysis.

2.4.3 Proteasomal and protease activity assay

To differentiate between protease and proteasomal proteolysis, assays were performed with and without proteasomal inhibition. Epoxomicin is the most specific proteasomal

inhibitor currently known and its only identified function is inhibition of the proteasome (Dr. Alexei Kisselev, Dartmouth Medical School, USA, personal communication). Assays were performed as above, except either 2.5 μ l of 2.04 mM epoxomicin (BIOMOL) in DMSO or 2.5 μ l DMSO alone (no inhibition) was added in addition to the fluorogenic substrate. This addition of inhibitor produces a final concentration of 20 μ M epoxomicin, which is sufficient to inhibit chymotrypsin-like, trypsin-like and PGPH-like proteolytic activities of the 20s proteasome. Any activity in the presence of epoxomicin is considered to be non-proteasomal or protease proteolytic activity, and the difference between proteolysis in the presence and absence of epoxomicin (ie. epoximicin-sensitive component) is considered to be proteasomal activity.

2.4.4 Statistics

The unpaired student's *t* test was used to statistically evaluate the data from proteolytic activity assays and was performed both using Microsoft Excel and online (<http://www.physics.csbsju.edu/stats/t-test.html>). Differences were described as statistically significant when *p* values were below 0.05.

CHAPTER 3

Results

3.1 Overview

The initial aim of this project was to understand the nature of the insoluble protein aggregates found in the neurons of R6/2 mice and what role the UPS plays in the neuropathology of this neurodegenerative model. Firstly, electron microscopy and western blot analysis were used to demonstrate that aggregates are generally amorphous structures that are likely to be formed by the process of transglutamination (chapter 3.2.1). Confocal and immunoprecipitation studies were used to demonstrate that co-localisation of huntingtin and ubiquitin immunoreactivity in aggregates was due to direct ubiquitination of mutant huntingtin protein (chapter 3.2.2). To determine whether proteins involved in degradation (20s, 19s and 11s proteasome components) and folding (chaperones) displayed altered localisation in the R6/2 model, detailed immunohistochemical studies were carried out and showed redistribution of many of these proteins to aggregates (chapters 3.2.3-4).

As aggregates were shown to contain ubiquitinated mutant protein and many components of the ubiquitin-proteasome system, experiments were carried out to measure proteolysis in brains of R6/2 mice. These fluorometric-based assays revealed

increases in both chymotrypsin-like and PGPH-like and decreases in trypsin-like proteasomal activities (chapters 3.3.1-2). Additionally, all three activities were found to be decreased in non-proteasomal proteases. To explain the differential proteolytic profile found in R6/2 mice, the individual β -subunits responsible for the chymotrypsin-like, PGPH-like and trypsin-like activities of the proteasome were analysed by western blotting (chapter 3.3.3). The majority of β 1 and β 5 subunits (chymotrypsin-like, PGPH-like) were found to co-sediment with the aggregates, whilst the β 2 subunit, responsible for trypsin-like proteolysis, was shown to be predominantly present in the immature propeptide form.

To try to explain the increases seen in chymotrypsin-like and PGPH-like activities, western blotting was used to analyse levels of proteins known to regulate and alter the activities of the proteasome (chapters 3.4.1-3). No changes were seen in levels of 11s or immunoproteasome subunits, whilst increases were demonstrated in 19s protein levels. PA200 levels appeared increased in R6/2 brains and were shown to relocate to inclusions. Levels of PI31K, an inhibitor of chymotrypsin-like and PGPH-like peptidase activities, were demonstrated to be decreased in R6/2 brains.

Finally, immunohistochemical, confocal and western blotting analyses were used to ascertain the localisation and levels of additional proteins involved in the ubiquitin-proteasome system, such as those involved in ubiquitination and proteasomal maturation (E2(25k) and POMP) or ubiquitin-like proteins (SUMO-1, SUMO-2/3,

ubiquilin and VCP) (chapter 3.5.1-2). E2(25k), POMP and the ubiquitin-like proteins were shown to redistribute and insolubilise with aggregates.

3.2 Molecular composition of aggregates in R6/2 transgenic mice

One of the pathological hallmarks of polyglutamine diseases is the presence of insoluble NIIs, yet relatively little is known about their structure and molecular composition. Therefore, a series of experiments were conducted to further understand the structure and composition of the aggregates found in the R6/2 model.

3.2.1 Aggregates are amorphous structures containing Nε(γ glutamyl) lysine bonds

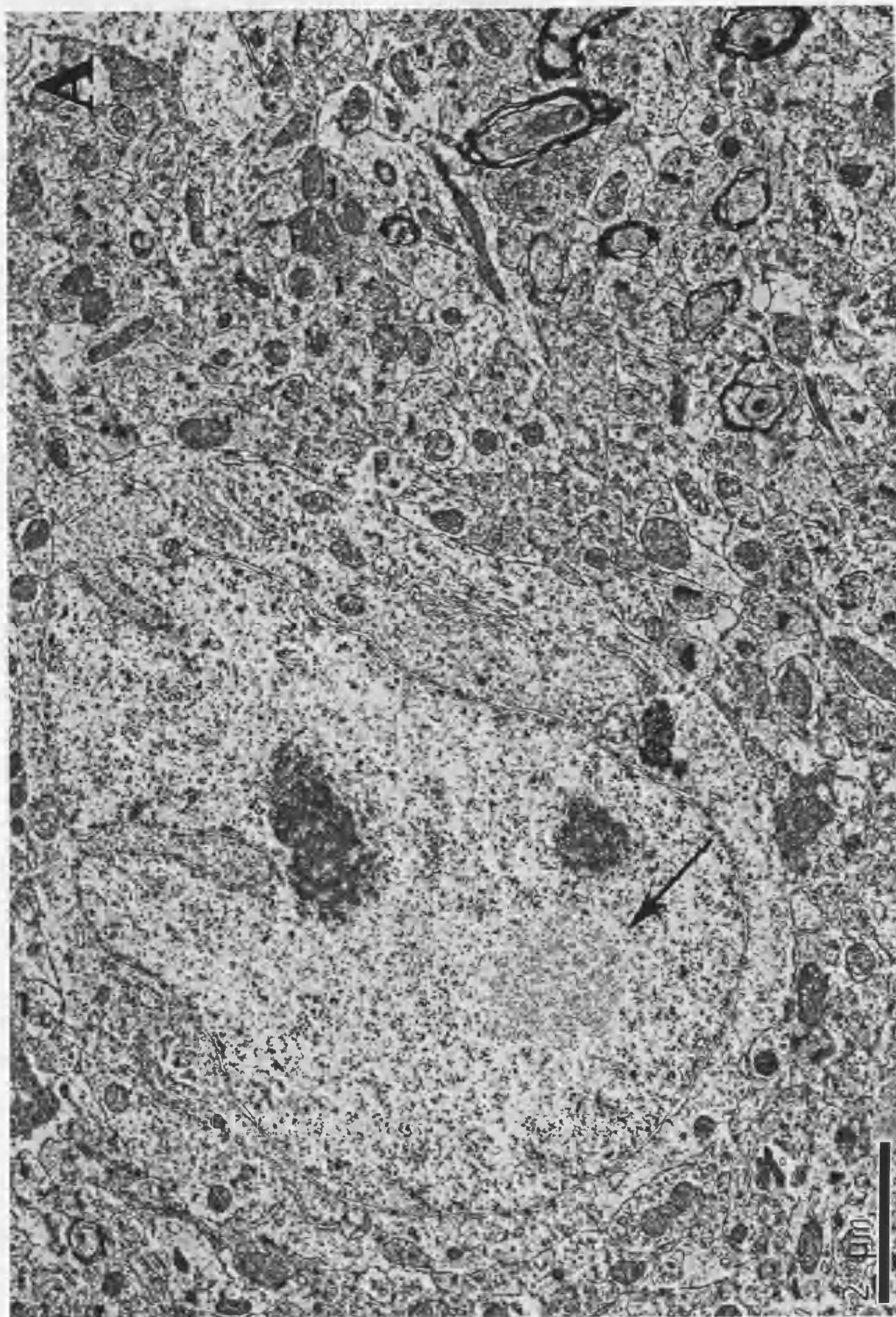
The two prevailing hypotheses concerning the structure of aggregates in polyglutamine disease state that expanded polyglutamine-containing proteins either form fibrils made up of hydrogen bonded β-pleated sheets or aggregate through the isopeptide cross links formed by the enzyme transglutaminase (Hoffner and Djian, 2002).

Transmission electron microscopy was used to examine the ultrastructure of aggregates in 13 week-old R6/2 mice. Cortical NIIs appear as predominantly amorphous, granular structures (Figure 7A & C) without the typically fibrous

ultrastructure that is clearly visible in aggregates in other neurodegenerative diseases, such as Lewy bodies in Parkinson's disease. From a purely ultrastructural viewpoint, NIIs do not seem to exhibit a defined ultrastructure characteristic of β -pleated fibrils. DNIs display a very similar granular morphology to nuclear aggregates. However, what can be construed as a fiber can occasionally be seen in neurite aggregates, it is important to state that these are the exception and not the norm (Figure 7B).

The commercial availability of antibodies against N ϵ (γ glutamyl) lysine bonds, the specific isopeptide links formed by transglutamination, allows for analysis of the mechanism of aggregation in neurodegenerative disease. Western blotting using such antibodies in R6/2 mice shows the presence of these isopeptide cross links in R6/2 mice as a smear from ~70 kDa upwards to the well of the gel (Figure 7D). Additionally, distinct bands appear at ~140, 210 kDa, possibly representing dimers and trimers of mutant huntingtin protein. These results support a role for transglutamination in the formation of aggregates in the brains of R6/2 mice.

Immunohistochemical analysis was employed to try and detect N ϵ (γ glutamyl) lysine bonds in aggregates. This proved unsuccessful, despite repeated attempts.



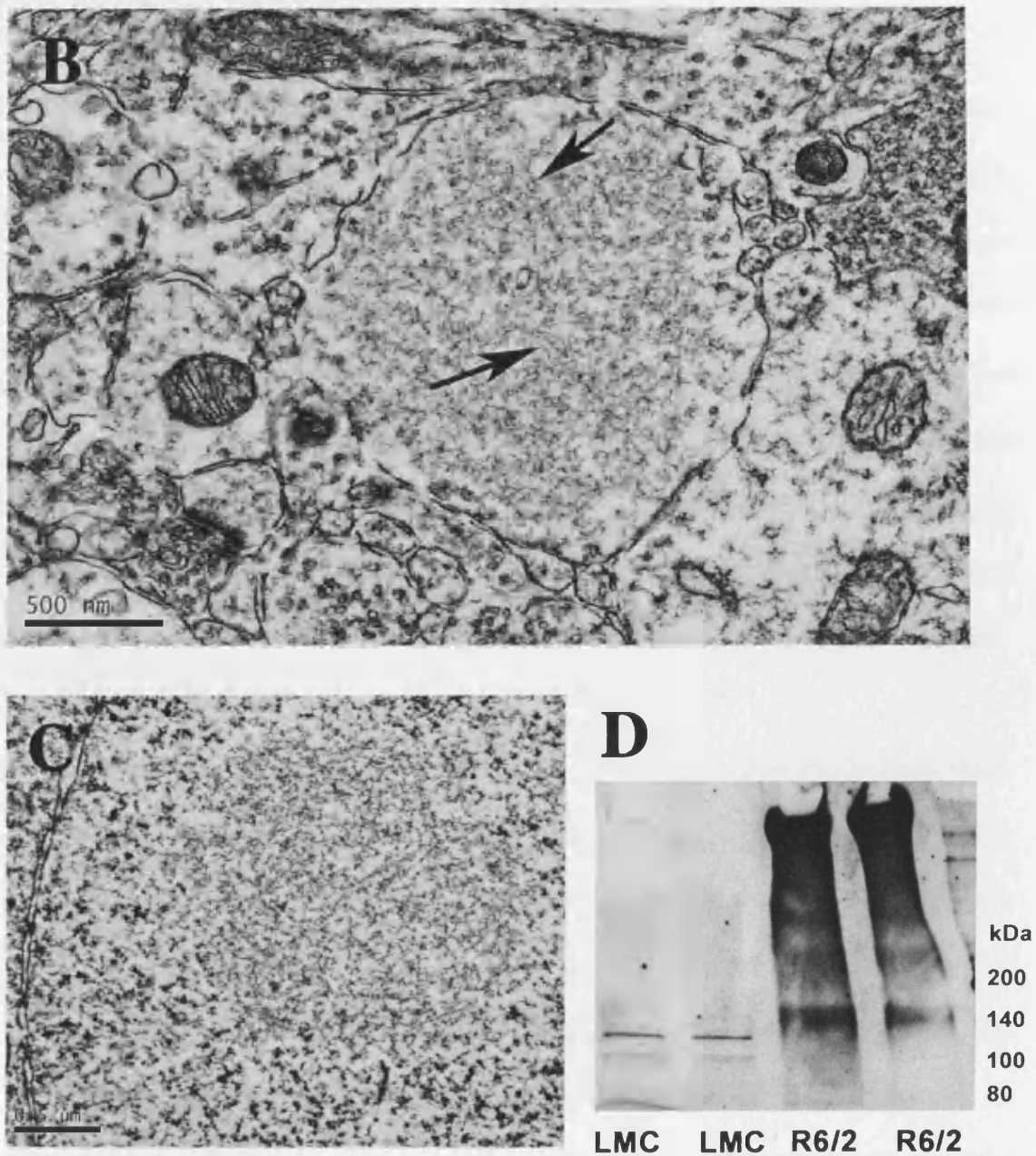


Figure 7: Inclusions in the R6/2 mouse model. Transmission electron micrographs showing the ultrastructure of cortical neuronal inclusions in 13 week-old R6/2 mice. NIIs (A, previous page, arrow) can be seen to have a predominantly granular and amorphous structure, similar in appearance to DNIs (B). However, DNIs occasionally contain fibres (B, arrows), not seen in NIIs, even at high magnification (C). (D) Whole-brain homogenates from 13 week-old R6/2 mice and age-matched litter-mate controls were separated by 4-20% SDS-PAGE (10 μ g total protein per lane) and blotted with antibodies against N ϵ (γ glutamyl) lysine bonds. The antibody detected transglutaminated aggregated proteins as a smear in R6/2, but not LMC samples.

3.2.2 Expanded polyglutamine proteins are ubiquitinated in R6/2 mice

Co-localisation of huntingtin and ubiquitin in NIIs and DNIs was demonstrated using double-labelled immunofluorescence in 13 week-old R6/2 mouse cortex (Figure 8A & B). All huntingtin-positive inclusions were also immunopositive for antibodies against ubiquitin. Whilst it has been shown in transformed cell lines that constructs of huntingtin can be ubiquitinated (Kalchman et al., 1996), mutant huntingtin protein has not yet been demonstrated to be directly ubiquitinated in R6/2 transgenic mice. Indeed, it is possible that the ubiquitin-immunopositivity of aggregates is due to ubiquitination of proteins other than huntingtin. Therefore, immunoprecipitation experiments were used to ascertain whether mutant huntingtin protein is ubiquitinated in the R6/2 model.

Initially, to show that expanded polyglutamine containing proteins can be detected in R6/2 mice with 1C2 antibody, western blots were performed on R6/2 and LMC whole brain homogenates. The 1C2 antibody, originally raised against the polyglutamine stretch in TATA-binding protein, is known to have an increasing affinity for increasingly long polyglutamine stretches (Trottier et al., 1995). As expected, the presence of aggregated mutant protein appeared as a smear from approximately 70 kDa up to the well of the gel in R6/2, but not litter mate control samples (Figure 8C). This is in agreement with the expected size of the transgene protein in the R6/2 model (Davies et al., 1997). To determine whether expanded polyglutamine containing proteins were ubiquitinated, magnetic Protein G-conjugated Dynal beads bound to

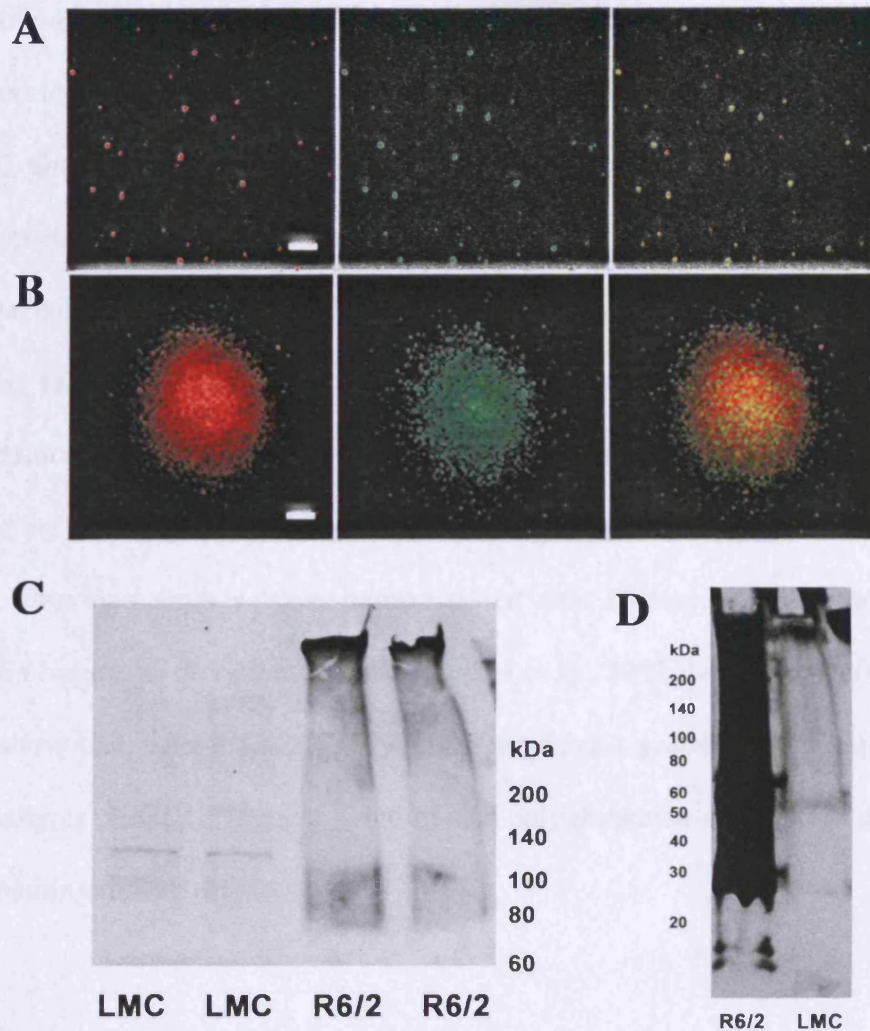


Figure 8: Huntingtin is ubiquitinated in the R6/2 model. (A, B) Confocal images showing co-localisation of huntingtin (EM48 antibody, red) and ubiquitin (Dako antibody, green) in cortical inclusions of 13 week-old R6/2 mice. Overlap, and hence co-localisation, is shown in yellow. (C) Whole-brain homogenates from R6/2 & LMC mice were separated by 4-20% SDS-PAGE (10 μ g total protein per lane) and blotted with anti-polyglutamine antibody (1C2). The antibody detected aggregated expanded polyglutamine-containing protein as a smear from ~70 kDa upwards in R6/2, but not LMC samples. (D) Polyglutamine containing proteins were purified by immunoprecipitation with FK2 antibody-bound magnetic Dynal beads from 13 week-old R6/2 and LMC whole-brain homogenates and separated by 4-20% SDS-PAGE. Membranes were then blotted with 1C2 antibody. A prominent smear from ~25 kDa upwards was detected in R6/2, but not LMC samples. The faint bands detected at ~22 and 55 kDa in both samples reflect the light and heavy chains of the non-covalently bound antibody that has dissociated from the magnetic beads. In addition to the smear detected in the R6/2 sample, the bands detected at ~70, 30, 18 and 15 kDa probably reflect proteolytically cleaved fragments of ubiquitinated polyglutamine-containing mutant protein. Scale bar 40 μ m upper panels, 0.5 μ m lower panels.

FK2 antibody (detects mono- and poly-ubiquitinated proteins, but not free ubiquitin) were used to purify ubiquitinated proteins from whole-brain homogenates in 13 week-old R6/2 and age-matched litter mate controls. These immunoprecipitated proteins were then electrophoresed and blotted with 1C2 antibody. A prominent smear (from ~25 kDa upwards) was detected in the R6/2, but not litter mate control, sample indicating that mutant huntingtin is indeed ubiquitinated in the R6/2 model (Figure 8D). Additionally, the R6/2 sample lane exhibited bands at ~70, 30, 18 and 15 kDa, possibly reflecting proteolytically cleaved fragments of ubiquitinated huntingtin protein. Previous studies have demonstrated that inclusions are comprised of huntingtin fragments of various lengths (Lunkes et al., 2002; Iuchi et al., 2003). These results show that, in the R6/2 line, mutant huntingtin protein is ubiquitinated and additionally, is cleaved into small ubiquitinated polyglutamine-containing fragments of mutant huntingtin.

3.2.3 20s, 19s and 11s proteasomal subunits relocate to aggregates in R6/2 brains

It has been shown that aggregates are ubiquitinated and have stained immunopositive for the 20s proteasome (Jana et al., 2001), yet it is not clear whether all components of the 26s proteasome, particularly the 19s and 11s regulatory subunits, localise to aggregates and whether they distribute to both nuclear and neurite aggregates in R6/2 mice. The advent of commercially available antibodies against various subunits of the proteasome, its regulatory subunits and associated proteins allows for this issue to be

addressed. Consequently, a detailed immunohistochemical study of the localisation of proteasome subunits in brains of R6/2 mice was performed.

NIIIs stained immunopositive for 20s, 19s and 11s subunits of the proteasome in cortex (Figures 9 & 10) and striatum (data not shown) of 13-week old R6/2 mice. Whilst antibodies raised against 19s subunits additionally labelled DNIs, 20s or 11s antibodies do not do so (Figure 10). Certain antibodies against 20s subunits ($\beta 1$ and $\beta 6$) did not label neuronal inclusions. Considering the demonstrated presence of the other 20s subunits in nuclear aggregates, this is more likely to represent either an unsuitability of these antibodies for immunohistochemistry or concealment of the epitopes within the structure of the proteasome or aggregate. Importantly, none of the antibodies raised against immunoproteasome subunits ($\beta 1i$, $\beta 2i$ and $\beta 5i$) were able to label either nuclear or neurite aggregates. This absence of γ -interferon inducible subunits in aggregates in R6/2 mice is in contradiction to findings from a previous study implicating them in the pathology of HD94 mice (Diaz-Hernandez et al., 2003). These results demonstrate that there is differential recruitment of proteasome components to NIIIs and DNIs and that immunoproteasome subunits are not recruited to aggregates in R6/2 mice.

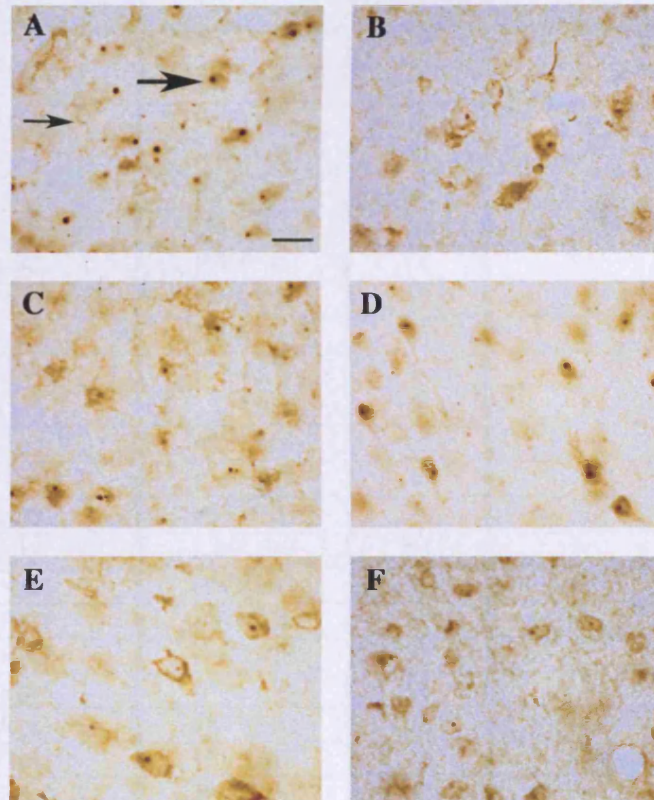


Figure 9: Components of the ubiquitin-proteasome system localise to aggregates in R6/2 mice. Antibodies recognising (A) polyubiquitinated proteins, (B) 20s “core”, (C) 20s α -subunits, (D) 19s RPN2, (E) 19s RPN10 and (F) 11s α -subunit all stain neuronal intranuclear inclusions in the cortex of 13-week R6/2 mice. Both anti-ubiquitin and anti-19s antibodies additionally stain dystrophic neurite inclusions, whilst anti-11s and anti-20s antibodies do not. Large and small arrows represent examples of NIIs and DNIs, respectively. Scale bar 20 μ m.

Protein	Antibody Code #	Species raised in	Staining of NIIs	Staining of DNIs
20s α 1,2,3,5,6 & 7	PW 8195	M	**	-
20s "core"	PW8155	R	***	-
20s β 1	PW8140	M	-	-
20s β 1i (LMP2)	PW8345	R	-	-
20s β 1i (LMP2)	PW8840	M	-	-
20s β 2	PW8145	M	**	-
20s β 2i (MECL1)	PW8350	R	-	-
20s β 3	PW8130	M	*	-
20s β 4	PW8890	R	*	-
20s β 5	PW8895	R	*	-
20s β 5i (LMP7)	PW8845	M	-	-
20s β 5i (LMP7)	PW8355	R	-	-
20s β 6	PW9000	R	-	-
20s β 7	PW8135	M	**	-
19s Rpt1	PW8165	R	***	**
19s Rpt1	PW8825	M	***	**
19s Rpt2	PW8305	R	*	-
19s Rpt3	PW8175	R	*	-
19s Rpt3	PW8310	R	*	-
19s Rpt3	PW8765	M	***	**
19s Rpt4	PW8220	R	*	-
19s Rpt4	PW8830	M	-	-
19s Rpt5	PW8770	M	*	-
19s Rpt6	PW8320	R	*	-
19s Rpn2	PW9270	M	***	**
19s Rpn6	PW8370	R	-	-
19s Rpn7	PW8225	R	-	-
19s Rpn8	PW8180	S	-	-
19s Rpn10	PW9250	M	**	*
19s Rpn12	PW8815	R	**	-
19s Rpn12	PW8835	M	*	-
11s PA28 α	PW8185	R	*	-
11s PA28 β	PW8240	R	-	-
11s PA28 γ	PW8190	R	-	-

Figure 10: Table showing which proteasome subunits localise to aggregates in R6/2 mice.

Table showing which proteasome subunits are present in neuronal intranuclear inclusions (NIIs) and dystrophic neurite inclusions (DNIs) as determined by immunohistochemical analysis in 13 week old R6/2 cortex. Most 11s, 19s and 20s components of the UPS are detected in NIIs, whilst only 19s subunits are detected in DNIs. "*" system indicates level of aggregate labelling. *** = high staining frequency (equivalent to that produced by ubiquitin or Huntingtin antibodies); ** = moderate quantity of aggregates immunopositive; * = immunostaining of aggregates rare or infrequent; - = antibody unable to label aggregates. See appendix for range of representative images to demonstrate scoring scale

3.2.4 Chaperones relocate to aggregates in R6/2 brains

The presence of 20s, 19s and 11s complexes of the proteasome in protein aggregates suggests the requirement for clearance by degradation of misfolded mutant huntingtin protein. However, as misfolded proteins are also targets for molecular chaperones, immunohistochemical and western blot studies were performed to ascertain whether they, too, recruit to aggregates in R6/2 mice.

Out of the chaperone antibodies tested, immunohistochemical analysis showed that only HDJ-2 and Hsc70 labelled NIIs (Figures 11A, B & 12). All tested chaperone antibodies failed to label DNIs (Figure 12). Western blot analysis confirmed the presence of both HDJ-2 and Hsc70 in insoluble aggregates as a smear in addition to soluble protein (Figure 11C & D). The smear in the case of HDJ-2 is particularly evident from ~80 kDa upwards, probably representing chaperone-bound fragments of mutant huntingtin protein. Further western blot analysis of two closely related chaperones, Hsp40 and Hsp70, confirmed immunohistochemical data by failing to show any insolubilisation of the respective proteins with the aggregates (Figure 11E & F). Levels of Hsp70 were unaltered in R6/2 brains. However, levels of Hsp40 appeared to be reduced in R6/2 brains compared to litter mate controls. The recruitment of Hsc70 to inclusions, and lack of increase in Hsp70 levels is not typical of a chaperone response, which has been shown to involve an increase in Hsp70. These results show that certain chaperones are recruited to NIIs, but not DNIs, in

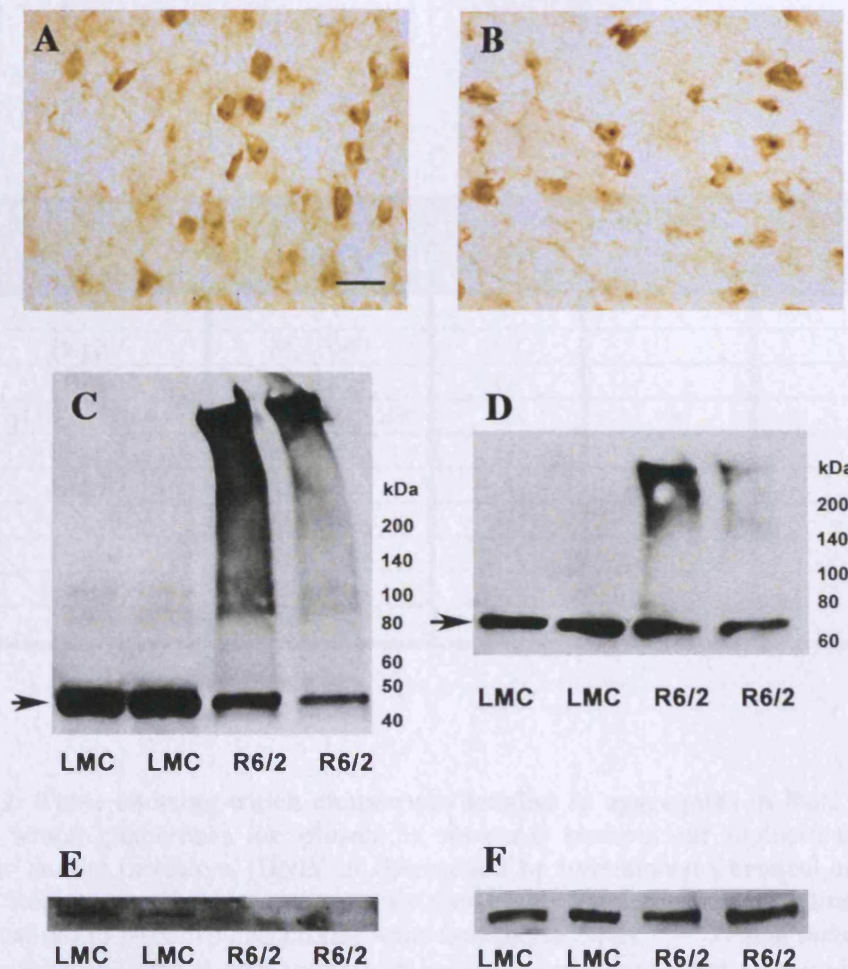


Figure 11: Chaperones aggregate in NIIs in R6/2 mice. Neuronal intranuclear inclusions in the cortex of 13-week old R6/2 mice are immunopositive for antibodies against (A) HDJ-2 and (B) Hsc70. Neither chaperones localise to dystrophic neurite inclusions. *Scale bar 20 μ m.* (C, D, E and F) Whole-brain homogenates from 13 week-old R6/2 mice and age-matched littermate controls were separated by 4-20% SDS-PAGE (10 μ g total protein per lane) and blotted with antibodies against (C) HDJ-2, (D) Hsc70, (E) Hsp40 or (F) Hsp70. In agreement with immunocytochemistry data, immunoblots of both (C) HDJ-2 and (D) Hsc70 demonstrate that both chaperones insolubilise with the aggregates in R6/2 samples, as shown by the smear from ~80 kDa upwards. Additionally, levels of soluble HDJ-2 and Hsc70 are slightly decreased (C & D, arrows). Levels of (E) Hsp40 are reduced in R6/2 samples compared to LMC, whilst levels of (F) Hsp70 appear unaltered.

Protein	Antibody Code #	Species raised in	Staining of NIIs	Staining of DNIs
Hsp27	SC-1049	Gt	-	-
Hsp40	SC-1801	Gt	-	-
HDJ-2 / DNAJ	MS-225-PIABX	Ms	**	-
Hsp70	SC-1060	Gt	-	-
Hsp70	SPA-810	Ms	-	-
Hsc70	SC-1059	Gt	**	-
Hsc70	SPA-815	Rt	*	-
Hsp105	SC-1804	Gt	-	-

Figure 12: Table showing which chaperones localise to aggregates in R6/2 mice. Table showing which chaperones are present in neuronal intranuclear inclusions (NIIs) and dystrophic neurite inclusions (DNIs) as determined by immunohistochemical analysis in 13 week old R6/2 cortex. Out of the chaperones tested, only antibodies raised against HDJ-2 and Hsc70 localised to NIIs. No chaperones were detected in DNIs. "*" system indicates level of aggregate labelling. *** = high staining frequency (equivalent to that produced by ubiquitin or huntingtin antibodies); ** = moderate quantity of aggregates immunopositive; * = immunostaining of aggregates rare or infrequent; - = antibody unable to label aggregates. See appendix for range of representative images to demonstrate scoring scale

brains of R6/2 mice and are accompanied by a decrease in levels of Hsp40.

Additionally, antibodies against BAG-1 and CHIP, proteins involved in linking the proteasome to chaperones were subject to immunohistochemical and western blot analysis. However, they were unable to detect the relevant proteins in either case.

3.3 Proteolytic activity in brains of R6/2 mice

The presence of ubiquitinated NIIs and DNIs in the brains of R6/2 mice, in addition to the redistribution of proteasomes to aggregates implies that proteasomal inhibition is a feature of polyglutamine disorders. The vast majority of studies of proteasomal activity in polyglutamine diseases have been performed on cellular models, often expressing vast quantities of mutant protein, which is likely to have an impact on a cellular system of protein degradation. Additionally, experiments have typically relied on measuring only one of the peptidase activities (usually chymotrypsin-like activity) as an indicator of proteasome activity, whereas recent data suggests that to gain a more accurate assessment of proteasomal activity all three main peptidase activities (chymotrypsin, trypsin and PGPH) should be examined (Kisselev et al., 2006).

3.3.1 Altered total proteolysis in R6/2 mice

Initially, as a precursor to experiments specifically measuring proteasomal activity, total proteolytic activity was measured in the R6/2 model, as compared to wild-type. This was performed by assaying the emitted fluorescence, and therefore degradation, of AMC-conjugated substrates of chymotrypsin, trypsin and PGPH peptidase activities in whole brain homogenates. Measurements of fluorescence were taken every 30 minutes over a period of 4 hours and this data were used to give average rates of degradation (in arbitrary units of fluorescence per hour). Assays were performed both in the presence and absence of SDS, a detergent thought to activate and open the 20S channel by removing control of access to the channel pore (Shibatani and Ward, 1995). All activities were expressed as a percentage of litter-mate control values (Figure 13).

In the presence of SDS, trypsin-like activity was found to be unchanged at 145.7%(±69.8%) of control values, whilst both chymotrypsin-like and PGPH-like activities were increased at 436.4%(±71.1%) and 435.4%(±24.1%) of control values, respectively.

In the absence of SDS, reflecting a more physiological state of cellular proteolysis, trypsin like activities are decreased at 50.7%(±28%) of control activities, whilst both chymotrypsin-like and PGPH-like activities are increased at 211.5%(±74%) and 375.4%(±55.5%) of control values, respectively. These preliminary results indicate

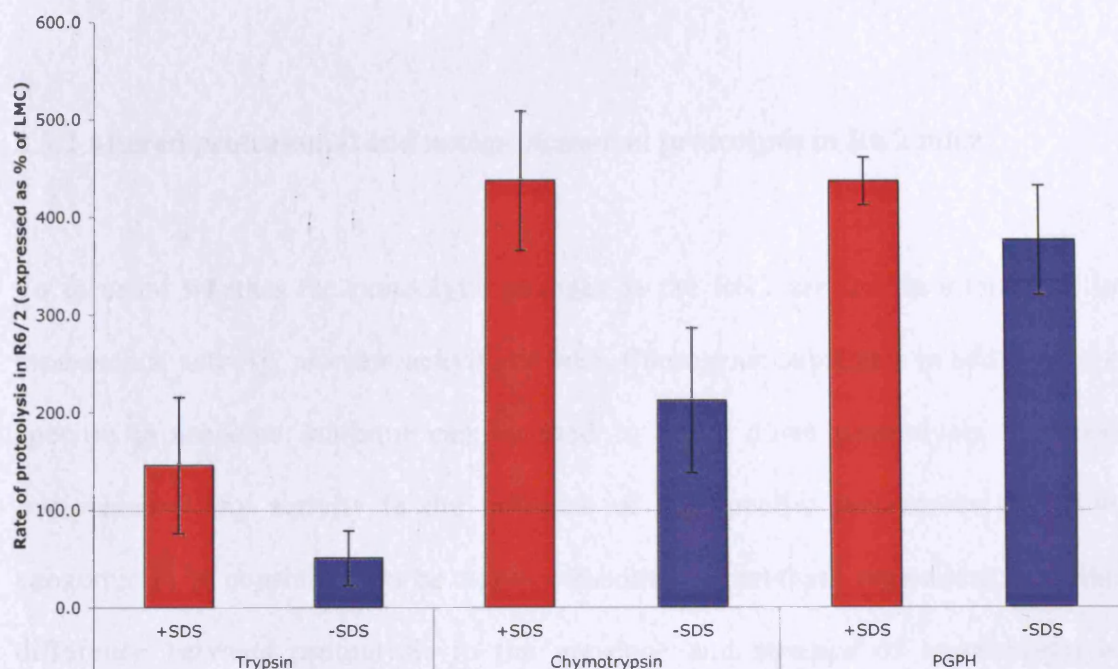


Figure 13: Rate of trypsin, chymotrypsin and PGPH peptidase activities in R6/2 mice. 13 week-old R6/2 and LMC whole-brain homogenates ($1 \mu\text{g} / \mu\text{l}$) were incubated with AMC-conjugated substrates specific for trypsin, chymotrypsin or PGPH peptidase cleavage. Proteolytic activity was determined by measuring the emitted fluorescence over time and expressed as a percentage of litter mate control values. Experiments were performed either in the presence or absence of SDS. In the absence of SDS, trypsin-like activities are decreased whilst both chymotrypsin-like and PGPH activities are increased in R6/2 samples. In the presence of SDS, both chymotrypsin-like and PGPH activities are both increased in R6/2 samples, whilst trypsin-like activities appear unaltered. $n=2$.

that proteolysis is altered in the R6/2 model, with trypsin-like activity decreased and both PGPH-like and chymotrypsin-like activity increased.

3.3.2 Altered proteasomal and non-proteasomal proteolysis in R6/2 mice

To measure whether the proteolytic changes in the R6/2 are due to alterations in proteasomal activity, protease activity or both, fluorogenic substrates in addition to a specific proteasome inhibitor can be used to break down proteolysis into two components. Any activity in the presence of the specific proteasome inhibitor, epoxomicin, is considered to be non-proteasomal or protease dependent, and the difference between proteolysis in the presence and absence of epoxomicin is considered to be proteasomal activity. Additionally, all assays were done in the absence of SDS to represent a more physiological profile of proteolytic activity.

Total trypsin-like activity was decreased by 67.6%(±2.1%; $p<0.001$), whilst chymotrypsin-like (105.7%(±7.2%; $p<0.001$)) and PGPH-like activities (94.4%(±42.2%)) were increased. Proteasomal trypsin-like activity was decreased by 42.2%(±8%; $p<0.05$), whilst chymotrypsin-like (202.4%(±9.6%; $p<0.001$)) and PGPH-like activities (146.4%(±55.9%; $p<0.05$)) were increased. Non-proteasomal proteolysis of trypsin-like (86%(±2.4%; $p<0.001$)), chymotrypsin-like (89.5%(±3.1%; $p<0.001$)) and PGPH-like (39.3%(±15.1%; $p<0.05$)) activities were all decreased (Figure 14). These results show that whilst there is inhibition of non-proteosomal

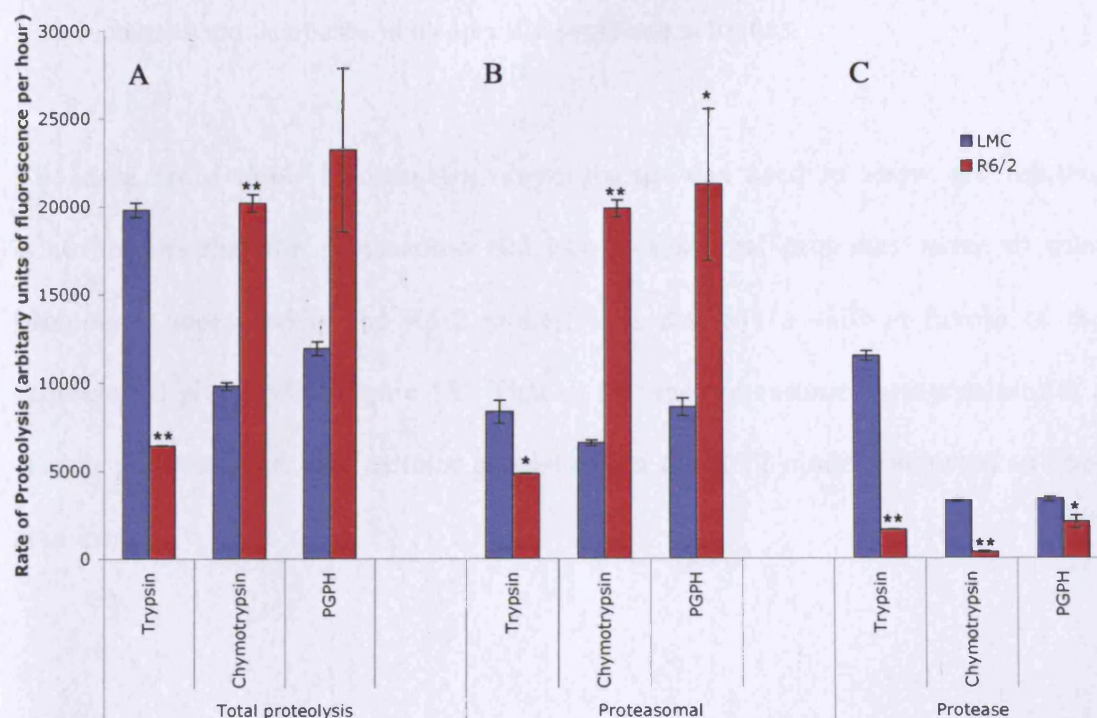


Figure 14: Rate of trypsin, chymotrypsin and PGPH proteasomal and protease activities in brains of R6/2 and LMC mice. 13 week-old R6/2 and LMC whole-brain homogenates (1 μ g / μ l) were incubated with fluorophore-conjugated substrates specific for trypsin, chymotrypsin or PGPH pepsidase cleavage. Proteolytic activity was determined by measuring the emitted fluorescence over time. In order to determine whether changes in proteolytic activity were due to proteasomal or non-proteasomal proteolysis, experiments were performed either in the presence or absence of the specific proteasome inhibitor epoxomicin. Hence, (A) total proteolysis can be divided into (B) proteasomal and (C) non-proteasomal protease components. (A) Total chymotrypsin pepsidase activities are significantly increased, whilst trypsin pepsidase activity are significantly reduced in R6/2 samples compared to litter-mate controls. (B) Proteasomal chymotrypsin-like and PGPH-like activities are significantly increased, whilst trypsin-like proteolysis is significantly decreased in R6/2 samples compared to litter mate controls. (C) All three pepsidase activities are significantly decreased in non-proteasomal proteases in R6/2 samples compared to litter mate controls (* p <0.05, ** p <0.001). $n=3$

proteases in R6/2 mice, the proteasome exhibits a differential proteolytic profile, with both increases and decreases in its specific peptidase activities.

The data from these fluorometric experiments was used to show the relative contributions that the proteasome and non-proteasomal proteases make to total proteolysis measured in the R6/2 model. This displays a shift in favour of the proteasomal proteolysis (Figure 15). That is, that the proteasome is responsible for a greater percentage of total cellular proteolysis in the R6/2 model compared to litter mate control.

3.3.3 Alterations in proteasomal subunits in R6/2 mice

To determine whether levels of proteasome subunits, or any obvious post-translational modifications could account for the differential proteolytic profile of the proteasome in R6/2 mice, western blots were performed using antibodies against 20S α subunits and the 20S catalytic subunits, β_1 , β_2 and β_5 .

Soluble levels of 20S α were increased in R6/2 mice, in addition to higher molecular weight aggregates (Figure 16A). Additionally, higher molecular weight species were detected at 55, 70 and ~95 kDa in the R6/2 mice, but not litter mate controls. Soluble levels of both β_1 (Figure 16B) & β_5 (Figure 16D) were markedly decreased, but as both β_1 and β_5 proteins heavily stain the insoluble aggregates (top of gel), proteins levels of

A

		Proteasome	Protease
LMC	Trypsin	42.1	57.9
	Chymotrypsin	66.9	33.1
	PGPH	72	28
R6/2	Trypsin	74.9	25.1
	Chymotrypsin	98.3	1.7
	PGPH	91.3	8.7

B

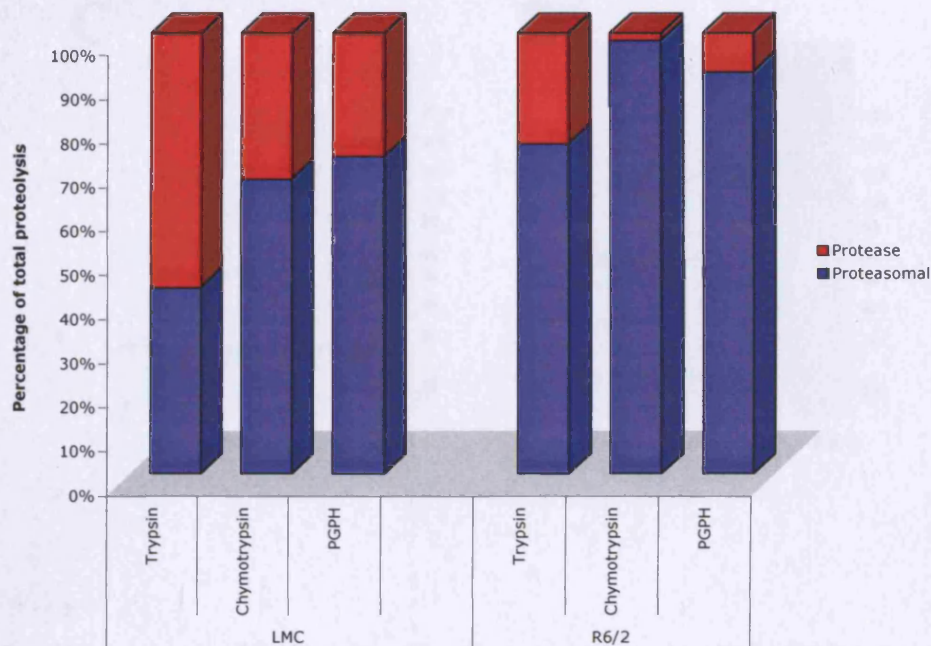


Figure 15: Relative contributions of the proteasome and non-proteasomal proteases to total proteolysis in brains of R6/2 and litter mate controls. (A) Table showing the relative percentage of trypsin, chymotrypsin and PGPH proteasomal and non-proteasomal proteolysis in R6/2 and LMC brains. In litter-mate controls, proteasomal proteolysis is responsible for ~40% of trypsin-like proteolysis and ~70% of chymotrypsin-like and PGPH proteolysis. However, in the R6/2, ~75% of trypsin-like proteolysis and nearly all of chymotrypsin-like and PGPH proteolysis is proteasomal. This demonstrates that in R6/2 samples, a higher percentage of the total proteolysis is due to the proteasome. (B) Visual representation of data from (A)

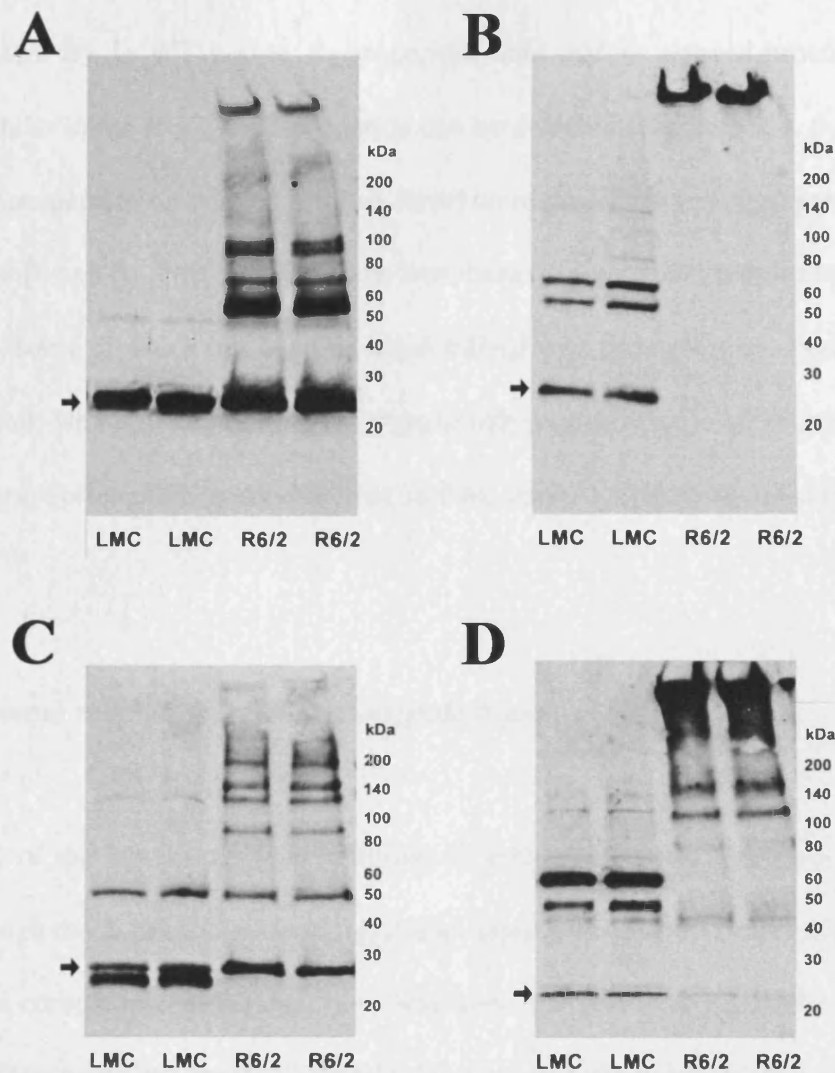


Figure 16: Altered expression / localisation of proteasome subunits in R6/2 mice. Whole-brain homogenates from 13 week-old R6/2 mice and age-matched litter-mate controls were separated by 4-20% SDS-PAGE (20 μ g total protein per lane) and blotted with antibodies against (A) 20s α -subunits (B) 20s β_1 -subunits (C) 20s β_2 -subunits and (D) 20s β_5 -subunits. Immunoblots demonstrate increased levels of soluble 20s α -subunits (A, arrow) in addition to aggregated protein (A, top of gel) and prominent bands at 55, 70 & 90 kDa in R6/2 mice compared to litter-mate controls. Soluble 20s β_1 (B, arrow) & β_5 -subunits (D, arrow) are almost absent in R6/2 mice, but are abundant in aggregated protein (B, D, top of gels). β_2 -subunits present in propeptide and mature cleaved states can be seen in LMC mice, whilst only propeptide is seen in R6/2 mice (C, arrow). Higher molecular weight bands detected in R6/2 samples (A, C and D) are probably aggregated forms of the respective subunits.

particularly β_5 can be considered to be increased, but insolubilised with the aggregate (Figure 16B & D), In WT brains, β_2 propeptide, and mature cleaved protein can be detected, whilst in the R6/2, only propetide can be detected (Figure 16C). β_2 subunits (whether in propeptide or cleaved product form) were present in the aggregate, but not as heavily as β_1 and β_5 . These results show that there is increased expression of the 20s proteasome, some of which has become insolubilised with the aggregate. Furthermore, the β_2 subunit, which is responsible for trypsin-like peptidase activity, is present only as the immature propeptide in soluble form in R6/2 mice compared to controls.

3.4 Proteasomal regulation in R6/2 transgenic mice

The activity of the 20s proteasome is known to be modulated in a number of ways. Firstly, through the presence and binding of additional proteasome components such as 19s and 11s complexes, which can bind and open the 20s pore channel and act as molecular chaperones by “feeding” proteins directly into the catalytic core. Secondly, via the γ -interferon inducible immunoproteasome subunits (β_{1i} , β_{2i} and β_{5i}) that directly replace the catalytically active β -subunits, β_1 , β_2 and β_5 . Or thirdly, via accessory proteins, such as PI31k and PA200, which have recently been shown to alter the proteolytic profile of the proteasome.

3.4.1 Levels of 11s and 19s proteasomal regulatory proteins in R6/2 mice

To ascertain whether proteolytic alterations shown in R6/2 mice could be attributable to altered regulation, western blot analysis was undertaken to determine any potential changes in levels of 11s and 19s components. Immunoblots showed that there was no difference in the levels of 11s α , 11s β or 11s γ between R6/2 mice and litter-mate controls (Figure 17A, B & C). Based on previous data showing a strong immunopositivity of aggregates using anti-Rpn2 antibodies, this antibody was used to gauge levels of 19s regulatory complexes. An increase was detected in levels of the 19s subunit Rpn2 in R6/2 mice compared to litter-mate controls (Figure 17D). Previous immunohistochemical studies (chapter 3.2.3) demonstrated that 19s antibodies were particularly strong markers of both NIIs and DNIs, yet western blot analysis did not detect 19s Rpn2 subunits insolubilising with aggregates as a “smear” (top of gel, data not shown). Likewise, none of the immunoblots of 11s subunits detected aggregate smears (top of gel, data not shown), including the 11s α subunit, shown by immunohistochemical studies (chapter 3.2.3) to recruit to NIIs. It could be argued, therefore, that both 11s and 19s proteins are not insolubilised with aggregates and represent transient components of inclusions, being sequestered purely by their high affinity for 20s proteasomes.

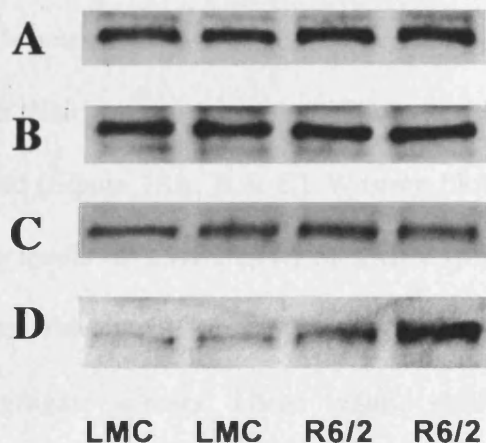


Figure 17: Levels of 11s and 19s regulatory subunits in R6/2 mice. Whole-brain homogenates from 13 week-old R6/2 mice and age-matched litter-mate controls were separated by 4-20% SDS-PAGE (10 μ g total protein per lane) and blotted with antibodies against (A) 11s α (B) 11s β (C) 11s γ and (D) 19s s10 (check other name) subunits. No differences were found in levels of 11s α , β or γ subunits between R6/2 and LMC samples. An increase in levels of 19s Rpn2 subunits was found in R6/2 when compared to LMC samples.

3.4.2 No change in immunoproteasome subunits

Immunoproteasomes are known to have different activity profiles to constitutive 20s proteasomes via substitution of the β -subunits known to possess catalytic activity. To see whether the differential proteolytic profile displayed in R6/2 brains was attributable to altered 20s proteasome composition, levels of immunoproteasome subunits were measured (Figure 18A, B & C). Western blot analysis revealed that no differences in protein levels of LMP2 (β 1i) or LMP7 (β 5i), and of MECL1 (β 2i), which was barely detectable. Furthermore, none of these proteins were detected in R6/2 samples as aggregate smears. These results confirm previous data from immunohistochemical studies (chapter 3.2.3) demonstrating that immunoproteasome subunits are not recruited (or aggregate) with inclusions in R6/2 mice, nor is there any alterations to immunoproteasome subunit protein levels. This finding is contrary to a previous study describing upregulation of LMP2 and LMP7 subunits in HD94 mice (Diaz-Hernandez et al., 2003). Therefore, it is unlikely that immunoproteasomes are implicated in any alterations to the ubiquitin-proteasome system in R6/2 mice.

3.4.3 Levels and localisation of PA200 and PI31k

To see if there was any difference in the levels of accessory proteins that could explain the differential proteolytic profile demonstrated in R6/2 mice, western blot analysis of PA200 and PI31k proteins was undertaken.

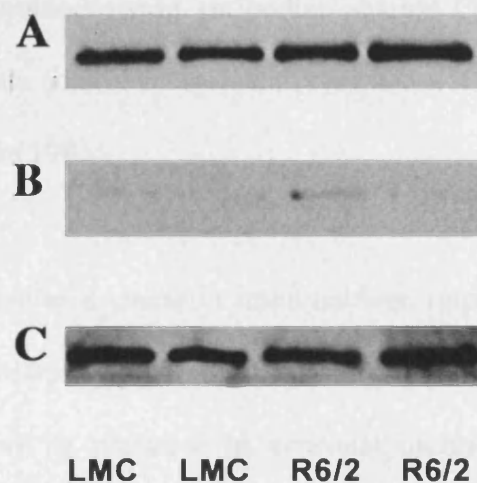


Figure 18: Levels of immunoproteasome subunits in R6/2 mice. Whole-brain homogenates from 13 week-old R6/2 mice and age-matched litter-mate controls were separated by 4-20% SDS-PAGE (10 μ g total protein per lane) and blotted with antibodies against (A) LMP2 (B) MECL-1 and (C) LMP7 subunits. No differences were found in levels of immunoproteasome subunits (A) LMP2 and (C) LMP7 between R6/2 and LMC samples. (B) MECL-1 was barely detectable in both R6/2 and LMC samples.

Western blots showed the presence of two bands (160 and 200 kDa) corresponding to the two described mammalian forms of PA200 in litter-mate controls. In the R6/2 samples, these soluble forms of PA200 were not detectable, yet a high molecular weight smear was detected (Figure 19A), implying that PA200 has insolubilised with the aggregate. Immunoblots using antibodies against PI31k detected the 31 kDa protein in the litter-mate control samples and revealed a significant decrease in levels in R6/2 samples (Figure 19B).

As PA200 was detected as a smear in immunoblots, implying insolubilisation with aggregates, immunohistochemical studies were performed on R6/2 brains to conclusively determine its presence in neuronal inclusions. PA200 was weakly detected in nuclear, but not neurite, inclusions (Figure 19C). Additionally, to further determine whether PI31k is present in inclusions immunohistochemistry was also performed using antibodies against PI31k. PI31k antibodies were unable to positively stain aggregates in the R6/2 mouse

These results demonstrate that PA200 is sequestered into NIIs. Furthermore, protein levels of the chymotrypsin-like and PGPH-like proteasome inhibitor, PI31k, are greatly reduced in the R6/2 model.

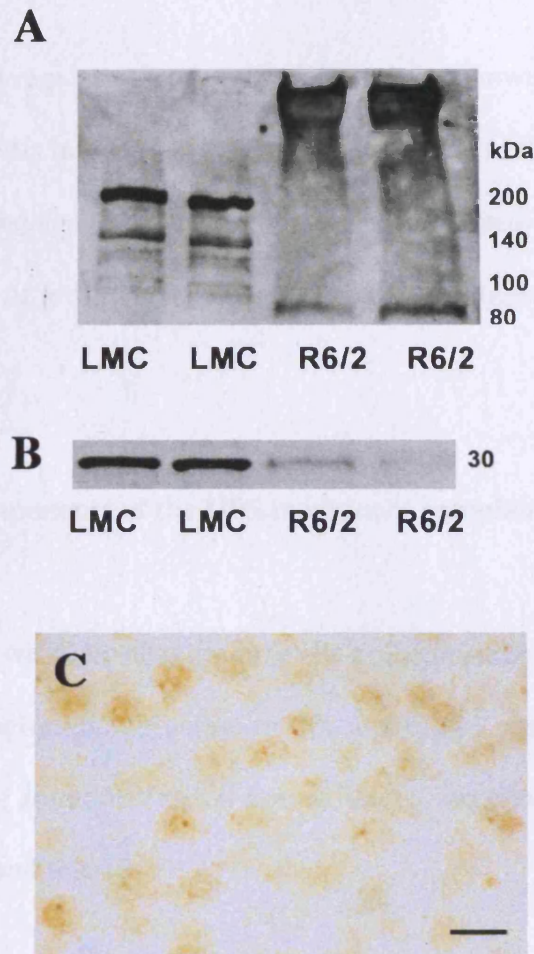


Figure 19: Altered expression / localisation of proteasome regulatory components PA200 and PI31k in R6/2 mice. (A, B) Whole-brain homogenates from 13 week-old R6/2 mice and age-matched litter-mate controls were separated by 4-20% SDS-PAGE (20 μ g total protein per lane) and blotted with antibodies against (A) PA200 and (B) PI31k. (A) Immunoblots demonstrate decreased levels of soluble PA200 (~160 and 200 kDa) in addition to aggregated protein (top of gel) in R6/2 samples compared to litter-mate controls. (B) Soluble PI31k is markedly decreased in R6/2 samples. (C) Immunohistochemistry showing the presence of PA200 in neuronal intranuclear inclusions in the cortex of 13 week-old R6/2 mice. *Scale bar* 20 μ m.

3.5 Additional components of the UPS in the R6/2 transgenic model

20s proteasomes and regulatory components have been shown to redistribute to and insolubilise with the NIIs in brains of R6/2 mice. This leads to the possibility that other proteins involved or related to the ubiquitin proteasome system might be altered in the R6/2 model, in terms of protein level and recruitment to aggregates.

3.5.1 Additional components of the UPS machinery associate with NIIs

To see whether there were any changes in levels or localisation of components that are involved with huntingtin ubiquitination or 20s assembly / maturation, western blots were performed using antibodies raised against the E2 enzyme shown to interact with huntingtin, E2(25k), and POMP.

Soluble levels of both E2(25k) and POMP (detected at 16 kDa) were reduced in the R6/2 compared to litter-mate control (Figure 20A & D). A longer exposure of the immunoblot revealed that POMP insolubilised with the aggregates and appeared on immunoblots as a smear (Figure 20B). Additionally, E2(25k) produced a high molecular weight smear on the blot indicating that it had also insolubilised with the aggregates (Figure 20D).

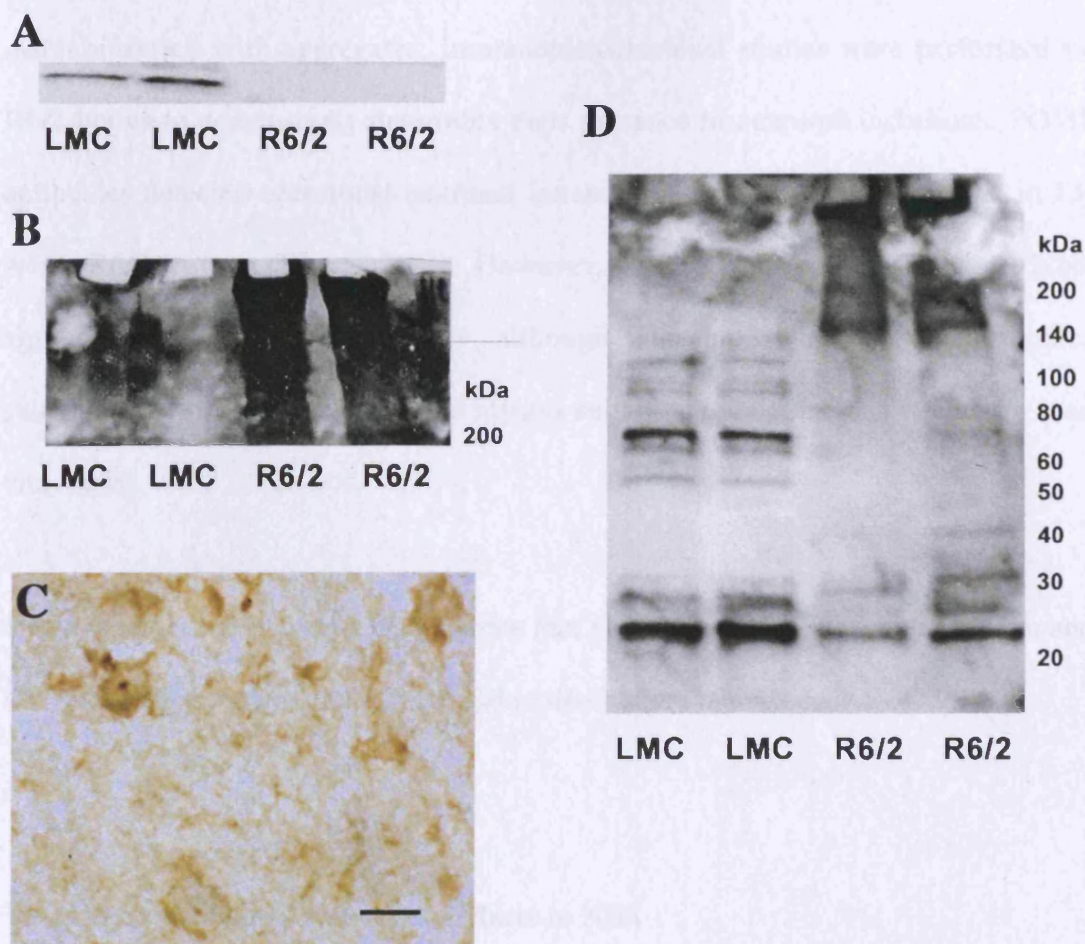


Figure 20: Altered expression / localisation of proteasome maturation protein (POMP) and E2 ubiquitinating enzyme in R6/2 mice. (A, B, D) Whole-brain homogenates from 13 week-old R6/2 mice and age-matched litter-mate controls were separated by 4-20% SDS-PAGE (20 μg total protein per lane) and blotted with antibodies against (A, B) POMP and (D) E25k. (A) Immunoblots demonstrate absence of soluble POMP (~16 kDa) in R6/2 samples compared to litter-mate controls. (B) Overexposure of nitrocellulose membranes show aggregated POMP appearing as a smear in western blots. (D) Soluble E25k is markedly decreased in addition to aggregated protein (top of gel) in R6/2 samples compared to litter-mate controls. (C) Immunohistochemistry showing the presence of POMP in neuronal intranuclear inclusions, but not dystrophic neurite inclusions in the cortex of 13 week-old R6/2 mice. Scale bar 20 μm.

As both E2(25k) and POMP were detected as smears in immunoblots, implying insolubilisation with aggregates, immunohistochemical studies were performed on R6/2 brains to conclusively determine their presence in neuronal inclusions. POMP antibodies detected occasional neuronal intranuclear inclusion, but not DNIs, in 13-week R6/2 cortex (Figure 20C). However, E2(25k) antibodies failed to label aggregates immunohistochemically, although this could well be that antibodies suitable for western blotting are not always suitable for immunohistochemistry (and vice versa).

Taken together, these results demonstrate that proteins required for ubiquitination and UPS assembly become insolubilised and redistribute to inclusions in R6/2 mice.

3.5.2 Ubiquitin-like proteins redistribute to NIIs

Among their currently identified function, both ubiquilin and VCP are known to target multi-ubiquitinated proteins to the proteasome. Additionally, SUMO-1, SUMO-2/3 and NEDD8 are all bound to target proteins through a series of E1, E2 and E3 enzymes, similar to that of ubiquitin. To see whether there were any changes in levels or localisation of ubiquitin-like proteins, western blots were performed using antibodies raised against SUMO-1, SUMO-2/3, ubiquilin, NEDD8 and VCP.

Antibodies against NEDD8 were used for both immunocytochemistry and western blot analysis of R6/2 tissue. However, NEDD8 was unable to be detected in both immunoblots and immunohistochemistry.

Western blot analysis showed a loss of soluble SUMO-1 (14 kDa), SUMO-2/3 (14 kDa), ubiquitin (66 kDa) and VCP (97 kDa) (Figure 21A, B, C & D), and a insolubilisation of the respective proteins with the aggregate, as detected by smears on the tops of the gels. Additionally, high molecular weight conjugates of SUMO-1, at about 80 kDa, and SUMO-2/3, at about 110 kDa) were absent in the R6/2 samples.

As western blots of SUMO-1, SUMO-2/3, ubiquitin and VCP all appeared as smears or were retained in the wells, immunocytochemistry was used to conclusively determine their presence in aggregates (Figure 22A, B, C). All tested ubiquitin-like proteins (except VCP) recruited to NIIs, but failed to label DNIs. Both SUMO-1 and SUMO-2/3 labelled a large frequency of nuclear aggregates, comparable with the immunopositivity of antibodies against huntingtin or ubiquitin, whilst ubiquitin antibodies labelled nuclear aggregates, albeit infrequently. Valoisin containing protein antibodies, however, failed to label aggregates. It is possible that this is due to a lack of suitability of the antibody for immunocytochemistry.

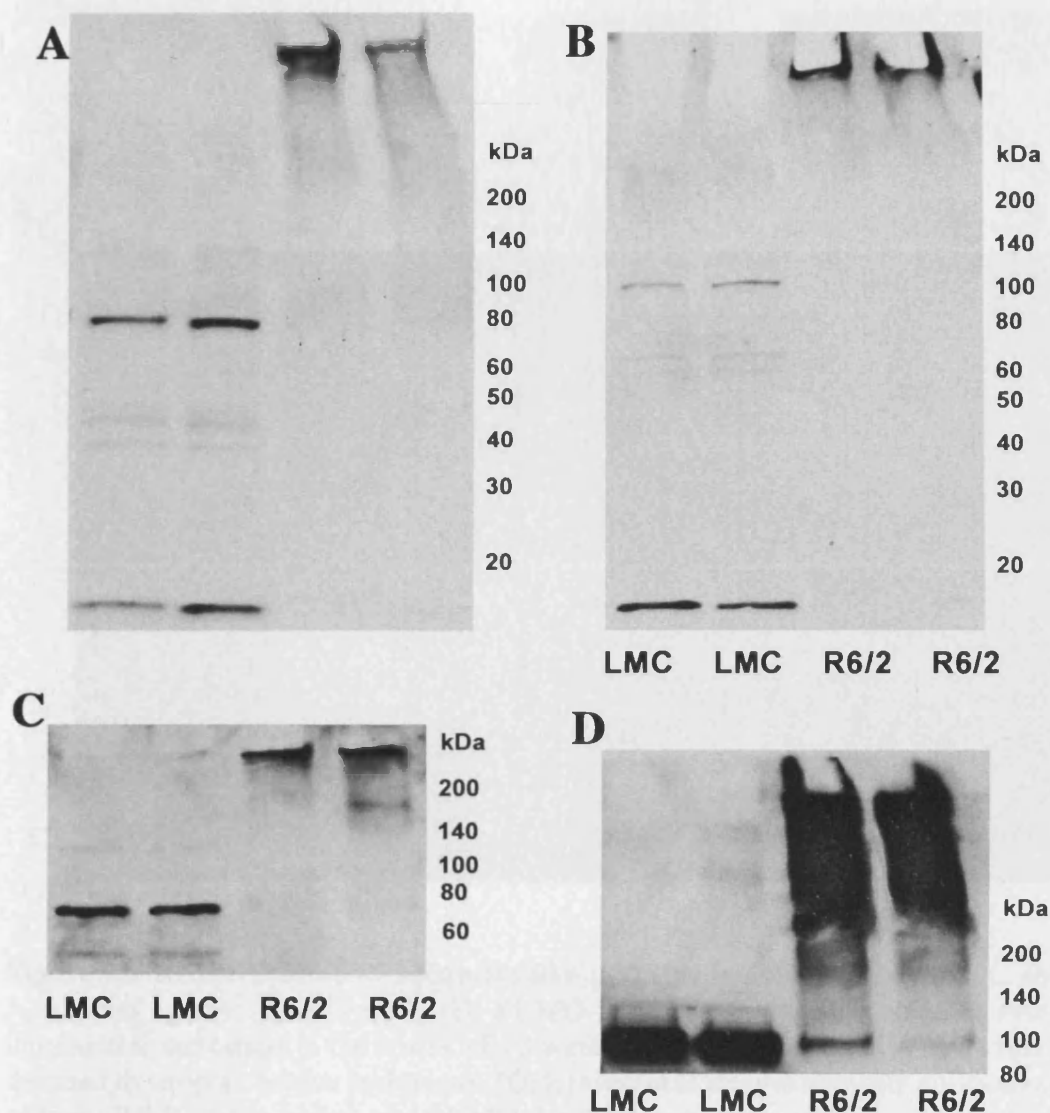


Figure 21: Altered expression / localisation of ubiquitin-like proteins (UBLs) in R6/2 mice. Whole-brain homogenates from 13 week-old R6/2 mice and age-matched litter-mate controls were separated by 4-20% SDS-PAGE (10 μ g total protein per lane) and blotted with antibodies against (A) SUMO-1 (B) SUMO-2/3 (C) Ubiquilin and (D) VCP. Immunoblots demonstrate a loss of soluble SUMO-1 (A, ~14 kDa), SUMO-2/3, (B, ~14 kDa), ubiquilin (C, ~66 kDa) and a decrease of soluble VCP (D, ~97 kDa) in R6/2 compared to LMC samples. SUMO-1, SUMO-2/3, Ubiquilin and VCP are all present in the insoluble aggregate (A, B, C, D, top of gel). Additionally, proteins that are conjugated with SUMO-1 (A, ~80, 45 and 40 kDa) and SUMO-2/3 (B, ~110, 70 and 60 kDa) in LMC samples are absent in the R6/2 samples.

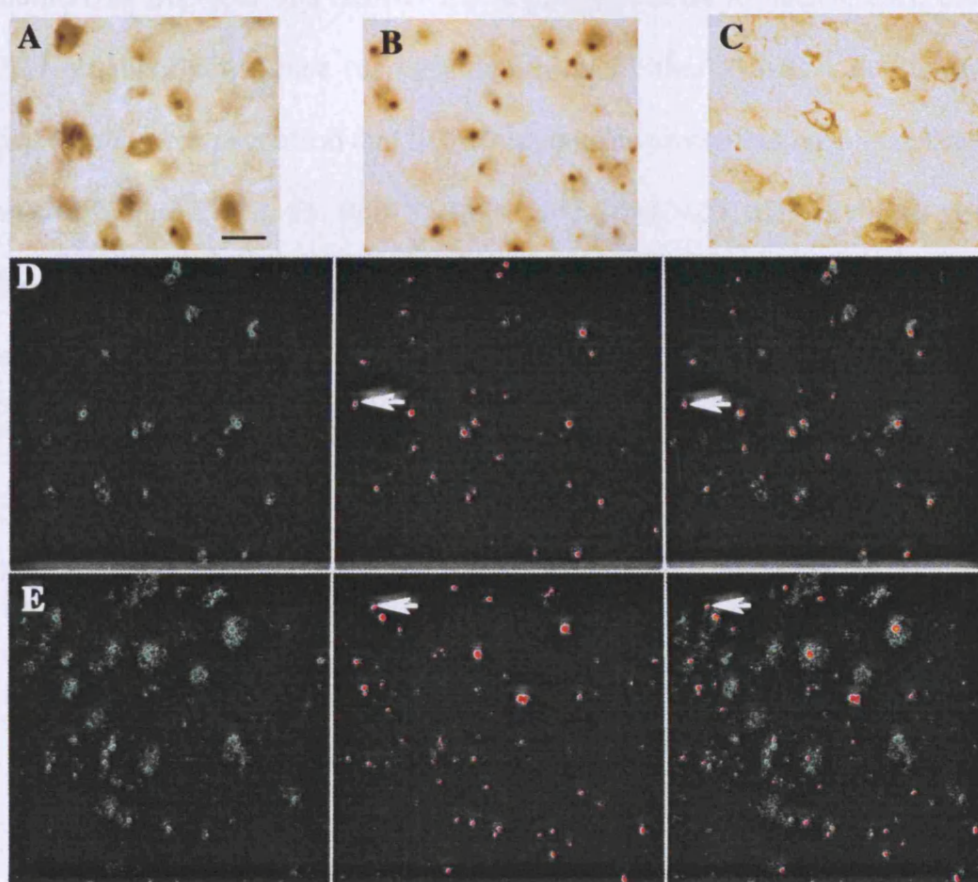


Figure 22: Redistribution of ubiquitin-like proteins in R6/2 mice. (A, B, C and D) Antibodies against (A) SUMO-1, (B) SUMO-2/3 and (C) ubiquitin all label neuronal intranuclear inclusions in the cortex of 13 week-old R6/2 mice. None of the antibodies detected dystrophic neurite inclusions. (D, E) Confocal images showing co-localisation of both SUMO-1 (D, green) and SUMO-2/3 (E, green) with ubiquitin (FK2 antibody, red) in cortical inclusions of 13 week-old R6/2 mice. Overlap, and hence co-localisation, is shown in yellow. Note that as SUMO-1 and SUMO-2/3 only label nuclear inclusions and not dystrophic neurite inclusions, the overlapped images show some ubiquitin-positive inclusions that do not stain for SUMO-1 or SUMO-2/3 (shown by arrows in D and E). *Scale bar 20 μ m.*

In addition, as SUMO-1 and SUMO-2/3 normally localise in nuclear foci, double-labelled immunofluorescence (using ubiquitin and either SUMO-1 or SUMO-2/3 antibodies) was used to confirm that SUMO immunopositivity was labelling of nuclear aggregates (Figure 22D & E). Both SUMO-1 and SUMO-2/3 labelled a high number of ubiquitin positive nuclear aggregates. Additionally, immunofluorescence confirmed immunohistochemical studies that neither SUMO-1 or SUMO-2/3 antibodies label DNIs. These results demonstrate that, in addition to proteasomal components, UBLs relocate to and insolubilise with aggregates and, in the case of SUMO-1 and SUMO-2/3, higher molecular weight conjugates are absent in the R6/2 model.

CHAPTER 4

Discussion

4.1 Molecular composition of polyglutamine containing aggregates

Perhaps one of the most controversial topics within the polyglutamine expansion disease field is the role that protein aggregation plays in neurological dysfunction. Whilst it has been suggested that protein aggregates are benign neuropathological features, which are simply a by-product of disease, more commonly the controversy is whether aggregates are harmful to the affected neuron or whether they serve a neuroprotective role by sequestering potentially harmful soluble toxic species. One fact remains clear, however, and that is that protein aggregation is a feature common to all polyglutamine expansion diseases, and indeed many other neurodegenerative diseases, including Alzheimer's and Parkinson's diseases. Unlike the plaques and tangles found in Alzheimer's patients brains and the Lewy bodies found in Parkinson's disease brains, relatively little is known about the structure and composition of protein aggregates in polyglutamine diseases. As a deeper understanding into the structure and formation of these entities could provide important clues into the pathogenesis of these diseases, the first approach of this study was to try and ascertain more information regarding the structure and molecular composition of aggregates in the R6/2 model.

4.1.1 Clues about the ultrastructure of protein aggregates in R6/2 mice

The two prevailing hypotheses regarding the nature of polyglutamine aggregation postulate that expanded polyglutamine containing proteins either forms fibrils composed of β -pleated sheets or aggregates via transglutaminase crosslinking. Electron microscopy is an established tool to identify filamentous structures in neurodegenerative diseases. A good example of this is the Lewy body, found in Parkinson's disease, which has been shown to be comprised of filaments of α -synuclein. These α -synuclein filaments are clearly visible at the electron microscopic level (Forno *et al.*, 1976; Spillantini *et al.*, 1998). Thus, using standard transmission electron microscopy, the ultrastructure of cortical neuronal aggregates was examined in R6/2 mice. NIIs appeared to display a predominantly amorphous, granular structure. Indeed, DNIs were also found to be predominantly granular, amorphous structures, and, although they occasionally contained what could be construed as a filament-like structure, it is important to state that these were very rare and were the exception rather than the norm. This implies that whilst filamentous elements were very occasionally visible in DNIs, the underlying structure of aggregates in the R6/2 model does not appear to be filamentous in nature.

There are a variety of proteins that have been shown to insolubilise and / or relocalise with aggregates in R6/2 mice (see 4.1.2) and this heterogenous protein content could explain the predominantly disordered and amorphous structure seen. This, as mentioned, is unlike Lewy bodies in Parkinson's disease patients, which can be clearly

seen to be primarily composed of filaments of α -synuclein. This could represent an important distinction. Often, neurodegenerative disorders are clumped together based upon the common presence of insoluble protein aggregates, yet their differing localisation, composition and solubility would have different effects on the functionality of the cell. Furthermore, the fact that in R6/2 mice, neurite aggregates occasionally contain filament-like structures unlike nuclear aggregates implies that there might be differences in the composition of these aggregates. This could be due to differences between the nuclear and cytoplasmic compartments such as presence of certain chaperones, proteasome subtypes and other proteases which could affect the mechanism and kinetics of aggregation. For example, it is thought that calpains and cathepsins (cytoplasmic and lysosomal proteases, respectively) cleave mutant huntingtin prior to inclusion formation, and that this cleaved N-terminal product has a high propensity to aggregate (Kegel et al., 2000; Kim et al., 2001). As cleavage via these proteases is thought to occur in the cytoplasmic and lysosomal compartments, different species of mutant protein would be expected to present in nuclear versus cytoplasmic aggregates, which has been demonstrated in one study (Lunkes et al., 2002). This study has indeed highlighted differential recruitment of proteins to nuclear and neurite aggregates (discussed in 4.1.2).

A study which initially showed huntingtin filaments to be present in both a conditional mouse model of HD and HD patients, using both electron and atomic-force microscopy, is of particular relevance here (Diaz-Hernandez *et al.*, 2004). A follow up study using these same mice showed that after shutting down transgene expression, the

majority of huntingtin-containing inclusions were cleared, whilst a small fraction of Thioflavin-S-positive inclusions remained (Diaz-Hernandez *et al.*, 2005). This implies that, even in a study showing huntingtin filaments present in inclusions, filaments do not form the main structure of polyglutamine inclusions, in keeping with the results presented here.

As electron microscopy implied that aggregates in R6/2 mice did not appear to be primarily composed of filaments, transglutamination represents an attractive alternative. In order to test whether aggregates in the R6/2 model are formed by the process of transglutamination, western blot and immunohistochemical experiments were performed using antibodies raised against N ϵ (γ glutamyl) lysine bonds, the isopeptide bonds formed by transglutamination. The high molecular weight “smear” seen in these western blots is typical of aggregated proteins and these results imply that aggregated proteins in this model contain these specific bonds. Mutant N-terminal huntingtin expressed in the R6/2 model is approximately 70 kDa (Davies *et al.*, 1997) and the additional bands seen at ~140 kDa and ~210 kDa are likely to represent transglutaminated dimers and trimers of N-terminal huntingtin. Indeed, it has been shown that inclusions in HD patients contain a broad range of N-terminal fragments (Hoffner *et al.*, 2005). This result implies that N-terminal huntingtin is a target for transglutamination and that aggregates are formed via N ϵ (γ glutamyl) lysine bonds, despite immunohistochemistry failing to reveal the presence of these N ϵ (γ glutamyl) lysine bonds in either DNIs or NIIs. It should be noted here that whilst this antibody has been used successfully in immunohistochemical studies examining α -synuclein

cross-linking in Parkinsons disease (Andringa et al., 2004), a recent paper cautioned that this antibody is not consistent at recognising these bonds (Johnson *et al.*, 2004). It is possible that the antigen is obscured in R6/2 aggregates using immunohistochemistry and is only revealed upon denaturation for western blotting.

Based on the observations that NIIs and DNIs are immunopositive for both huntingtin and ubiquitin – confirmed in this study through confocal microscopy - it is understandably assumed that it is the mutant huntingtin in the R6/2 model that is ubiquitinated. Indeed, it has been shown that in transformed lymphoblasts derived from a patient heterozygote for HD that huntingtin immunoprecipitates with ubiquitin (Kalchman et al., 1996). However, as the possibility remains that it is other proteins within aggregates that are ubiquitinated, and in order to determine the situation in the R6/2 model, immunoprecipitation and western blotting techniques were used to answer this. The 1C2 antibody recognises expanded polyglutamine stretches (Trottier et al., 1995) and was shown here to recognise mutant huntingtin in R6/2 mice as a smear from ~70 kDa upwards, as expected and in agreement with published data (Davies et al., 1997). When 1C2 antibody was used to blot against proteins immunoprecipitated using anti-ubiquitin antibodies from R6/2 whole-brain lysates, a prominent smear was detected from ~25 kDa upwards, implying that aggregated mutant huntingtin is ubiquitinated in the R6/2 model. Additionally, bands are detectable at ~70, 30, 18 and 15 kDa, with the 70 kDa band most likely to represent soluble, ubiquitinated mutant N-terminal huntingtin and the other bands representing proteolytically cleaved ubiquitinated fragments. It is possible that their absence from 1C2 western blots could

be due to their low levels that become concentrated upon ubiquitin-conjugate immunoprecipitation. It should be mentioned here that whilst this study shows that huntingtin protein is ubiquitinated in the R6/2 model, it does not demonstrate that ubiquitinated huntingtin is exclusively a proteasomal substrate. As mentioned previously, there are several types of polyubiquitin chains, (Lys-11, Lys-48, Lys-63 etc), and only Lys-48 is known to signal proteasomal degradation. However, a recent paper examined the ratios of polyubiquitin chains to unconjugated ubiquitin in several HD models, including the R6/2, and found that Lys-48 polyubiquitin chains, as well as Lys-11 and Lys-63 chains, progressively accumulated with the disease (Bennett *et al.*, 2007). The authors concluded that the UPS was impaired in HD, and combined with the immunoprecipitation data presented here, it seems likely that, the proteasome is a target, amongst other destinations, for ubiquitinated huntingtin protein in the R6/2 model.

These results demonstrate that the mutant huntingtin found in aggregates is ubiquitinated in R6/2 mice and at least a proportion of this is likely to be a substrate for proteasomal degradation. Through ultrastructural analysis, R6/2 aggregates appear to be generally amorphous and granular in nature implying that they are not primarily composed of filaments. This study also shows that N ϵ (γ glutamyl) lysine bonds are increased in brains of R6/2 mice, are present in aggregated proteins, and specific bands detected via western blot are likely to correspond to dimers and trimers of N-terminal mutant huntingtin. Taken together, these results suggest that nuclear and cytoplasmic aggregates are likely to be formed via the process of transglutamination in R6/2 mice.

4.1.2 Protein recruitment to nuclear and neurite aggregates

Whilst some immunohistochemical and immunofluorescence studies have reported staining of huntingtin-positive aggregates with antibodies against proteasome subunits, it is unclear whether all complexes of the proteasome relocate. Often, no distinction is made between nuclear and cytoplasmic inclusions and consequently, whether the proteins recruited to these compartmentalised aggregates differ. Indeed, this is compounded by the fact that often many cellular models of polyglutamine expansion diseases are characterised by the presence of cytoplasmic aggregates and do not produce nuclear aggregates. Therefore, caution should be taken in compiling data regarding the protein composition of aggregates from various models of polyglutamine disease. This study provides the first thorough immunohistochemical analysis of proteasomal subunits / complexes recruited to neuronal nuclear and cytoplasmic inclusions in the most studied model of HD, the R6/2.

There appears to be clear differences in the recruitment of proteasomal complexes to nuclear and cytoplasmic inclusions in the R6/2 model. Immunohistochemical analysis presented here showed that nuclear aggregates contained 20s and 19s complexes and also weakly stained immuno-positive for 11s α , but not 11s β or 11s γ , in a small proportion of nuclear aggregates. Whilst 11s γ has been suggested to play a role in the pathology of HD (Goellner *et al.*, 2003), as it is only small subset of NIs that label

immunopositive for these proteins, it is likely that any potential role played by 11sy is not particularly significant. Indeed, 11sy regulatory complexes may even localise to NIIs purely through affinity for the concentrated pools of 20s proteasomes present. As 11sy are known to alter peptidase activities of the proteasome, it is likely that in this small subset of 11sy-positive NIIs, proteasomes exhibit a slightly different proteolytic pattern to 11sy-negative NIIs due to the presence of different proteasomal subtypes. Unexpectedly, this study showed that cytoplasmic aggregates only stained immunopositive for 19s subunits and failed to be stained by antibodies against 20s or 11s subunits. Although the results presented here show that antibodies recognising proteasome subunits generally seem to stain DNIs slightly more weakly than NIIs, this is unlikely to account for the lack of 20s proteasome immunodetection in DNIs as both the 20s α and 20s “core” antibodies stain NIIs intensely and fail to stain any DNIs. Additionally, as electron microscopic analysis of aggregates in R6/2 mice showed that NIIs and DNIs both appeared very similar ultrastructurally, it is unlikely that 20s antigens are differentially obscured between these types of inclusions.

The finding that nuclear and cytoplasmic aggregates differ in terms of proteasome complexes is interesting for several reasons. Firstly, whilst 20s proteasomes have been described in the nucleus, they are predominantly thought of as cytoplasmic complexes, (Knuehl et al., 1996) and, as such, would be expected to be able to localise to and attempt to degrade cytoplasmic aggregates. Secondly, as DNIs are strongly immunopositive for 19s complexes, one would expect the 20s proteasome to be there additionally, even if purely by affinity for protein-protein interactions with 19s

complexes. Thirdly, and perhaps most pertinent to this study, this would reflect differences in the ability of nuclear and cytoplasmic aggregates to be degraded by the proteasome. The 20s complex, containing the catalytic sites is the central element of the proteasome, and without it the 19s and 11s subunits are largely redundant, in terms of protein degradation. Therefore, it follows that if cytoplasmic aggregates contain 19s subunits, but no 20s proteasomes, then proteasomal proteolysis is comparatively inactive in DNIs compared to NIIs. This is not to say that proteolysis does not occur in the cytoplasmic aggregates; 20s proteasomes might well be present, but to a far lesser degree than in NIIs; additionally, non-proteasomal proteases, such as calpains present in the cytoplasm could play a role in proteolysis-dependent formation of DNIs. One of the implications of differences in proteasomes present in cytoplasmic and nuclear aggregates is that one would expect that they should contain different length fragments as a result of differential proteolysis in the two compartments. Interestingly, one of the few papers highlighting differences between cytoplasmic and nuclear aggregates, demonstrated that like nuclear aggregates, cytoplasmic aggregates are made up of N-terminal fragments, although slightly larger in size (Lunkes et al., 2002), implying differences in the cleavage patterns between the two compartments. This could play a role in why cytoplasmic aggregates occasionally contain fibers, whilst NIIs do not appear to.

The question remains as to why DNIs are strongly immunopositive for 19s complexes when there are no 20s complexes there. It is known that certain 19s subunit bind polyubiquitin chains and could, therefore, be recruited to aggregates containing

ubiquitinated N-terminal mutant huntingtin. It seems strange, however, given the 19s' affinity for 20s complexes that 20s complexes do not localise to DNIs.

As this study showed that NIIs in R6/2 mice contained a heterogeneous mix of ubiquitinated huntingtin, 20s and 19s proteasomes (and in some cases 11sy), the possibility remained that NIIs are additionally sites of proteasome formation and ubiquitination. To test this hypothesis, western blotting and immunohistochemical analysis was performed using antibodies against proteins involved in these processes. Proteasome maturation protein (POMP) is the mammalian homologue of UMP1, a yeast protein, that is thought to act as a chaperone in the complex biogenesis of 20s proteasomes (Witt et al., 2000). In the present study, POMP was shown to localise to a proportion of NIIs, but not to DNIs, implying that proteasomal biogenesis takes place within the NII. Whether this represents a high level of 20s biogenesis in NIIs or is indicative of incomplete maturation remains unclear. However, once again, this highlights another difference between NIIs and DNIs, although, in this case, the absence of POMP was not wholly unexpected from DNIs based on this study's previous observations that they are not immuno-positive for 20s complexes. Western blot analysis presented here revealed that soluble POMP is depleted in R6/2 mice, although overexposure of the blot revealed the presence of aggregated and insolubilised POMP appearing as a smear. It would seem understandable that, considering that 20s α and β subunits form high molecular weight species, insolubilise and aggregate, too, in the R6/2 model (discussed in 4.2.2), that POMP, which would bind to them would also insolubilise.

The ubiquitination of huntingtin is still relatively poorly understood. Currently, huntingtin has been shown, through yeast two-hybrid screening, to interact directly with two enzymes involved in ubiquitination, the ubiquitin conjugating enzyme, E2(25k)(Kalchman et al., 1996) and more recently, the ubiquitin ligase, Hrd1 (Yang et al., 2007). Western blot analysis presented here revealed a significant decrease in soluble E2(25k) coupled with its insolubilisation, denoted by the appearance of a high molecular weight smear in R6/2 mice. That E2(25k) would insolubilise and aggregate is not wholly unexpected as the mutant huntingtin to which it is postulated to bind to, does so. Interestingly, the protein smear is detected clearly from ~140 kDa upwards, the size of the first band clearly visible in isopeptide blots which is postulated in this study to represent a dimer of N-terminal mutant huntingtin. It seems likely that monomers of huntingtin are more readily able to be degraded, but oligomers, possibly formed via transglutamination, become progressively more resistant to proteolysis, and are therefore more persistent in the cell. This would give rise to the smear from ~140 kDa upwards seen here. Whilst immunohistochemistry failed to label E2(25k) in aggregates in R6/2 mice, it is possibly due to this particular antibodies unsuitability for this particular application.

Ubiquitin-like proteins (UBLs), such as SUMO-1, SUMO-2/3, NEDD8 and ubiquitin, represent a particularly interesting family of proteins in the context of R6/2 pathology. SUMO-1, SUMO-2/3 and NEDD8 have all been shown to act as protein modifiers, binding to target proteins in a similar manner to ubiquitin, through a series of E1, E2

and E3 enzymes (Kerscher et al., 2006). The data presented here shows that in the R6/2 model, aggregates are heavily ubiquitinated and contain proteasome components and ubiquitin-conjugating enzymes; as UBLs bind similarly to ubiquitin, it seems possible their levels or that of their conjugates may be affected, as may localisation. To investigate these possibilities, immunohistochemical and immunofluorescent analysis was used to demonstrate that NIIs, but not DNIs, were strongly immuno-positive for SUMO-1 and SUMO-2/3. As mentioned previously, SUMO proteins have been implicated in the nuclear transport of proteins, and are attached to target proteins through similar mechanisms to ubiquitin. If the enzymatic machinery to ubiquitinate proteins is aggregated in R6/2 mice, then it is possible that similar enzymes responsible for SUMOylation are there, too. It seems plausible that in addition to NIIs acting as sites of proteolysis and ubiquitination, they could also be sites of UBL processing and attachment.

Additionally, this study performed western blot analysis using antibodies against SUMO-1 and SUMO-2/3 to analyse protein levels and those of their conjugates in R6/2 mice. This demonstrated that, in both cases, the soluble pools were absent or severely depleted when compared to control animals. Instead, aggregated SUMOylated conjugates were detected retained in the well of the stacking gel and as a very high molecular weight smear (250 kDa+). Whilst it would be attractive to suggest that it is mutant huntingtin that is SUMOylated, this would seem to be unlikely given that, in the R6/2, mutant huntingtin is detectable as a smear from ~70 kDa. Interestingly, the high molecular weight conjugates of SUMO-1 and SUMO-2/3 (~80 and ~110 kDa,

respectively) that are detectable in the litter-mate control are absent in R6/2 brains. This would seem to indicate that either normal SUMO conjugates aggregate or that the depleted soluble pool of free SUMO, due to insolubilisation in aggregates and therefore reduced SUMO recycling, reduces conjugation to SUMO's normal protein targets. Another possibility is that these proteins which are SUMOylated in litter mate controls are absent in the R6/2 model. However, it seems more likely that a depletion of the pool of free SUMO would serve to limit the normal processes of SUMO.

The UBL, ubiquilin, has been suggested to target polyubiquitinated proteins to the proteasome (Ko et al., 2004). Whilst not a UBL, the type II AAA (ATPases associated with a variety of activities) ATPases, valosin-containing protein (VCP) was also investigated here, because amongst its various diverse cellular functions is the targeting of polyubiquitinated proteins to the proteasome (Woodman, 2003). Therefore, immunohistochemistry and western blot analysis were used to investigate VCP and ubiquilins potential involvement in R6/2 neuropathology.

It was unexpected that ubiquilin labelled nuclear but not cytoplasmic aggregates, as ubiquilin is known to bind both polyubiquitin chains and 19s proteasome subunits (Ko et al., 2004), which this study has shown that DNIs are abundant in. However the potential role that ubiquilin plays is somewhat confusing as, whilst it has been shown to bind both polyubiquitin chains and the proteasome, in overexpression studies, it's binding to target proteins perversely enhances their stability (Funakoshi et al., 1999; Massey et al., 2004). If ubiquilin indeed binds to mutant huntingtin, then whilst it

might seem like an attractive explanation for its persistence in the cell and presence in NIIIs, it would seem odd that DNIs do not label, given their mutant huntingtin and ubiquitin content. Despite repeated attempts in this study, VCP antibodies failed to label either aggregates, but given its aggregation and insolubility, as determined by western blot analysis (see below), it seems likely that this represents an unsuitability of this antibody for immunohistochemistry.

This study also used western blot analysis to analyse the levels and potential insolubility of VCP and ubiquilin. As in the case of SUMO proteins, soluble ubiquilin and VCP were greatly reduced and accompanied by a smear on the membrane, implying aggregation. It seems likely that the reduced soluble pools of these proteins will have implications on the targeting of normal cellular substrates of these proteins to the proteasome and it remains possible that this would result in their reduced degradation. Furthermore, as VCP has been implicated in cellular functions other than degradation such as membrane fusion and DNA replication (Woodman, 2003), a reduced soluble pool is likely to have an impact on cellular homeostasis. Interestingly, the blot for VCP displays a slightly different smear pattern to that of the UBLs; it seems to be split into two densities of smear; initially, the smear begins at ~160 kDa and then becomes much more intense from ~230 kDa. These blots bear similarities to western blots against the isopeptidase bonds formed by transglutamination. It is possible that this represents VCP binding to dimers and trimers of N-terminal huntingtin with increasing efficiency. A recent study has shown that the degradation of N-terminal huntingtin (with an expanded polyglutamine tract), overexpressed in cells,

is VCP-dependent (Yang et al., 2007). This would favour the notion that in the R6/2 model, N-terminal huntingtin is bound to VCP, perhaps in a shuttling role. However, the function that VCP is playing here is difficult to assess as, somewhat similarly to the case of ubiquilin, a recent paper has demonstrated a role for VCP in both the formation and elimination of polyglutamine aggregates (Kobayashi et al., 2007).

Chaperones, too, represent an interesting family of proteins in the context of neurodegenerative diseases of aggregation. Chaperones are known to bind to misfolded proteins and either assist in their refolding or present them to the proteasome (Esser et al., 2004). In the present study, immunohistochemistry was initially employed to identify which chaperones localised to aggregates in the R6/2 model, the rationale being that these would be relevant to pathology. Out of the extensive range of antibodies tested, only members of the Hsp70 family (Hsc70 and HDJ-2 / DNAJ), although noticeably, not Hsp70 itself, were shown to localise to NIIs and, once again, not to DNIs. It was reasoned that as Hsc70 and HDJ-2 / DNAJ seemed to be involved in R6/2 neuropathology, western blot analysis of the Hsp70 family should be undertaken to analyse their protein levels. In agreement with the immunohistochemical data neither Hsp40 nor Hsp70 were aggregated or insolubilised as determined by the absence of smear on western blots. A somewhat unexpected result, given Hsc70's redistribution to NIIs, was that levels of Hsp70 were unaffected in the R6/2 model. As Hsc70 is constitutively present in neural tissue, and Hsp70 is upregulated in cellular stress (Pavlik *et al.*, 2007; Tytell, 2005), this would imply that brains of R6/2 mice do not undergo a typical heat-shock response in response to mutant huntingtin expression. However, this present study describes an absence, or

severe reduction, of Hsp40 in the R6/2 mice and this represents an interesting finding; Hsp40, like HDJ-2, is a co-chaperone of Hsc70 (Fink, 1999) and this absence would reduce Hsc70's ability in refolding. However, soluble levels of both Hsc70 and HDJ-2 were slightly decreased in the R6/2 model, yet both also aggregated and insolubilised, as detected by a smear. These findings are interesting because they seem to indicate that mutant huntingtin expression does not elicit a typical cell stress response in R6/2 mice brains. Rather, levels of the Hsc70 co-chaperone, Hsp40, are reduced, with no elevation of the inducible Hsp70 and both the constitutive protein, Hsc70, and HDJ-2 aggregate and relocate to NIIs but not DNIs. These findings are also consistent with another study detailing decreased HDJ-2 levels, and redistribution of Hsc70 and HDJ-2 to nuclear, but not neurite aggregates in R6/2 mice (Hay *et al.*, 2004). Another study crossed R6/2 mice with those overexpressing Hsp70 and found a modest delaying effect on disease phenotype (including aggregate formation), implying that the role that Hsp70 plays in R6/2 alleviating neuropathology might be not as significant as previously suggested (Hansson *et al.*, 2003). Proteins such as BAG-1 and CHIP are known to bind both proteasomes and Hsc70, and can serve to present Hsc70 bound proteins to the proteasome for degradation (McDonough *et al.*, 2003). This shift from refolding to degradation could be particularly relevant here, given that a non-typical cell stress response is displayed. However, as immunostaining and western blotting with antibodies raised against both CHIP and BAG-1 failed to label aggregates or detect the relevant proteins, this role was unable to be investigated.

NIIIs seem to act as focal points for proteasomal proteolysis, similar to the concept of clastosomes. The term clastosomes was coined by Lafarga *et al.*, who described them as nuclear bodies, enriched in 19s and 20s components, ubiquitin conjugates and UPS substrates. Clastosomes are rarely found in normal conditions, but occur when proteasomal activity is stimulated and curiously disappear upon proteasomal inhibition (Lafarga *et al.*, 2002). Interestingly, inhibition of the proteasome suppresses NII formation in cultured postmitotic neurons (Kim *et al.*, 2004). This study concludes that in the R6/2 line, as global proteolysis is increased (chymotrypsin is thought to be the most important peptidase activity of the proteasome; see 4.2), and NIIIs have been shown to contain 11s, 19s and 20s components, NIIIs can be considered to be clastosomes. Additionally, this study has shown that NIIIs also contain POMP, E2(25k) and PA200, insinuating that not only are clastosomes areas of intense proteasomal activity, but areas of ubiquitination and proteasomal formation / maturation. Additionally, this study shows that UBL proteins also recruit and aggregate in these clastosomes. This extends the current definition of clastosomes.

Interestingly, another focal point of proteasomal activity has been described, with a juxtannuclear localisation, the aggresome (Taylor *et al.*, 2003). Whilst DNIs are also cytoplasmic, unlike aggresomes they are found in the neurites of affected neurons. Additionally, aggresomes become membrane bound and have been known to fuse with lysosomes. There appears to be no such comparison with inclusions in R6/2 mice (Professor Stephen W. Davies, UCL, UK, personal communication) and contrary to what some studies have suggested, NIIIs and DNIs are not analogous to aggresomes.

4.2 Proteolysis in the R6/2 model

The presence of insoluble protein aggregates, shown to contain ubiquitinated expanded polyglutamine-containing protein and proteasome components, has led to suggestions that the UPS is inhibited in models of polyglutamine expansion disease. Therefore, fluorometric assays were used to determine proteolytic activity in the brains of R6/2 mice.

4.2.1 Altered Proteolysis in the R6/2 model

Initially, fluorometric degradation assays were performed without the use of a specific proteasome inhibitor, thereby measuring total (both proteasomal and non-proteasomal) proteolysis, and in the presence or absence of SDS. SDS is a known potentiator of the proteasome and is thought to activate latent 20s proteasomes by opening the channel pore (Shibatani *et al.*, 1995). This study showed that in the absence of SDS, both PGPH and chymotrypsin-like activity were increased, whilst trypsin-like activity was decreased. That chymotrypsin-like activity is significantly increased in the presence of SDS implies that additional to the proteasomes expressing elevated chymotrypsin-like peptidase activity in the R6/2 model are proteasomes present in a latent state. This represents an interesting finding because it implies that there are additional functional

but inactivated proteasomes, when compared to litter-mate controls, that could be harnessed to increase cellular degradation, which would have implications for future therapeutic approaches. Additionally, that the decrease in trypsin-like activity is abolished in the presence of SDS could mean that there are proteasomes capable of normal trypsin-like activity. It has been postulated that expanded polyglutamine containing proteins could become physically stuck in the 20s pore, thus causing proteasomal inhibition. It is plausible that, in this scenario, mutant huntingtin could block the active sites relevant to trypsin-like activity and leave the others relatively unaffected. SDS could open the channel enough to “free” the 20s pore from mutant huntingtin, which would have the effect of normalising the trypsin-like activity as seen. However, as these were preliminary experiments analysing total peptidase activity (proteasomal and non-proteasomal) and were intended to serve as a starting point to gauge any gross changes prior to more specific experiments aimed at measuring proteasomal activity, further proteolytic assays were performed in the absence of SDS in order to represent a more physiological assessment of proteolysis.

Whilst there have been studies investigating proteolysis in cells transfected with mutant huntingtin / polyglutamine, the *in vivo* studies have not always reflected accurate measures of proteasomal activity. Diaz-Hernandez *et al.*, reported increases in both chymotrypsin and trypsin-like proteasomal activities in HD94 mice (Diaz-Hernandez *et al.*, 2003). However, this study used lactacystin, which has been shown to be a non-specific inhibitor of the proteasome (Rodgers *et al.*, 2003; Vigouroux *et al.*, 2003a; Vigouroux *et al.*, 2003b), and Triton X-100, which has been shown to

inhibit the proteasome (Arribas *et al.*, 1990). Other detergents, such as SDS, have been shown to increase the activity of the proteasome by opening the pore (Shibatani *et al.*, 1995). Consequently, detergents should not be used in assays to ascertain the state of proteasomal activity in neurodegenerative disease, as by increasing or inhibiting the proteasome, they do not reflect a physiological representation of peptidase activity. Another study has attempted to study proteasomal activity in HD brains and skin fibroblasts (Seo *et al.*, 2004), finding both PGPH and chymotrypsin-like activity to be decreased. However, this study measured PGPH and chymotrypsin-like and not trypsin-like activity and did so in without the use of a specific proteasome inhibitor, thereby also measuring protease activity. In the present study, to differentiate between proteasomal and non-proteasomal proteolysis, peptidase activity was measured in the presence and absence of epoxomicin. Epoxomicin is the most specific proteasomal inhibitor currently known and a concentration of 20 μ M, is sufficient to inhibit chymotrypsin-like, trypsin-like and PGPH-like proteolytic activities of the 20s proteasome (Dr. Alexei Kisselev, Dartmouth Medical School, USA, personal communication and (Sin *et al.*, 1999). Therefore, this represents the first accurate study of both proteasomal and non-proteasomal chymotrypsin, trypsin and PGPH-like peptidase activity in a murine model of HD.

This study shows that in the R6/2 model, the 20s proteasome is not inhibited, but exhibits a differential proteolytic profile when compared to litter mate controls, with some activities increased (PGPH and chymotrypsin-like) and one decreased (trypsin-like). Furthermore it shows that chymotrypsin-like, trypsin-like and PGPH non-

proteasomal peptidase activities are all decreased. However, which specific non-proteasomal protease contributes to the cleavage of these fluorogenic substrates is unclear at present. One study has described the presence of a novel 105 kDa protease in brain that exhibits both chymotrypsin-like and trypsin-like activity (Vigouroux et al., 2003b). This is likely to be one of many cellular proteases that contributes to cleavage of fluorogenic compounds in these types of proteasomal activity assays. It is known that several proteases function and reside within the highly acidic, membrane-bound environment of the lysosome and, because the fluorometric assays were conducted at a higher pH, it is unlikely that lysosomal proteases would, or indeed could, contribute to the measured non-proteasomal peptidase activity in this study. Whilst this thesis is predominantly concerned with the contribution of the proteasome to cellular proteolysis, other non-proteasomal proteases play a significant part in the degradation of the measured fluorometric substrates. For example, this study shows that in control animals, nearly 60% of all measured trypsin-like activity is via non-proteasomal proteases, compared to just 25% in R6/2 animals. In fact, as all of these non-proteasomal activities are greatly reduced in the R6/2, and two activities (PGPH and chymotrypsin-like) are increased in proteasomes, it implies that the cell becomes much more dependent on the proteasome to degrade proteins. To the authors knowledge, this apparent shift in favour of proteasomal proteolysis in the R6/2 has not been noted before in the literature.

There are certain problems associated with interpreting the data from these fluorometric assays. Firstly, unlike global proteasomal changes (ie. increases or

decreases in all of the peptidase activities), the data from the R6/2 model shows that some activities are increased, whilst one, the trypsin-like activity, is decreased. The actual effects on protein degradation are therefore very difficult to estimate. Chymotrypsin-like activity has often been reported to be the most important of the proteasomes peptidase activities and is seen to be increased dramatically in the R6/2 model alongside increases in PGPH activity, so global proteasomal proteolysis might be seen to be increased. This problem is compounded by the fact that all of the non-proteasomal proteases activities are decreased in R6/2 mice, and, as mentioned before, because they are responsible for a significant proportion of proteolytic activity, it is difficult to take into account when considering total protein degradation. Secondly, it should be borne in mind that this study demonstrates differential proteolysis in whole brain samples in R6/2 mice as opposed to measuring the proteasomal activity in specific brain regions or even cellular compartments. A recent study shows regional differences in proteasomal activity in the brain (Zeng et al., 2005), highlighting the fact that there are different heterogeneous populations of proteasomes in different brain areas anyway. It is possible, and perhaps even likely, that specific regions of the brain are more dramatically affected than others; measuring proteolysis in whole brain homogenates is likely to mask some of those differences and therefore makes the changes seen here that much more striking. Additionally, it seems likely that there are compartmental differences in the proteolytic profiles of, for example, nuclear versus cytoplasmic proteasomes. This is highlighted by the differential recruitment of proteasome components to NIIs and DNIs and could potentially be a factor in why

cytoplasmic and nuclear inclusions appear to be made up of different fragments of mutant huntingtin (Lunkes et al., 2002).

Three very recent studies, published during the writing of this thesis, are pertinent and should be mentioned here. The first study employed a novel method to analyse proteasome activity using mass-spectrometry to measure polyubiquitin chains, which the authors concluded was a valid method to measure proteasome impairment, and found that in both R6/2 and HD brains, global proteasomal function was decreased (Bennett et al., 2007). However, this does not mean decreases in overall proteasomal proteolysis, ie. decrease in protein degradation (one of the problems with interpreting the data from fluorometric methods). The authors essentially use a comparison of free ubiquitin to polyubiquitin chains with the implication being that increased “build up” of polyubiquitinated conjugates represents UPS dysfunction. Whilst this is a novel and useful system to measure *general* UPS function it is plausible to imagine several scenarios which would caution against using this method as a measure of *proteasomal function*: increased rates of ubiquitination could cause a build up of polyubiquitinated conjugates; perturbations of polyubiquitin shuttling proteins to the proteasome would increase conjugates; polyubiquitinated proteins could be insoluble (as is the case with many neurodegenerative proteins), aggregate and be resistant to degradation and therefore persistent in the cell regardless of proteasome function etc. So whilst the authors say that the UPS is dysfunctional to a greater extent in the R6/2 model (this present study confirms this and sees many changes to various elements of the UPS) and HD patients than previously thought, at which level this first occurs is unclear.

Another study of interest here used both fluorometric substrates and a series of reporters to analyse UPS function and proteasomal proteolysis in a striatal cell model of HD (Hunter et al., 2007). This study used a comprehensive methodology to investigate UPS function and activity and also found that the proteasome was differentially regulated. However, the authors discovered that PGPH and chymotrypsin-like activities were slightly decreased, whilst trypsin-like activity was increased; the opposite pattern of what is seen in this present study. There could be several reasons for this discrepancy. Firstly, the present study was performed using whole brain homogenates, whilst the study by Hunter *et al.* specifically used a striatal cell line. It is expected that neural cell type will affect proteasomal profile and the use of whole brain homogenates masks cell-specific differences in proteasome activity. It would be ideal to compare the proteasomal profile of several cell types derived from HD and control brains. Secondly, the model from which these cells are derived differ in their neuropathology from R6/2 mice. It is possible that the proteolytic profiles are slightly different between these models (as in the immunoproteasome involvement in HD94 mice) and as mentioned before, caution should be exercised extrapolating data from one model to another. However, the present study, like the work of Hunter *et al.* interestingly shows differential proteolytic profiles as a result of polyglutamine expansion. The third interesting recent study measured chymotrypsin-like activity in R6/2 mice and, in agreement with the present study, found increases when compared to control animals (Bett et al., 2006). Additionally, whilst Bett *et al.* reported smaller increases in chymotrypsin-like activity than those reported in this study, they also noted that this increase was not significant at 8 weeks of age, only becoming apparent

by 13 weeks. This would imply that changes in proteasomal activity occur fairly late in the pathology of R6/2 mice and are not a primary event. All the mice used in the present study are 13 weeks old; it would be of interest to know at what stage more sensitive assay conditions would note a change in proteolysis. However, it should be noted that Bett *et al.* only measured chymotrypsin-like activity and it is wholly possible that early changes can be detected in PGPH or trypsin-like activity.

The UPS is a fundamental mechanism for controlled protein degradation in all cells and is central to many different cellular processes. As proteasomes in the R6/2 model exhibit very different proteolytic profiles when compared to litter mate controls, it is probable that some of the pathological features of polyglutamine expansion diseases could be either exacerbated or come as a direct consequence of altered proteolysis. For example, the proteasome is involved in the regulation of transcription factors (Lipford *et al.*, 2003) and transcriptional dysregulation has been suggested as a mechanism of neurodegeneration in polyglutamine expansion diseases (Helmlinger *et al.*, 2006; Thomas, 2006). It is possible that the described changes in gene regulation are a result of altered proteolysis, and therefore transcription factor regulation. Additionally, amongst the many described functions of the UPS, a role in mediating morphological changes in dendritic spines has been proposed, whereby UPS-dependent degradation of certain proteins (eg. spine-associated Rap GTPase activating protein (SPAR)) result in dissipation of dendritic spines (Yi *et al.*, 2005). Indeed, morphological changes have been reported in dendrites and their spines in HD brains (Ferrante *et al.*, 1991; Graveland *et al.*, 1985). Furthermore, dendritic retraction and spine dysmorphia is a

pathological feature of striatal, cortical and hippocampal neurons in the R6/2 model (Aysha Raza, UCL, personal communication and (Klapstein *et al.*, 2001). It seems plausible to suggest that the altered proteasomal activation seen in R6/2 mice brains could be a contributory or, indeed, causative factor in dendritic dysmorphia. Taking this idea a step further, it is known that R6/2 brains weigh considerably less than their age-matched litter mate controls (Davies *et al.*, 1997) and that this may be due to neuronal shrinkage and not cell death (Aysha Raza, UCL, personal communication). Perhaps, on a larger scale, the altered peptidase activity displayed by the proteasome could result in increased degradation of cellular proteins and cell shrinkage. It is already known that muscle cachexia, a feature of cancer and AIDS patients, can occur through a proteasome dependent mechanism, and that attempts have been made to inhibit muscle breakdown through inhibition of the proteasome (Acharyya *et al.*, 2007).

4.2.2 Regulation of the proteasome in the R6/2 model

There are several possible factors that could contribute towards the altered proteasomal proteolysis seen in the R6/2 mice: 1) Altered levels of the 20s core particle, 2) changes in maturation of the proteasome, 3) changes in the subunit composition of the 20s proteasome or 4) changes in one (or more) regulatory particles of the 20s proteasome.

As the various peptidase activities of the proteasome can be attributed to specific subunits of the proteasome, initially western blot analysis was used to determine levels or potential changes to these 20s β -subunits in addition to 20s α -subunits in the R6/2 20s proteasome. It should be noted here that there are inherent problems that can present when comparing proteins levels in the R6/2 model versus litter-mate controls. Whilst soluble protein levels may be readily compared, it is difficult to interpret levels of aggregated protein when coupled with decreases in soluble protein, as higher molecular weight proteins (including aggregates) are known to transfer less efficiently to nitrocellulose membranes. Having stated that, in the case of 20s α -subunits in the R6/2 model compared to litter-mate controls, there is a clear increase in soluble 20s α -subunits in addition to several higher molecular weight species and aggregated protein. As the 20s α antibody is raised against and recognises many 20s proteasome α -subunits, it can be seen as a useful tool for comparing levels of the 20s proteasome per se. Whilst increases in protein levels cannot be confirmed from western blot analysis of 20s β -subunits (due to decreases in soluble protein, coupled with higher molecular weight bands and aggregated protein) it seems probable that the entire 20s proteasome is upregulated, and not just the α -subunits. An implication of this is that the increases in PGPH-like and chymotrypsin-like peptidase activities could be simply due to increases in levels of 19s (see below) and 20s core particles. However, as altered levels of PI31K (see below) were also noted, the increased levels of 20s core particles in the R6/2 model is more likely to represent a contributory factor to increased PGPH and chymotrypsin-like activities.

In the cases of β_1 and β_5 subunits, the soluble form of the proteins was absent and greatly reduced, respectively. As mentioned previously with regards to comparing soluble and insoluble proteins, it is impossible to infer whether or not the protein levels of these subunits is altered, but it is clear that immunodetection of both subunits was almost exclusively in insoluble smears. It has been argued that sequestration of proteins into polyglutamine aggregates could reduce or even nullify their function, thus contributing to neurological dysfunction (Donaldson *et al.*, 2003). For example, in a cell culture model of SCA-3, it has been shown that CREB-binding protein (CBP) relocalises to aggregates, resulting in reduced levels of soluble CBP, despite an increase seen in CBP mRNA, and that rescue of cellular toxicity could be achieved by overexpression of CBP (McCampbell *et al.*, 2000). Data from the various experimental approaches can be used to answer important questions regarding the functionality of proteins that have been retarded in aggregates. Both immunohistochemical and western blot data show that nearly all of the detected 20s β_1 and β_5 subunits in R6/2 brains is present within insoluble aggregates (retained at the top of the gel in western blots or localised to aggregates in immunohistochemistry analysis) and that soluble forms of the protein are near absent. However, data from the fluorometric assays show elevation of the corresponding chymotrypsin-like and PGPH-like proteasomal activities (see 4.2). Importantly, this implies that whilst these 20s proteasomal subunits may become insolubilised in aggregates, they are still functionally active. This is somewhat surprising as it is expected that aggregation of certain 20s proteasome subunits would physically interfere with subunit-subunit interactions and result in them not being able to form whole functional 20s proteasomes. It could still be argued,

however, that sequestration of 20s proteasomes into aggregates could still lead to cellular dysfunction, as the proteasome is not distributed throughout the neuron in a normal manner and could be unable to perform degradative duties in compartments other than aggregates.

The case of the 20s β_2 subunit is slightly different; this subunit corresponds to the trypsin-like peptidase activities of the proteasome, which were found to be decreased in the R6/2 model. 20s β -subunits are initially translated as propeptides that are autolytically cleaved to form mature subunits. For example, 20s β_6 -subunits exist as free propeptides (25 kDa) within the cell, and are cleaved into mature polypeptides (23 kDa) concomitant with their incorporation into intermediate or mature proteasomes (Rodriguez-Vilarino et al., 2000). Western blot analysis using antibodies raised against 20s β_2 subunits revealed the presence of two low molecular weight bands in control samples at ~25 and 28 kDa, likely to correspond to precursor and mature forms of the protein. However, in the R6/2 samples, only the propeptide is detected and the mature polypeptide is absent. This implies that the 20s β_2 subunit may not be normally autolytically cleaved in the R6/2 model. It is possible that there is incomplete maturation of this subunit, and this would help to explain the decrease seen in trypsin-like activity. However, a potential problem with this interpretation is whether or not complete 20s proteasomes are able to form in the absence of a mature β_2 -subunit and utilise a precursor in its formation. Data regarding the assembly of mammalian proteasomes is currently not as well documented as that for yeast proteasomes, and, as such, there are several conflicting models describing formation and the potential

presence of intermediate proteasomes with unprocessed β -subunits (Rodriguez-Vilarino et al., 2000). It is wholly possible that in R6/2 brains, immature β_2 -subunits are incorporated into intermediate proteasomes that exhibit functional peptidase activity. In support of this idea is that intermediate proteasomes have been described with functional catalytic properties (Dahlmann et al., 2000).

To explore the possibility of whether the altered proteasomal proteolytic profile seen in R6/2 mice was due to changes in proteasomal regulation, the protein levels of known 20s regulators were analysed by western blot. Perhaps the best known and comprehensively described regulators of the 20s proteasome are the 11s and 19s regulatory complexes. However, in this study, western blot analysis failed to detect any differences in the levels of soluble 11s α , β or γ subunits between R6/2 and litter mate controls and additionally, unlike that of the 20s subunits tested, higher molecular weight species or insolubilised protein were undetectable. As the immunohistochemical data (discussed in 4.1.2) showed that a small proportion of NIIs were immunopositive for 11s α subunits (and not 11s β or γ), it is unlikely that any of the 11s subunits play a significant role in R6/2 pathology or altered proteolytic profile, and that the 11s α subunits presence in a few NIIs is more likely to be due to its affinity for the 20s proteasome, concentrated in NIIs. As the 11s α regulator is known to alter the proteolytic profile (Li *et al.*, 2001a; Li *et al.*, 2001b) of the 20s proteasome, it would be expected that the 20s proteasomes cleavage pattern will be different in the nuclei containing 11s immunopositive aggregates versus those containing 11s

immunonegative aggregates, although this is only a small proportion of NII containing nuclei.

The 19s complex is thought to activate the proteasome by recognizing ubiquitinated substrates, then unfolding and translocating them into the lumen of the 20s core. Without 19s regulatory complexes, or similar (eg. PA200), 20s proteasomes would effectively not be able to efficiently degrade ubiquitinated substrates. Western blotting was used to analyse the levels of 19s Rpn2 subunits and revealed an increase in protein levels. Whilst it is recognised that this antibody recognises only one subunit of the 19s regulatory complex, as two of the other tested 19s antibodies failed to detect any protein via western blotting in either the R6/2 or litter mate controls, the Rpn2 antibody was relied upon to give an indication of the protein levels of the whole 19s regulatory complex. As the immunohistochemical data revealed that both DNIs and NIIs were strongly immunopositive for antibodies raised against various 19s subunits, and as 20s antibodies labelled NIIs but not DNIs, it could be expected that an increased level of 19s complexes would increase the proteasomal degradation in NIIs. As both 20s and 19s complexes seem to be increased in the R6/2 compared to litter mate controls, it is probable that the increases seen in PGPH-like and chymotrypsin-like peptidase activities are partially due to elevated levels of 19s-20s complexes.

Immunoproteasomes represent another subtype of proteasome with altered proteolytic profiles and, particularly pertinent to this study, when compared to constitutive proteasomes, depress chymotrypsin-like and PGPH activity whilst enhancing trypsin-

like activity (Dahlmann et al., 2000). However, in this study western blot analysis of the levels of the γ -interferon inducible subunits, LMP2, MECL-1 and LMP7 failed to reveal any differences between R6/2 or litter-mate controls. Furthermore, that western blotting failed to show any high molecular weight species or aggregated protein smears coupled with their absence from either nuclear or cytoplasmic aggregates in immunohistochemical studies, clearly demonstrates that immunoproteasomes are not involved in the pathology or differential proteolysis seen in R6/2 mice. This is in contrast to the work of Diaz-Hernandez *et al.*, who detected increased immunoproteasome subunits LMP2 and LMP7 in HD94 brains. Whilst the authors suggest a role in HD neurodegeneration for immunoproteasomes, the significance of this role is questionable given that recruitment of LMP2 only occurs in a very small population (5%) of ubiquitin-positive cortical aggregates. A further difference to what this present study describes in R6/2 mice, as mentioned before, was that the authors reported increases in trypsin and chymotrypsin-like activities in the HD94 model (Diaz-Hernandez et al., 2003). Taken together, this shows that the proteasome expresses a different proteolytic profile and regulation in the R6/2 mouse when compared to the HD94 model and reiterates the differences that exist between models of polyglutamine expansion diseases and the pitfalls of extrapolating data from one model to another.

Two further known regulators of proteasomes were examined, PA200 and PI31K. Western blot analysis of PA200, a proteasome activator that is known to increase proteolysis by opening the 20s pore (Ortega et al., 2005), revealed that soluble species

of PA200 are absent in the R6/2 model and instead form smears on western blots and remain as aggregated in the stacking gel. Whilst this demonstrates redistribution of this protein to, and insolubilisation with, aggregates, as described before, it is impossible to infer any difference in protein levels between the samples. This, again, raises the question of why expression of mutant huntingtin protein would induce the selective aggregation and insolubilisation of seemingly unconnected proteins. For example, it seems odd that 19s, 11s and immunoproteasome subunits do not seem to insolubilise, whilst 20s subunits and PA200, a protein that binds 20s core particle in a similar manner to 19s complexes, do. However, in the case of PI31K, there is a marked decrease in protein levels in R6/2 mice. PI31 is a 31 kDa protein that competes for 20s binding with 11s $\alpha\beta$ and PA200 and is thought to affect proteasomal activity. Whilst not a lot is currently known about PI31K, it has been shown that PI31 inhibits chymotrypsin-like and PGPH-like activity, whilst sparing trypsin-like activity (Zaiss et al., 1999; Zaiss et al., 2002). It seems that the decrease seen in PI31 levels in R6/2 brains, and hence lack of inhibition, could partially account for increased chymotrypsin- and PGPH-like peptidase activity of the proteasome.

The altered proteolytic profile seen in R6/2 mice is due to complex changes in regulation and protein levels of various proteasomal components. In summation, it seems probable that increased chymotrypsin-like and PGPH peptidase activities are likely to be due to a combination of elevated 19s and 20s levels and a decrease in the inhibitory protein, PI31K. The depression of trypsin-like activities clearly requires further examination, but the initial findings presented here potentially indicate

immaturity and incomplete cleavage of 20s β_2 subunits could be responsible for changes in this peptidase activity.

4.3 Future studies

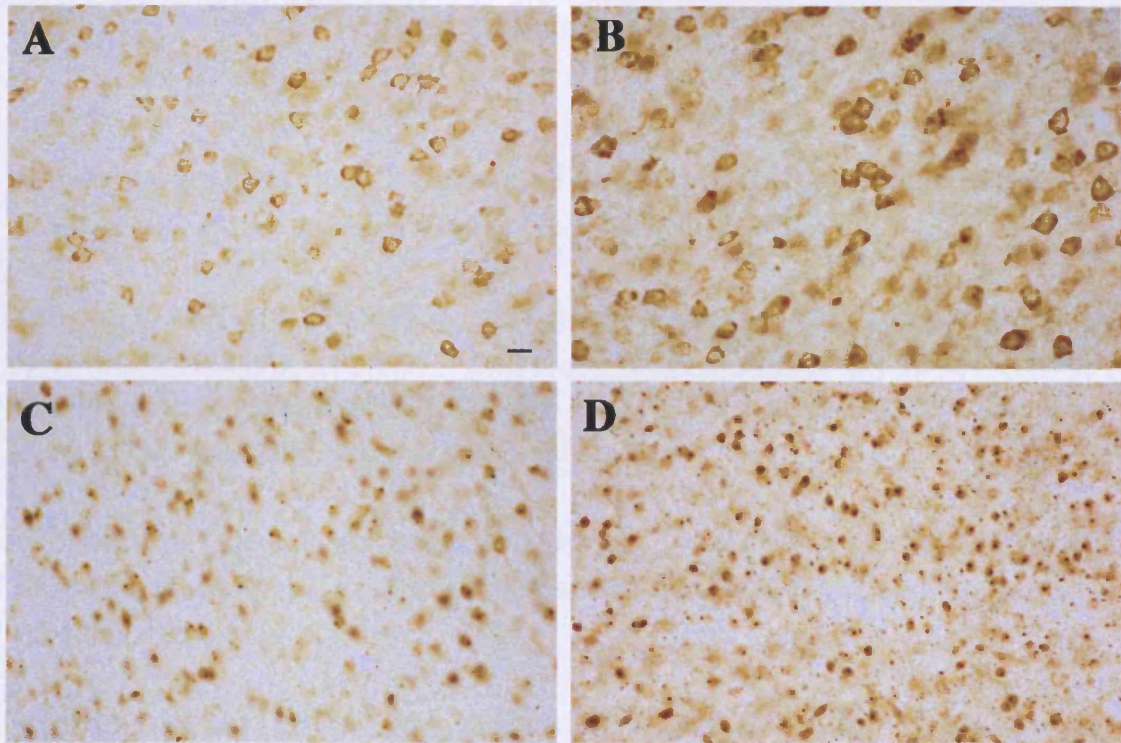
Several areas of future study are clearly required to follow up the questions that this work raises. Firstly, the altered proteolytic profile of R6/2 proteasomes needs to be addressed. A previous study has identified different proteasomes subtypes using negative staining electron microscopy (Cascio *et al.*, 2002). This technique would allow for ratios of proteasome subtypes, for example 19s-20s-19s : 11s-20s-11s : uncapped 20s, to be measured between R6/2 and control samples. Furthermore, combining this approach with a cellular fractionation method (nuclear and cytoplasmic) and further fluorometric assays would provide insights into the differences between cytoplasmic and nuclear proteasomes and how they could contribute to differing cytoplasmic and nuclear aggregates, an area particularly highlighted by this present study. Indeed, a recent study has shown that there is differential regulation of nuclear and synaptic proteasomes in *Aplysia* (Upadhyaya *et al.*, 2006).

Secondly, a combination of western blotting, trypsin gel-digests and mass-spectrometry could be employed to further explore the nature of the post-translational modifications of 20s β_2 subunits and of the high molecular weight species detected in the 20s α blots. This approach could also be used to clarify whether there are any further post-translational modifications of the 20s proteasome that could account for the altered proteolytic profile seen in R6/2 mice. For example, a recent paper described the profound effect of phosphorylation (via PKA) of specific 20s subunits, including β_2 , in altering peptidase activities of murine cardiac proteasomes (Zong et al., 2006).

Several other questions remain: What other proteins regulate the proteolytic profile of 20s proteasomes and are they involved in R6/2 neuropathology? What proteases are responsible for the decreased non-proteasomal proteolysis in R6/2 mice? What is the effect of decreased UBL free pools on the cell? Is deubiquitination affected in the R6/2 model? At what stage does proteolysis first become affected in R6/2 mice?

Conclusions

The work presented here strongly implicates the UPS in the neuropathology of the Huntington's disease mouse model, the R6/2. Both NIIs and DNIs are typically granular, amorphous structures unlikely to be primarily composed of fibrils formed by β -pleated sheets. Instead ubiquitinated mutant huntingtin protein is likely to form oligomers and aggregate through the process of transglutamination. NIIs and DNIs were shown to differentially recruit proteins involved in degradation and refolding. NIIs are rich in many proteasome components, UBLs, and proteins involved in ubiquitination and proteasome biogenesis, further developing the concept of the clastosome. DNIs appear to include far fewer proteins than NIIs and this might be important when considering their respective effects on the cell. Fundamentally, the proteasome is not inhibited in this model, rather it is differentially regulated, whilst the activity of many cellular non-proteasomal proteases is decreased. Global increases in 20s and 19s proteasome levels and decreases in the levels of the proteasomal inhibitor, PI31K, are both likely to be contributory factors involved in increased PGPH and chymotrypsin-like peptidase activities, whilst decreased trypsin-like activity may be as a result of incomplete maturation of the 20s proteasome.



Appendix 2: Representative images demonstrating the “*” scoring scale used for strength of immunohistochemical staining. “-” = antibody unable to label aggregates (A) * = immunostaining of aggregates rare or infrequent (B); ** = moderate quantity of aggregates immunopositive (C); *** = high staining frequency (equivalent to that produced by ubiquitin or Huntingtin antibodies (D). Scale bar=20 μ m.

References

- ACHARYYA, S. & GUTTRIDGE, D.C. (2007). Cancer cachexia signaling pathways continue to emerge yet much still points to the proteasome. *Clin Cancer Res*, **13**, 1356-61.
- AHN, J.Y., TANAHASHI, N., AKIYAMA, K., HISAMATSU, H., NODA, C., TANAKA, K., CHUNG, C.H., SHIBMARA, N., WILLY, P.J., MOTT, J.D., SLAUGHTER, C.A. & DEMARTINO, G.N. (1995). Primary structures of two homologous subunits of PA28, a gamma-interferon-inducible protein activator of the 20S proteasome. *FEBS Lett*, **366**, 37-42.
- ANDRINGA, G., LAM, K.Y., CHEGARY, M., WANG, X., CHASE, T.N. & BENNETT, M.C. (2004). Tissue transglutaminase catalyzes the formation of alpha-synuclein crosslinks in Parkinson's disease. *Faseb J*, **18**, 932-4.
- ARRIBAS, J. & CASTANO, J.G. (1990). Kinetic studies of the differential effect of detergents on the peptidase activities of the multicatalytic proteinase from rat liver. *J Biol Chem*, **265**, 13969-73.
- BAUMEISTER, W., WALZ, J., ZUHL, F. & SEEMULLER, E. (1998). The proteasome: paradigm of a self-compartmentalizing protease. *Cell*, **92**, 367-80.
- BAYER, P., ARNDT, A., METZGER, S., MAHAJAN, R., MELCHIOR, F., JAENICKE, R. & BECKER, J. (1998). Structure determination of the small ubiquitin-related modifier SUMO-1. *J Mol Biol*, **280**, 275-86.
- BENCE, N.F., SAMPAT, R.M. & KOPITO, R.R. (2001). Impairment of the ubiquitin-proteasome system by protein aggregation. *Science*, **292**, 1552-5.
- BENNETT, E.J., SHALER, T.A., WOODMAN, B., RYU, K.Y., ZAITSEVA, T.S., BECKER, C.H., BATES, G.P., SCHULMAN, H. & KOPITO, R.R. (2007). Global changes to the ubiquitin system in Huntington's disease. *Nature*, **448**, 704-8.
- BETT, J.S., GOELLNER, G.M., WOODMAN, B., PRATT, G., RECHSTEINER, M. & BATES, G.P. (2006). Proteasome impairment does not contribute to pathogenesis in R6/2 Huntington's disease mice: exclusion of proteasome activator REGgamma as a therapeutic target. *Hum Mol Genet*, **15**, 33-44.

BOCHTLER, M., DITZEL, L., GROLL, M., HARTMANN, C. & HUBER, R. (1999). The proteasome. *Annu Rev Biophys Biomol Struct*, **28**, 295-317.

BRAUN, B.C., GLICKMAN, M., KRAFT, R., DAHLMANN, B., KLOETZEL, P.M., FINLEY, D. & SCHMIDT, M. (1999). The base of the proteasome regulatory particle exhibits chaperone-like activity. *Nat Cell Biol*, **1**, 221-6.

BUSCHMANN, T., FUCHS, S.Y., LEE, C.G., PAN, Z.Q. & RONAI, Z. (2000). SUMO-1 modification of Mdm2 prevents its self-ubiquitination and increases Mdm2 ability to ubiquitinate p53. *Cell*, **101**, 753-62.

CASCIO, P., CALL, M., PETRE, B.M., WALZ, T. & GOLDBERG, A.L. (2002). Properties of the hybrid form of the 26S proteasome containing both 19S and PA28 complexes. *Embo J*, **21**, 2636-45.

CATTANEO, E., ZUCCATO, C. & TARTARI, M. (2005). Normal huntingtin function: an alternative approach to Huntington's disease. *Nat Rev Neurosci*, **6**, 919-30.

CHAN, H.Y., WARRICK, J.M., ANDRIOLA, I., MERRY, D. & BONINI, N.M. (2002). Genetic modulation of polyglutamine toxicity by protein conjugation pathways in *Drosophila*. *Hum Mol Genet*, **11**, 2895-904.

CHU-PING, M., SLAUGHTER, C.A. & DEMARTINO, G.N. (1992). Purification and characterization of a protein inhibitor of the 20S proteasome (macropain). *Biochim Biophys Acta*, **1119**, 303-11.

CHUANG, J.Z., ZHOU, H., ZHU, M., LI, S.H., LI, X.J. & SUNG, C.H. (2002). Characterization of a brain-enriched chaperone, MRJ, that inhibits Huntingtin aggregation and toxicity independently. *J Biol Chem*, **277**, 19831-8.

CHUN, W., LESORT, M., TUCHOLSKI, J., FABER, P.W., MACDONALD, M.E., ROSS, C.A. & JOHNSON, G.V. (2001). Tissue transglutaminase selectively modifies proteins associated with truncated mutant huntingtin in intact cells. *Neurobiol Dis*, **8**, 391-404.

CICCHETTI, F., PRENSA, L., WU, Y. & PARENT, A. (2000). Chemical anatomy of striatal interneurons in normal individuals and in patients with Huntington's disease. *Brain Res Brain Res Rev*, **34**, 80-101.

CIECHANOVER, A. & BRUNDIN, P. (2003). The ubiquitin proteasome system in neurodegenerative diseases: sometimes the chicken, sometimes the egg. *Neuron*, **40**, 427-46.

CLABOUGH, E.B. & ZEITLIN, S.O. (2006). Deletion of the triplet repeat encoding polyglutamine within the mouse Huntington's disease gene results in subtle behavioral/motor phenotypes in vivo and elevated levels of ATP with cellular senescence in vitro. *Hum Mol Genet*, **15**, 607-23.

CUMMINGS, C.J., MANCINI, M.A., ANTALFFY, B., DEFRANCO, D.B., ORR, H.T. & ZOGHBI, H.Y. (1998). Chaperone suppression of aggregation and altered subcellular proteasome localization imply protein misfolding in SCA1. *Nat Genet*, **19**, 148-54.

CUMMINGS, C.J., SUN, Y., OPAL, P., ANTALFFY, B., MESTRIL, R., ORR, H.T., DILLMANN, W.H. & ZOGHBI, H.Y. (2001). Over-expression of inducible HSP70 chaperone suppresses neuropathology and improves motor function in SCA1 mice. *Hum Mol Genet*, **10**, 1511-8.

DAHLMANN, B., RUPPERT, T., KUEHN, L., MERFORTH, S. & KLOETZEL, P.M. (2000). Different proteasome subtypes in a single tissue exhibit different enzymatic properties. *J Mol Biol*, **303**, 643-53.

DAI, R.M., CHEN, E., LONGO, D.L., GORBEA, C.M. & LI, C.C. (1998). Involvement of valosin-containing protein, an ATPase Co-purified with IkappaBalpha and 26 S proteasome, in ubiquitin-proteasome-mediated degradation of IkappaBalpha. *J Biol Chem*, **273**, 3562-73.

DAI, R.M. & LI, C.C. (2001). Valosin-containing protein is a multi-ubiquitin chain-targeting factor required in ubiquitin-proteasome degradation. *Nat Cell Biol*, **3**, 740-4.

DAVIES, S.W., TURMAINE, M., COZENS, B.A., DIFIGLIA, M., SHARP, A.H., ROSS, C.A., SCHERZINGER, E., WANKER, E.E., MANGIARINI, L. & BATES, G.P. (1997). Formation of neuronal intranuclear inclusions underlies the neurological dysfunction in mice transgenic for the HD mutation. *Cell*, **90**, 537-48.

DE LA MONTE, S.M., VONSATTEL, J.P. & RICHARDSON, E.P., JR. (1988). Morphometric demonstration of atrophic changes in the cerebral cortex, white matter, and neostriatum in Huntington's disease. *J Neuropathol Exp Neurol*, **47**, 516-25.

- DENG, Y.P., ALBIN, R.L., PENNEY, J.B., YOUNG, A.B., ANDERSON, K.D. & REINER, A. (2004). Differential loss of striatal projection systems in Huntington's disease: a quantitative immunohistochemical study. *J Chem Neuroanat*, **27**, 143-64.
- DESTERRO, J.M., RODRIGUEZ, M.S. & HAY, R.T. (1998). SUMO-1 modification of IkappaBalpha inhibits NF-kappaB activation. *Mol Cell*, **2**, 233-9.
- DIAZ-HERNANDEZ, M., HERNANDEZ, F., MARTIN-APARICIO, E., GOMEZ-RAMOS, P., MORAN, M.A., CASTANO, J.G., FERRER, I., AVILA, J. & LUCAS, J.J. (2003). Neuronal induction of the immunoproteasome in Huntington's disease. *J Neurosci*, **23**, 11653-61.
- DIAZ-HERNANDEZ, M., MORENO-HERRERO, F., GOMEZ-RAMOS, P., MORAN, M.A., FERRER, I., BARO, A.M., AVILA, J., HERNANDEZ, F. & LUCAS, J.J. (2004). Biochemical, ultrastructural, and reversibility studies on huntingtin filaments isolated from mouse and human brain. *J Neurosci*, **24**, 9361-71.
- DIAZ-HERNANDEZ, M., TORRES-PERAZA, J., SALVATORI-ABARCA, A., MORAN, M.A., GOMEZ-RAMOS, P., ALBERCH, J. & LUCAS, J.J. (2005). Full motor recovery despite striatal neuron loss and formation of irreversible amyloid-like inclusions in a conditional mouse model of Huntington's disease. *J Neurosci*, **25**, 9773-81.
- DIFIGLIA, M., SAPP, E., CHASE, K., SCHWARZ, C., MELONI, A., YOUNG, C., MARTIN, E., VONSATTEL, J.P., CARRAWAY, R., REEVES, S.A., BOYCE, F.M. & ARONIN, N. (1995). Huntingtin is a cytoplasmic protein associated with vesicles in human and rat brain neurons. *Neuron*, **14**, 1075-81.
- DIFIGLIA, M., SAPP, E., CHASE, K.O., DAVIES, S.W., BATES, G.P., VONSATTEL, J.P. & ARONIN, N. (1997). Aggregation of huntingtin in neuronal intranuclear inclusions and dystrophic neurites in brain. *Science*, **277**, 1990-3.
- DJOUSSE, L., KNOWLTON, B., HAYDEN, M., ALMQVIST, E.W., BRINKMAN, R., ROSS, C., MARGOLIS, R., ROSENBLATT, A., DURR, A., DODE, C., MORRISON, P.J., NOVELLETTO, A., FRONTALI, M., TRENT, R.J., MCCUSKER, E., GOMEZ-TORTOSA, E., MAYO, D., JONES, R., ZANKO, A., NANCE, M., ABRAMSON, R., SUCHOWERSKY, O., PAULSEN, J., HARRISON, M., YANG, Q., CUPPLES, L.A., GUSELLA, J.F., MACDONALD, M.E. & MYERS, R.H. (2003). Interaction of normal and expanded CAG repeat sizes influences age at onset of Huntington disease. *Am J Med Genet A*, **119**, 279-82.

- DOI, H., MITSUI, K., KUROSAWA, M., MACHIDA, Y., KUROIWA, Y. & NUKINA, N. (2004). Identification of ubiquitin-interacting proteins in purified polyglutamine aggregates. *FEBS Lett*, **571**, 171-6.
- DONALDSON, K.M., LI, W., CHING, K.A., BATALOV, S., TSAI, C.C. & JOAZEIRO, C.A. (2003). Ubiquitin-mediated sequestration of normal cellular proteins into polyglutamine aggregates. *Proc Natl Acad Sci U S A*, **100**, 8892-7.
- DUBIEL, W., PRATT, G., FERRELL, K. & RECHSTEINER, M. (1992). Purification of an 11 S regulator of the multicatalytic protease. *J Biol Chem*, **267**, 22369-77.
- DUYAO, M.P., AUERBACH, A.B., RYAN, A., PERSICHETTI, F., BARNES, G.T., MCNEIL, S.M., GE, P., VONSATTEL, J.P., GUSELLA, J.F., JOYNER, A.L. & MACDONALD, M.A. (1995). Inactivation of the mouse Huntington's disease gene homolog Hdh. *Science*, **269**, 407-10.
- ESSER, C., ALBERTI, S. & HOHFELD, J. (2004). Cooperation of molecular chaperones with the ubiquitin/proteasome system. *Biochim Biophys Acta*, **1695**, 171-88.
- FERRANTE, R.J., KOWALL, N.W. & RICHARDSON, E.P., JR. (1991). Proliferative and degenerative changes in striatal spiny neurons in Huntington's disease: a combined study using the section-Golgi method and calbindin D28k immunocytochemistry. *J Neurosci*, **11**, 3877-87.
- FERRELL, K., WILKINSON, C.R., DUBIEL, W. & GORDON, C. (2000). Regulatory subunit interactions of the 26S proteasome, a complex problem. *Trends Biochem Sci*, **25**, 83-8.
- FINK, A.L. (1999). Chaperone-mediated protein folding. *Physiol Rev*, **79**, 425-49.
- FORNO, L.S. & NORVILLE, R.L. (1976). Ultrastructure of Lewy bodies in the stellate ganglion. *Acta Neuropathol (Berl)*, **34**, 183-97.
- FOROUD, T., GRAY, J., IVASHINA, J. & CONNEALLY, P.M. (1999). Differences in duration of Huntington's disease based on age at onset. *J Neurol Neurosurg Psychiatry*, **66**, 52-6.
- FUNAKOSHI, M., GELEY, S., HUNT, T., NISHIMOTO, T. & KOBAYASHI, H. (1999). Identification of XDRP1; a Xenopus protein related to yeast Dsk2p binds to the N-terminus of cyclin A and inhibits its degradation. *Embo J*, **18**, 5009-18.

GANDELMAN, K.Y., GIBSON, L., MEYN, M.S. & YANG-FENG, T.L. (1992). Molecular definition of the smallest region of deletion overlap in the Wolf-Hirschhorn syndrome. *Am J Hum Genet*, **51**, 571-8.

GERARDS, W.L., DE JONG, W.W., BLOEMENDAL, H. & BOELEN, W. (1998). The human proteasomal subunit HsC8 induces ring formation of other alpha-type subunits. *J Mol Biol*, **275**, 113-21.

GLICKMAN, M.H., RUBIN, D.M., COUX, O., WEFES, I., PFEIFER, G., CJEKA, Z., BAUMEISTER, W., FRIED, V.A. & FINLEY, D. (1998). A subcomplex of the proteasome regulatory particle required for ubiquitin-conjugate degradation and related to the COP9-signalosome and eIF3. *Cell*, **94**, 615-23.

GOELLNER, G.M. & RECHSTEINER, M. (2003). Are Huntington's and polyglutamine-based ataxias proteasome storage diseases? *Int J Biochem Cell Biol*, **35**, 562-71.

GOMEZ-TORTOSA, E., DEL BARRIO, A., GARCIA RUIZ, P.J., PERNAUTE, R.S., BENITEZ, J., BARROSO, A., JIMENEZ, F.J. & GARCIA YEBENES, J. (1998). Severity of cognitive impairment in juvenile and late-onset Huntington disease. *Arch Neurol*, **55**, 835-43.

GRAVELAND, G.A., WILLIAMS, R.S. & DIFIGLIA, M. (1985). Evidence for degenerative and regenerative changes in neostriatal spiny neurons in Huntington's disease. *Science*, **227**, 770-3.

GREEN, H. (1993). Human genetic diseases due to codon reiteration: relationship to an evolutionary mechanism. *Cell*, **74**, 955-6.

GUO, D., LI, M., ZHANG, Y., YANG, P., ECKENRODE, S., HOPKINS, D., ZHENG, W., PUROHIT, S., PODOLSKY, R.H., MUIR, A., WANG, J., DONG, Z., BRUSKO, T., ATKINSON, M., POZZILLI, P., ZEIDLER, A., RAFFEL, L.J., JACOB, C.O., PARK, Y., SERRANO-RIOS, M., LARRAD, M.T., ZHANG, Z., GARCHON, H.J., BACH, J.F., ROTTER, J.I., SHE, J.X. & WANG, C.Y. (2004). A functional variant of SUMO4, a new I kappa B alpha modifier, is associated with type 1 diabetes. *Nat Genet*, **36**, 837-41.

GUSELLA, J.F. & MACDONALD, M.E. (2000). Molecular genetics: unmasking polyglutamine triggers in neurodegenerative disease. *Nat Rev Neurosci*, **1**, 109-15.

GUTEKUNST, C.A., NORFLUS, F. & HERSCH, S.M. (2002). Neuropathology of Huntington's disease. In *Huntington's Disease*. ed Bates, G., Harper, P. & Jones, L. pp. 251-257. Oxford: Oxford.

- HANSSON, O., NYLANDSTED, J., CASTILHO, R.F., LEIST, M., JAATTELA, M. & BRUNDIN, P. (2003). Overexpression of heat shock protein 70 in R6/2 Huntington's disease mice has only modest effects on disease progression. *Brain Res*, **970**, 47-57.
- HARJES, P. & WANKER, E.E. (2003). The hunt for huntingtin function: interaction partners tell many different stories. *Trends Biochem Sci*, **28**, 425-33.
- HARPER, P.S. (1992). The epidemiology of Huntington's disease. *Hum Genet*, **89**, 365-76.
- HARTL, F.U. (1996). Molecular chaperones in cellular protein folding. *Nature*, **381**, 571-9.
- HAY, D.G., SATHASIVAM, K., TOBABEN, S., STAHL, B., MARBER, M., MESTRIL, R., MAHAL, A., SMITH, D.L., WOODMAN, B. & BATES, G.P. (2004). Progressive decrease in chaperone protein levels in a mouse model of Huntington's disease and induction of stress proteins as a therapeutic approach. *Hum Mol Genet*, **13**, 1389-405.
- HEDREEN, J.C. & FOLSTEIN, S.E. (1995). Early loss of neostriatal striosome neurons in Huntington's disease. *J Neuropathol Exp Neurol*, **54**, 105-20.
- HEDREEN, J.C., PEYSER, C.E., FOLSTEIN, S.E. & ROSS, C.A. (1991). Neuronal loss in layers V and VI of cerebral cortex in Huntington's disease. *Neurosci Lett*, **133**, 257-61.
- HEINEMEYER, W., RAMOS, P.C. & DOHMEN, R.J. (2004). The ultimate nanoscale mincer: assembly, structure and active sites of the 20S proteasome core. *Cell Mol Life Sci*, **61**, 1562-78.
- HELMLINGER, D., TORA, L. & DEVYS, D. (2006). Transcriptional alterations and chromatin remodeling in polyglutamine diseases. *Trends Genet*, **22**, 562-70.
- HERSHKO, A. & CIECHANOVER, A. (1998). The ubiquitin system. *Annu Rev Biochem*, **67**, 425-79.
- HIRANO, Y., HENDIL, K.B., YASHIRODA, H., IEMURA, S., NAGANE, R., HIOKI, Y., NATSUME, T., TANAKA, K & MURATA, S. (2005) A heterodimeric complex that promotes the assembly of mammalian 20S proteasomes. *Nature*, **437**, 1381-5.
- HOCHSTRASSER, M. (2000). Evolution and function of ubiquitin-like protein-conjugation systems. *Nat Cell Biol*, **2**, E153-7.

- HOFFMAN, L., PRATT, G. & RECHSTEINER, M. (1992). Multiple forms of the 20 S multicatalytic and the 26 S ubiquitin/ATP-dependent proteases from rabbit reticulocyte lysate. *J Biol Chem*, **267**, 22362-8.
- HOFFMAN, L. & RECHSTEINER, M. (1994). Activation of the multicatalytic protease. The 11 S regulator and 20 S ATPase complexes contain distinct 30-kilodalton subunits. *J Biol Chem*, **269**, 16890-5.
- HOFFNER, G. & DJIAN, P. (2002). Protein aggregation in Huntington's disease. *Biochimie*, **84**, 273-8.
- HOFFNER, G., ISLAND, M.L. & DJIAN, P. (2005). Purification of neuronal inclusions of patients with Huntington's disease reveals a broad range of N-terminal fragments of expanded huntingtin and insoluble polymers. *J Neurochem*. **95**, 125-36.
- HOLMBERG, C.I., STANISZEWSKI, K.E., MENSAH, K.N., MATOUSCHEK, A. & MORIMOTO, R.I. (2004). Inefficient degradation of truncated polyglutamine proteins by the proteasome. *Embo J*, **23**, 4307-18.
- HUANG, C.C., FABER, P.W., PERSICHETTI, F., MITTAL, V., VONSATTEL, J.P., MACDONALD, M.E. & GUSELLA, J.F. (1998). Amyloid formation by mutant huntingtin: threshold, progressivity and recruitment of normal polyglutamine proteins. *Somat Cell Mol Genet*, **24**, 217-33.
- HUNTER, J.M., LESORT, M. & JOHNSON, G.V. (2007). Ubiquitin-proteasome system alterations in a striatal cell model of Huntington's disease. *J Neurosci Res*, **85**, 1774-88.
- HUNTINGTON'S DISEASE COLLABORATIVE RESEARCH GROUP (1993). A novel gene containing a trinucleotide repeat that is expanded and unstable on Huntington's disease chromosomes. *Cell*, **72**, 971-83.
- ISHIGAKI, S., HISHIKAWA, N., NIWA, J., IEMURA, S., NATSUME, T., HORI, S., KAKIZUKA, A., TANAKA, K. & SOBUE, G. (2004). Physical and functional interaction between Dornin and Valosin-containing protein that are colocalized in ubiquitylated inclusions in neurodegenerative disorders. *J Biol Chem*, **279**, 51376-85.
- IUCHI, S., HOFFNER, G., VERBEKE, P., DJIAN, P. & GREEN, H. (2003). Oligomeric and polymeric aggregates formed by proteins containing expanded polyglutamine. *Proc Natl Acad Sci U S A*, **100**, 2409-14.

- JANA, N.R., TANAKA, M., WANG, G. & NUKINA, N. (2000). Polyglutamine length-dependent interaction of Hsp40 and Hsp70 family chaperones with truncated N-terminal huntingtin: their role in suppression of aggregation and cellular toxicity. *Hum Mol Genet*, **9**, 2009-18.
- JANA, N.R., ZEMSKOV, E.A., WANG, G. & NUKINA, N. (2001). Altered proteasomal function due to the expression of polyglutamine-expanded truncated N-terminal huntingtin induces apoptosis by caspase activation through mitochondrial cytochrome c release. *Hum Mol Genet*, **10**, 1049-59.
- JEITNER, T.M., BOGDANOV, M.B., MATSON, W.R., DAIKHIN, Y., YUDKOFF, M., FOLK, J.E., STEINMAN, L., BROWNE, S.E., BEAL, M.F., BLASS, J.P. & COOPER, A.J. (2001). N(epsilon)-(gamma-L-glutamyl)-L-lysine (GGEL) is increased in cerebrospinal fluid of patients with Huntington's disease. *J Neurochem*, **79**, 1109-12.
- JEONG, S.J., KIM, M., CHANG, K.A., KIM, H.S., PARK, C.H. & SUH, Y.H. (2006). Huntingtin is localized in the nucleus during preimplantation embryo development in mice. *Int J Dev Neurosci*, **24**, 81-5.
- JOHNSON, G.V. & LESHOURE, R., JR. (2004). Immunoblot analysis reveals that isopeptide antibodies do not specifically recognize the epsilon-(gamma-glutamyl)lysine bonds formed by transglutaminase activity. *J Neurosci Methods*, **134**, 151-8.
- KAHLEM, P., GREEN, H. & DJIAN, P. (1998). Transglutaminase action imitates Huntington's disease: selective polymerization of Huntingtin containing expanded polyglutamine. *Mol Cell*, **1**, 595-601.
- KALCHMAN, M.A., GRAHAM, R.K., XIA, G., KOIDE, H.B., HODGSON, J.G., GRAHAM, K.C., GOLDBERG, Y.P., GIETZ, R.D., PICKART, C.M. & HAYDEN, M.R. (1996). Huntingtin is ubiquitinated and interacts with a specific ubiquitin-conjugating enzyme. *J Biol Chem*, **271**, 19385-94.
- KARPUJ, M.V., GARREN, H., SLUNT, H., PRICE, D.L., GUSELLA, J., BECHER, M.W. & STEINMAN, L. (1999). Transglutaminase aggregates huntingtin into nonamyloidogenic polymers, and its enzymatic activity increases in Huntington's disease brain nuclei. *Proc Natl Acad Sci U S A*, **96**, 7388-93.
- KEGEL, K.B., KIM, M., SAPP, E., MCINTYRE, C., CASTANO, J.G., ARONIN, N. & DIFIGLIA, M. (2000). Huntingtin expression stimulates endosomal-lysosomal activity, endosome tubulation, and autophagy. *J Neurosci*, **20**, 7268-78.

- KERSCHER, O., FELBERBAUM, R. & HOCHSTRASSER, M. (2006). Modification of Proteins by Ubiquitin and Ubiquitin-Like Proteins. *Annu Rev Cell Dev Biol.* **22**, 159-80.
- KIM, W.Y., HORBINSKI, C., SIGURDSON, W. & HIGGINS, D. (2004). Proteasome inhibitors suppress formation of polyglutamine-induced nuclear inclusions in cultured postmitotic neurons. *J Neurochem*, **91**, 1044-56.
- KIM, Y.J., YI, Y., SAPP, E., WANG, Y., CUIFFO, B., KEGEL, K.B., QIN, Z.H., ARONIN, N. & DIFIGLIA, M. (2001). Caspase 3-cleaved N-terminal fragments of wild-type and mutant huntingtin are present in normal and Huntington's disease brains, associate with membranes, and undergo calpain-dependent proteolysis. *Proc Natl Acad Sci U S A*, **98**, 12784-9.
- KISSELEV, A.F., CALLARD, A. & GOLDBERG, A.L. (2006). Importance of the different proteolytic sites of the proteasome and the efficacy of inhibitors varies with the protein substrate. *J Biol Chem*, **281**, 8582-90.
- KISSELEV, A.F. & GOLDBERG, A.L. (2005). Monitoring activity and inhibition of 26S proteasomes with fluorogenic peptide substrates. *Methods Enzymol*, **398**, 364-78.
- KLAPSTEIN, G.J., FISHER, R.S., ZANJANI, H., CEPEDA, C., JOKEL, E.S., CHESSELET, M.F. & LEVINE, M.S. (2001). Electrophysiological and morphological changes in striatal spiny neurons in R6/2 Huntington's disease transgenic mice. *J Neurophysiol*, **86**, 2667-77.
- KLIMASCHEWSKI, L. (2003). Ubiquitin-dependent proteolysis in neurons. *News Physiol Sci*, **18**, 29-33.
- KNUEHL, C., SEELIG, A., BRECHT, B., HENKLEIN, P. & KLOETZEL, P.M. (1996). Functional analysis of eukaryotic 20S proteasome nuclear localization signal. *Exp Cell Res*, **225**, 67-74.
- KO, H.S., UEHARA, T., TSURUMA, K. & NOMURA, Y. (2004). Ubiquitin interacts with ubiquitylated proteins and proteasome through its ubiquitin-associated and ubiquitin-like domains. *FEBS Lett*, **566**, 110-4.
- KOBAYASHI, T., MANNO, A. & KAKIZUKA, A. (2007). Involvement of valosin-containing protein (VCP)/p97 in the formation and clearance of abnormal protein aggregates. *Genes Cells*, **12**, 889-901.

LA SPADA, A.R., PAULSON, H.L. & FISCHBECK, K.H. (1994). Trinucleotide repeat expansion in neurological disease. *Ann Neurol*, **36**, 814-22.

LAFARGA, M., BERCIANO, M.T., PENA, E., MAYO, I., CASTANO, J.G., BOHMANN, D., RODRIGUES, J.P., TAVANEZ, J.P. & CARMO-FONSECA, M. (2002). Clastosome: a subtype of nuclear body enriched in 19S and 20S proteasomes, ubiquitin, and protein substrates of proteasome. *Mol Biol Cell*, **13**, 2771-82.

LAM, Y.A., LAWSON, T.G., VELAYUTHAM, M., ZWEIER, J.L. & PICKART, C.M. (2002). A proteasomal ATPase subunit recognizes the polyubiquitin degradation signal. *Nature*, **416**, 763-7.

LESORT, M., CHUN, W., JOHNSON, G.V. & FERRANTE, R.J. (1999). Tissue transglutaminase is increased in Huntington's disease brain. *J Neurochem*, **73**, 2018-27.

LI, J., GAO, X., ORTEGA, J., NAZIF, T., JOSS, L., BOGYO, M., STEVEN, A.C. & RECHSTEINER, M. (2001). Lysine 188 substitutions convert the pattern of proteasome activation by REGgamma to that of REGs alpha and beta. *Embo J*, **20**, 3359-69.

LI, J. & RECHSTEINER, M. (2001). Molecular dissection of the 11S REG (PA28) proteasome activators. *Biochimie*, **83**, 373-83.

LI, S.H. & LI, X.J. (2004). Huntingtin-protein interactions and the pathogenesis of Huntington's disease. *Trends Genet*, **20**, 146-54.

LI, S.H., SCHILLING, G., YOUNG, W.S., 3RD, LI, X.J., MARGOLIS, R.L., STINE, O.C., WAGSTER, M.V., ABBOTT, M.H., FRANZ, M.L., RANEN, N.G., FOLSTEIN, N.G., HEDREEN, J.C. & ROSS, C.A. (1993). Huntington's disease gene (IT15) is widely expressed in human and rat tissues. *Neuron*, **11**, 985-93.

LIONE, L.A., CARTER, R.J., HUNT, M.J., BATES, G.P., MORTON, A.J. & DUNNETT, S.B. (1999). Selective discrimination learning impairments in mice expressing the human Huntington's disease mutation. *J Neurosci*, **19**, 10428-37.

LIPFORD, J.R. & DESHAIES, R.J. (2003). Diverse roles for ubiquitin-dependent proteolysis in transcriptional activation. *Nat Cell Biol*, **5**, 845-50.

LU, X., MICHAUD, C. & ORLOWSKI, M. (2001). Heat shock protein-90 and the catalytic activities of the 20 S proteasome (multicatalytic proteinase complex). *Arch Biochem Biophys*, **387**, 163-71.

LUNKES, A., LINDENBERG, K.S., BEN-HAIEM, L., WEBER, C., DEVYS, D., LANDWEHRMEYER, G.B., MANDEL, J.L. & TROTTIER, Y. (2002). Proteases acting on mutant huntingtin generate cleaved products that differentially build up cytoplasmic and nuclear inclusions. *Mol Cell*, **10**, 259-69.

MA, C.P., SLAUGHTER, C.A. & DEMARTINO, G.N. (1992). Identification, purification, and characterization of a protein activator (PA28) of the 20 S proteasome (macropain). *J Biol Chem*, **267**, 10515-23.

MANGIARINI, L., SATHASIVAM, K., SELLER, M., COZENS, B., HARPER, A., HETHERINGTON, C., LAWTON, M., TROTTIER, Y., LEHRACH, H., DAVIES, S.W. & BATES, G.P. (1996). Exon 1 of the HD gene with an expanded CAG repeat is sufficient to cause a progressive neurological phenotype in transgenic mice. *Cell*, **87**, 493-506.

MARTIN, J. & HARTL, F.U. (1997). Chaperone-assisted protein folding. *Curr Opin Struct Biol*, **7**, 41-52.

MARTIN-APARICIO, E., YAMAMOTO, A., HERNANDEZ, F., HEN, R., AVILA, J. & LUCAS, J.J. (2001). Proteasomal-dependent aggregate reversal and absence of cell death in a conditional mouse model of Huntington's disease. *J Neurosci*, **21**, 8772-81.

MASSEY, L.K., MAH, A.L., FORD, D.L., MILLER, J., LIANG, J., DOONG, H. & MONTEIRO, M.J. (2004). Overexpression of ubiquilin decreases ubiquitination and degradation of presenilin proteins. *J Alzheimers Dis*, **6**, 79-92.

MAYER, R.J., LANDON, M. & LAYFIELD, R. (1998). Ubiquitin superfolds: intrinsic and attachable regulators of cellular activities? *Fold Des*, **3**, R97-9.

MCCAMPBELL, A., TAYLOR, J.P., TAYE, A.A., ROBITSCHKE, J., LI, M., WALCOTT, J., MERRY, D., CHAI, Y., PAULSON, H., SOBUE, G. & FISCHBECK, K.H. (2000). CREB-binding protein sequestration by expanded polyglutamine. *Hum Mol Genet*, **9**, 2197-202.

- MCCUTCHEN-MALONEY, S.L., MATSUDA, K., SHIMBARA, N., BINNS, D.D., TANAKA, K., SLAUGHTER, C.A. & DEMARTINO, G.N. (2000). cDNA cloning, expression, and functional characterization of PI31, a proline-rich inhibitor of the proteasome. *J Biol Chem*, **275**, 18557-65.
- MCDONOUGH, H. & PATTERSON, C. (2003). CHIP: a link between the chaperone and proteasome systems. *Cell Stress Chaperones*, **8**, 303-8.
- MCGOWAN, D.P., VAN ROON-MOM, W., HOLLOWAY, H., BATES, G.P., MANGIARINI, L., COOPER, G.J., FAULL, R.L. & SNELL, R.G. (2000). Amyloid-like inclusions in Huntington's disease. *Neuroscience*, **100**, 677-80.
- MICHALIK, A. & VAN BROECKHOVEN, C. (2004). Proteasome degrades soluble expanded polyglutamine completely and efficiently. *Neurobiol Dis*, **16**, 202-11.
- MULLER, S., HOEGE, C., PYROWOLAKIS, G. & JENTSCH, S. (2001). SUMO, ubiquitin's mysterious cousin. *Nat Rev Mol Cell Biol*, **2**, 202-10.
- MYERS, R.H. (2004). Huntington's disease genetics. *NeuroRx*, **1**, 255-62.
- MYERS, R.H., VONSATTEL, J.P., PASKEVICH, P.A., KIELY, D.K., STEVENS, T.J., CUPPLES, L.A., RICHARDSON, E.P., JR. & BIRD, E.D. (1991). Decreased neuronal and increased oligodendroglial densities in Huntington's disease caudate nucleus. *J Neuropathol Exp Neurol*, **50**, 729-42.
- NAKAMURA, K., JEONG, S.Y., UCHIHARA, T., ANNO, M., NAGASHIMA, K., NAGASHIMA, T., IKEDA, S., TSUJI, S. & KANAZAWA, I. (2001). SCA17, a novel autosomal dominant cerebellar ataxia caused by an expanded polyglutamine in TATA-binding protein. *Hum Mol Genet*, **10**, 1441-8.
- NANCE, M.A. (1998). Huntington disease: clinical, genetic, and social aspects. *J Geriatr Psychiatry Neurol*, **11**, 61-70.
- NANCE, M.A. & MYERS, R.H. (2001). Juvenile onset Huntington's disease--clinical and research perspectives. *Ment Retard Dev Disabil Res Rev*, **7**, 153-7.
- NANDI, D., WOODWARD, E., GINSBURG, D.B. & MONACO, J.J. (1997). Intermediates in the formation of mouse 20S proteasomes: implications for the assembly of precursor beta subunits. *Embo J*, **16**, 5363-75.

NODA, C., TANAHASHI, N., SHIMBARA, N., HENDIL, K.B. & TANAKA, K. (2000). Tissue distribution of constitutive proteasomes, immunoproteasomes, and PA28 in rats. *Biochem Biophys Res Commun*, **277**, 348-54.

NOVOSELOVA, T.V., MARGULIS, B.A., NOVOSELOV, S.S., SAPOZHNIKOV, A.M., VAN DER SPUY, J., CHEETHAM, M.E. & GUZHOVA, I.V. (2005). Treatment with extracellular HSP70/HSC70 protein can reduce polyglutamine toxicity and aggregation. *J Neurochem*, **94**, 597-606.

ORDWAY, J.M., TALLAKSEN-GREENE, S., GUTEKUNST, C.A., BERNSTEIN, E.M., CEARLEY, J.A., WIENER, H.W., DURE, L.S.T., LINDSEY, R., HERSCH, S.M., JOPE, R.S., ALBIN, R.L. & DETLOFF, P.J. (1997). Ectopically expressed CAG repeats cause intranuclear inclusions and a progressive late onset neurological phenotype in the mouse. *Cell*, **91**, 753-63.

ORLOWSKI, M. & WILK, S. (2000). Catalytic activities of the 20 S proteasome, a multicatalytic proteinase complex. *Arch Biochem Biophys*, **383**, 1-16.

ORTEGA, J., HEYMANN, J.B., KAJAVA, A.V., USTRELL, V., RECHSTEINER, M. & STEVEN, A.C. (2005). The axial channel of the 20S proteasome opens upon binding of the PA200 activator. *J Mol Biol*, **346**, 1221-7.

PAVESE, N., GERHARD, A., TAI, Y.F., HO, A.K., TURKHEIMER, F., BARKER, R.A., BROOKS, D.J. & PICCINI, P. (2006). Microglial activation correlates with severity in Huntington disease: a clinical and PET study. *Neurology*, **66**, 1638-43.

PAVLIK, A. & ANEJA, I.S. (2007). Cerebral neurons and glial cell types inducing heat shock protein Hsp70 following heat stress in the rat. *Prog Brain Res*, **162**, 417-31.

PERUTZ, M.F., JOHNSON, T., SUZUKI, M. & FINCH, J.T. (1994). Glutamine repeats as polar zippers: their possible role in inherited neurodegenerative diseases. *Proc Natl Acad Sci U S A*, **91**, 5355-8.

PICKART, C.M. & FUSHMAN, D. (2004) Polyubiquitin chains: polymeric protein signals. *Curr. Opin. Chem. Biol.*, **8**, 610-6.

POUNTNEY, D.L., HUANG, Y., BURNS, R.J., HAAN, E., THOMPSON, P.D., BLUMBERGS, P.C. & GAI, W.P. (2003). SUMO-1 marks the nuclear inclusions in familial neuronal intranuclear inclusion disease. *Exp Neurol*, **184**, 436-46.

PRATT, W.B. (1997). The role of the hsp90-based chaperone system in signal transduction by nuclear receptors and receptors signaling via MAP kinase. *Annu Rev Pharmacol Toxicol*, **37**, 297-326.

QIN, Z.H., WANG, Y., KEGEL, K.B., KAZANTSEV, A., APOSTOL, B.L., THOMPSON, L.M., YODER, J., ARONIN, N. & DIFIGLIA, M. (2003) Autophagy regulates the processing of amino terminal huntingtin fragments. *Hum. Mol. Genet.*, **12**, 3231-44.

RANGONE, H., PARDO, R., COLIN, E., GIRAULT, J.A., SAUDOU, F. & HUMBERT, S. (2005). Phosphorylation of arfaptin 2 at Ser260 by Akt Inhibits PolyQ-huntingtin-induced toxicity by rescuing proteasome impairment. *J Biol Chem*, **280**, 22021-8.

RASMUSSEN, A., MACIAS, R., YESCAS, P., OCHOA, A., DAVILA, G. & ALONSO, E. (2000). Huntington disease in children: genotype-phenotype correlation. *Neuropediatrics*, **31**, 190-4.

RAVIKUMAR, B., ACEVEDO-AROZENA, A., IMARISIO, S., BERGER, Z., VACHER, C., O'KANE, C.J., BROWN, S.D. & RUBINSZTEIN, D.C. (2005) Dynein mutations impair autophagic clearance of aggregate-prone proteins. *Nat. Genet.*, **37**, 771-6.

REALINI, C., JENSEN, C.C., ZHANG, Z., JOHNSTON, S.C., KNOWLTON, J.R., HILL, C.P. & RECHSTEINER, M. (1997). Characterization of recombinant REGalpha, REGbeta, and REGgamma proteasome activators. *J Biol Chem*, **272**, 25483-92.

RECHSTEINER, M. & HILL, C.P. (2005). Mobilizing the proteolytic machine: cell biological roles of proteasome activators and inhibitors. *Trends Cell Biol*, **15**, 27-33.

RECHSTEINER, M., REALINI, C. & USTRELL, V. (2000). The proteasome activator 11 S REG (PA28) and class I antigen presentation. *Biochem J*, **345 Pt 1**, 1-15.

RILEY, B.E., ZOGHBI, H.Y. & ORR, H.T. (2005). SUMOylation of the polyglutamine repeat protein, ataxin-1, is dependent on a functional nuclear localization signal. *J Biol Chem*, **280**, 21942-8.

- ROCK, K.L., GRAMM, C., ROTHSTEIN, L., CLARK, K., STEIN, R., DICK, L., HWANG, D. & GOLDBERG, A.L. (1994). Inhibitors of the proteasome block the degradation of most cell proteins and the generation of peptides presented on MHC class I molecules. *Cell*, **78**, 761-71.
- RODGERS, K.J. & DEAN, R.T. (2003). Assessment of proteasome activity in cell lysates and tissue homogenates using peptide substrates. *Int J Biochem Cell Biol*, **35**, 716-27.
- RODRIGUEZ-VILARINO, S., ARRIBAS, J., ARIZTI, P. & CASTANO, J.G. (2000). Proteolytic processing and assembly of the C5 subunit into the proteasome complex. *J Biol Chem*, **275**, 6592-9.
- ROIZIN, L., STELLAR, S. & LIU, J.D. (1979). Neuronal nuclear-cytoplasmic changes in Huntington chorea: electron microscope investigations. In: *Adv Neurol (New York: Raven Press.)* **23**, 95-122.
- ROSAS, H.D., KOROSHETZ, W.J., CHEN, Y.I., SKEUSE, C., VANGEL, M., CUDKOWICZ, M.E., CAPLAN, K., MAREK, K., SEIDMAN, L.J., MAKRIS, N., JENKINS, B.G. & GOLDSTEIN, J.M. (2003). Evidence for more widespread cerebral pathology in early HD: an MRI-based morphometric analysis. *Neurology*, **60**, 1615-20.
- ROSENBLATT, A., BRINKMAN, R.R., LIANG, K.Y., ALMQVIST, E.W., MARGOLIS, R.L., HUANG, C.Y., SHERR, M., FRANZ, M.L., ABBOTT, M.H., HAYDEN, M.R. & ROSS, C.A. (2001). Familial influence on age of onset among siblings with Huntington disease. *Am J Med Genet*, **105**, 399-403.
- RUDNICKI, D.D. & MARGOLIS, R.L. (2003). Repeat expansion and autosomal dominant neurodegenerative disorders: consensus and controversy. *Expert Rev Mol Med*, **2003**, 1-24.
- SAITOH, H. & HINCHEY, J. (2000). Functional heterogeneity of small ubiquitin-related protein modifiers SUMO-1 versus SUMO-2/3. *J Biol Chem*, **275**, 6252-8.
- SCHEEL, H., TOMIUK, S. & HOFMANN, K. (2003). Elucidation of ataxin-3 and ataxin-7 function by integrative bioinformatics. *Hum Mol Genet*, **12**, 2845-52.
- SCHERZINGER, E., LURZ, R., TURMAINE, M., MANGIARINI, L., HOLLENBACH, B., HASENBANK, R., BATES, G.P., DAVIES, S.W., LEHRACH, H. & WANKER, E.E. (1997). Huntingtin-encoded polyglutamine expansions form amyloid-like protein aggregates in vitro and in vivo. *Cell*, **90**, 549-58.

- SENECA, S., FAGNART, D., KEYMOLEN, K., LISSENS, W., HASAERTS, D., DEBULPAEP, S., DESPRECHINS, B., LIEBAERS, I. & DE MEIRLEIR, L. (2004). Early onset Huntington disease: a neuronal degeneration syndrome. *Eur J Pediatr*, **163**, 717-21.
- SEO, H., SONNTAG, K.C. & ISACSON, O. (2004). Generalized brain and skin proteasome inhibition in Huntington's disease. *Ann Neurol*, **56**, 319-28.
- SHARP, A.H., LOEV, S.J., SCHILLING, G., LI, S.H., LI, X.J., BAO, J., WAGSTER, M.V., KOTZUK, J.A., STEINER, J.P., LO, A. & ET AL. (1995). Widespread expression of Huntington's disease gene (IT15) protein product. *Neuron*, **14**, 1065-74.
- SHIBATANI, T. & WARD, W.F. (1995). Sodium dodecyl sulfate (SDS) activation of the 20S proteasome in rat liver. *Arch Biochem Biophys*, **321**, 160-6.
- SIERADZAN, K.A., MECHAN, A.O., JONES, L., WANKER, E.E., NUKINA, N. & MANN, D.M. (1999). Huntington's disease intranuclear inclusions contain truncated, ubiquitinated huntingtin protein. *Exp Neurol*, **156**, 92-9.
- SIN, N., KIM, K.B., ELOFSSON, M., MENG, L., AUTH, H., KWOK, B.H. & CREWS, C.M. (1999). Total synthesis of the potent proteasome inhibitor epoxomicin: a useful tool for understanding proteasome biology. *Bioorg Med Chem Lett*, **9**, 2283-8.
- SPILLANTINI, M.G., CROWTHER, R.A., JAKES, R., HASEGAWA, M. & GOEDERT, M. (1998). alpha-Synuclein in filamentous inclusions of Lewy bodies from Parkinson's disease and dementia with lewy bodies. *Proc Natl Acad Sci U S A*, **95**, 6469-73.
- STACK, E.C., KUBILUS, J.K., SMITH, K., CORMIER, K., DEL SIGNORE, S.J., GUELIN, E., RYU, H., HERSCH, S.M. & FERRANTE, R.J. (2005). Chronology of behavioral symptoms and neuropathological sequela in R6/2 Huntington's disease transgenic mice. *J Comp Neurol*, **490**, 354-70.
- STEFFAN, J.S., AGRAWAL, N., PALLOS, J., ROCKABRAND, E., TROTMAN, L.C., SLEPKO, N., ILLES, K., LUKACSOVICH, T., ZHU, Y.Z., CATTANEO, E., PANDOLFI, P.P., THOMPSON, L.M. & MARSH, J.L. (2004) SUMO modification of Huntingtin and Huntington's disease pathology. *Science*, **304**, 100-4.
- STENOIEN, D.L., CUMMINGS, C.J., ADAMS, H.P., MANCINI, M.G., PATEL, K., DEMARTINO, G.N., MARCELLI, M., WEIGEL, N.L. & MANCINI, M.A. (1999). Polyglutamine-expanded androgen

receptors form aggregates that sequester heat shock proteins, proteasome components and SRC-1, and are suppressed by the HDJ-2 chaperone. *Hum Mol Genet*, **8**, 731-41.

STOTT, K., BLACKBURN, J.M., BUTLER, P.J. & PERUTZ, M. (1995). Incorporation of glutamine repeats makes protein oligomerize: implications for neurodegenerative diseases. *Proc Natl Acad Sci U S A*, **92**, 6509-13.

TAN, J.M., WONG, E.S., DAWSON, V.L., DAWSON, T.M. & LIM, K.L. (2007) Lysine 63-linked polyubiquitin potentially partners with p62 to promote the clearance of protein inclusions by autophagy. *Autophagy*, **4**, 251-3.

TANAHASHI, N., YOKOTA, K., AHN, J.Y., CHUNG, C.H., FUJIWARA, T., TAKAHASHI, E., DEMARTINO, G.N., SLAUGHTER, C.A., TOYONAGA, T., YAMAMURA, K., SHIMBARA, N. & TANAKA, K. (1997). Molecular properties of the proteasome activator PA28 family proteins and gamma-interferon regulation. *Genes Cells*, **2**, 195-211.

TARLAC, V. & STOREY, E. (2003). Role of proteolysis in polyglutamine disorders. *J Neurosci Res*, **74**, 406-16.

TATHAM, M.H., JAFFRAY, E., VAUGHAN, O.A., DESTERRO, J.M., BOTTING, C.H., NAISMITH, J.H. & HAY, R.T. (2001). Polymeric chains of SUMO-2 and SUMO-3 are conjugated to protein substrates by SAE1/SAE2 and Ubc9. *J Biol Chem*, **276**, 35368-74.

TAYLOR, J.P., TANAKA, F., ROBITSCHKE, J., SANDOVAL, C.M., TAYE, A., MARKOVIC-PLESE, S. & FISCHBECK, K.H. (2003). Aggresomes protect cells by enhancing the degradation of toxic polyglutamine-containing protein. *Hum Mol Genet*, **12**, 749-57.

TERASHIMA, T., KAWAI, H., FUJITANI, M., MAEDA, K. & YASUDA, H. (2002). SUMO-1 co-localized with mutant atrophin-1 with expanded polyglutamines accelerates intranuclear aggregation and cell death. *Neuroreport*, **13**, 2359-64.

THOMAS, E.A. (2006). Striatal specificity of gene expression dysregulation in Huntington's disease. *J Neurosci Res*, **84**, 1151-64.

TROTTIER, Y., LUTZ, Y., STEVANIN, G., IMBERT, G., DEVYS, D., CANCEL, G., SAUDOU, F., WEBER, C., DAVID, G., TORA, L., AGID, Y., BRICE, A. & MANDEL, J.L. (1995). Polyglutamine

expansion as a pathological epitope in Huntington's disease and four dominant cerebellar ataxias. *Nature*, **378**, 403-6.

TSAI, H.F., LIN, S.J., LI, C. & HSIEH, M. (2005). Decreased expression of Hsp27 and Hsp70 in transformed lymphoblastoid cells from patients with spinocerebellar ataxia type 7. *Biochem Biophys Res Commun*. **334**(4), 1279-86.

TYTELL, M. (2005). Release of heat shock proteins (Hsps) and the effects of extracellular Hsps on neural cells and tissues. *Int J Hyperthermia*, **21**, 445-55.

UEDA, H., GOTO, J., HASHIDA, H., LIN, X., OYANAGI, K., KAWANO, H., ZOGHBI, H.Y., KANAZAWA, I. & OKAZAWA, H. (2002). Enhanced SUMOylation in polyglutamine diseases. *Biochem Biophys Res Commun*, **293**, 307-13.

UPADHYA, S.C., DING, L., SMITH, T.K. & HEGDE, A.N. (2006). Differential regulation of proteasome activity in the nucleus and the synaptic terminals. *Neurochem Int*, **48**, 296-305.

USTRELL, V., HOFFMAN, L., PRATT, G. & RECHSTEINER, M. (2002). PA200, a nuclear proteasome activator involved in DNA repair. *Embo J*, **21**, 3516-25.

VAN RAAMSDONK, J.M., GIBSON, W.T., PEARSON, J., MURPHY, Z., LU, G., LEAVITT, B.R. & HAYDEN, M.R. (2006). Body weight is modulated by levels of full-length Huntingtin. *Hum Mol Genet*, **15**, 1513-23.

VAN ROON-MOM, W.M., REID, S.J., FAULL, R.L. & SNELL, R.G. (2005). TATA-binding protein in neurodegenerative disease. *Neuroscience*, **133**, 863-72.

VAN ROON-MOM, W.M., REID, S.J., JONES, A.L., MACDONALD, M.E., FAULL, R.L. & SNELL, R.G. (2002). Insoluble TATA-binding protein accumulation in Huntington's disease cortex. *Brain Res Mol Brain Res*, **109**, 1-10.

VENKATRAMAN, P., WETZEL, R., TANAKA, M., NUKINA, N. & GOLDBERG, A.L. (2004). Eukaryotic proteasomes cannot digest polyglutamine sequences and release them during degradation of polyglutamine-containing proteins. *Mol Cell*, **14**, 95-104.

VERMA, R., ARAVIND, L., OANIA, R., MCDONALD, W.H., YATES, J.R., 3RD, KOONIN, E.V. & DESHAIES, R.J. (2002). Role of Rpn11 metalloprotease in deubiquitination and degradation by the 26S proteasome. *Science*, **298**, 611-5.

VIGOUROUX, S., FAROUT, L., CLAVEL, S., BRIAND, Y. & BRIAND, M. (2003a). Increased muscle proteasome activities in rats fed a polyunsaturated fatty acid supplemented diet. *Int J Biochem Cell Biol*, **35**, 749-55.

VIGOUROUX, S., FURUKAWA, Y., FAROUT, L., S, J.K., BRIAND, M. & BRIAND, Y. (2003b). Peptidase activities of the 20/26S proteasome and a novel protease in human brain. *J Neurochem*, **84**, 392-6.

VOGES, D., ZWICKL, P. & BAUMEISTER, W. (1999) The 26S proteasome: a molecular machine designed for controlled proteolysis. *Annu. Rev. Biochem.*, **68**, 1015-68.

VONSATTEL, J.P., MYERS, R.H., STEVENS, T.J., FERRANTE, R.J., BIRD, E.D. & RICHARDSON, E.P., JR. (1985). Neuropathological classification of Huntington's disease. *J Neuropathol Exp Neurol*, **44**, 559-77.

WACKER, J.L., ZAREIE, M.H., FONG, H., SARIKAYA, M. & MUCHOWSKI, P.J. (2004) Hsp70 and Hsp40 attenuate formation of spherical and annular polyglutamine oligomers by partitioning monomer. *Nat. Struct. Mol. Biol.*, **11**, 1215-22.

WAELETER, S., BOEDDRICH, A., LURZ, R., SCHERZINGER, E., LUEDER, G., LEHRACH, H. & WANKER, E.E. (2001). Accumulation of mutant huntingtin fragments in aggresome-like inclusion bodies as a result of insufficient protein degradation. *Mol Biol Cell*, **12**, 1393-407.

WANG, H., LIM, P.J., YIN, C., RIECKHER, M., VOGEL, B.E. & MONTEIRO, M.J. (2006). Suppression of polyglutamine-induced toxicity in cell and animal models of Huntington's disease by ubiquilin. *Hum Mol Genet*, **15**, 1025-41.

WARRICK, J.M., CHAN, H.Y., GRAY-BOARD, G.L., CHAI, Y., PAULSON, H.L. & BONINI, N.M. (1999). Suppression of polyglutamine-mediated neurodegeneration in *Drosophila* by the molecular chaperone HSP70. *Nat Genet*, **23**, 425-8.

WEISSMAN, A.M. (2001). Themes and variations on ubiquitylation. *Nat Rev Mol Cell Biol*, **2**, 169-78.

WELCHMAN, R.L., GORDON, C. & MAYER, R.J. (2005). Ubiquitin and ubiquitin-like proteins as multifunctional signals. *Nat Rev Mol Cell Biol*, **6**, 599-609.

WEXLER, N.S., LORIMER, J., PORTER, J., GOMEZ, F., MOSKOWITZ, C., SHACKELL, E., MARDER, K., PENCHASZADEH, G., ROBERTS, S.A., GAYAN, J., BROCKLEBANK, D., CHERNY, S.S., CARDON, L.R., GRAY, J., DLOUHY, S.R., WIKTORSKI, S., HODES, M.E., CONNEALLY, P.M., PENNEY, J.B., GUSELLA, J., CHA, J.H., IRIZARRY, M., ROSAS, D., HERSCH, S., HOLLINGSWORTH, Z., MACDONALD, M., YOUNG, A.B., ANDRESEN, J.M., HOUSMAN, D.E., DE YOUNG, M.M., BONILLA, E., STILLINGS, T., NEGRETTE, A., SNODGRASS, S.R., MARTINEZ-JAURRIETA, M.D., RAMOS-ARROYO, M.A., BICKHAM, J., RAMOS, J.S., MARSHALL, F., SHOULSON, I., REY, G.J., FEIGIN, A., ARNHEIM, N., ACEVEDO-CRUZ, A., ACOSTA, L., ALVIR, J., FISCHBECK, K., THOMPSON, L.M., YOUNG, A., DURE, L., O'BRIEN, C.J., PAULSEN, J., BRICKMAN, A., KRCH, D., PEERY, S., HOGARTH, P., HIGGINS, D.S., JR. & LANDWEHRMEYER, B. (2004). Venezuelan kindreds reveal that genetic and environmental factors modulate Huntington's disease age of onset. *Proc Natl Acad Sci U S A*, **101**, 3498-503.

WEXLER, N.S., YOUNG, A.B., TANZI, R.E., TRAVERS, H., STAROSTA-RUBINSTEIN, S., PENNEY, J.B., SNODGRASS, S.R., SHOULSON, I., GOMEZ, F., RAMOS ARROYO, M.A. & ET AL. (1987). Homozygotes for Huntington's disease. *Nature*, **326**, 194-7.

WITT, E., ZANTOPF, D., SCHMIDT, M., KRAFT, R., KLOETZEL, P.M. & KRUGER, E. (2000). Characterisation of the newly identified human Ump1 homologue POMP and analysis of LMP7(beta 5i) incorporation into 20 S proteasomes. *J Mol Biol*, **301**, 1-9.

WOJCIK, C. & DEMARTINO, G.N. (2003). Intracellular localization of proteasomes. *Int J Biochem Cell Biol*, **35**, 579-89.

WOODMAN, P.G. (2003). p97, a protein coping with multiple identities. *J Cell Sci*, **116**, 4283-90.

YANG, H., ZHONG, X., BALLAR, P., LUO, S., SHEN, Y., RUBINSZTEIN, D.C., MONTEIRO, M.J. & FANG, S. (2007). Ubiquitin ligase Hrd1 enhances the degradation and suppresses the toxicity of polyglutamine-expanded huntingtin. *Exp Cell Res*, **313**, 538-50.

YI, J.J. & EHLERS, M.D. (2005). Ubiquitin and protein turnover in synapse function. *Neuron*, **47**, 629-32.

- YOUNG, P., DEVERAUX, Q., BEAL, R.E., PICKART, C.M. & RECHSTEINER, M. (1998). Characterization of two polyubiquitin binding sites in the 26 S protease subunit 5a. *J Biol Chem*, **273**, 5461-7.
- ZAISS, D.M., STANDERA, S., HOLZHUTTER, H., KLOETZEL, P. & SIJTS, A.J. (1999). The proteasome inhibitor PI31 competes with PA28 for binding to 20S proteasomes. *FEBS Lett*, **457**, 333-8.
- ZAISS, D.M., STANDERA, S., KLOETZEL, P.M. & SIJTS, A.J. (2002). PI31 is a modulator of proteasome formation and antigen processing. *Proc Natl Acad Sci U S A*, **99**, 14344-9.
- ZEITLIN, S., LIU, J.P., CHAPMAN, D.L., PAPAIOANNOU, V.E. & EFSTRATIADIS, A. (1995). Increased apoptosis and early embryonic lethality in mice nullizygous for the Huntington's disease gene homologue. *Nat Genet*, **11**, 155-63.
- ZENG, B.Y., MEDHURST, A.D., JACKSON, M., ROSE, S. & JENNER, P. (2005). Proteasomal activity in brain differs between species and brain regions and changes with age. *Mech Ageing Dev*, **126**, 760-6.
- ZHANG, S., XU, L., LEE, J. & XU, T. (2002). Drosophila atrophin homolog functions as a transcriptional corepressor in multiple developmental processes. *Cell*, **108**, 45-56.
- ZONG, C., GOMES, A.V., DREWS, O., LI, X., YOUNG, G.W., BERHANE, B., QIAO, X., FRENCH, S.W., BARDAG-GORCE, F. & PING, P. (2006). Regulation of murine cardiac 20S proteasomes: role of associating partners. *Circ Res*, **99**, 372-80.

